Australian Government
Geoscience Australia

NSW GOVERNMENT Industry & Investment

New SHRIMP U-Pb zircon ages from the eastern Lachlan Orogen, New South Wales

July 2008–June 2009

Bodorkos, S., Simpson, C.J., Thomas, O.D., Trigg, S.J., Blevin, P.L., Campbell, L.M., Deyssing, L.J. and Fitzherbert, J.A.

Record
2010/31

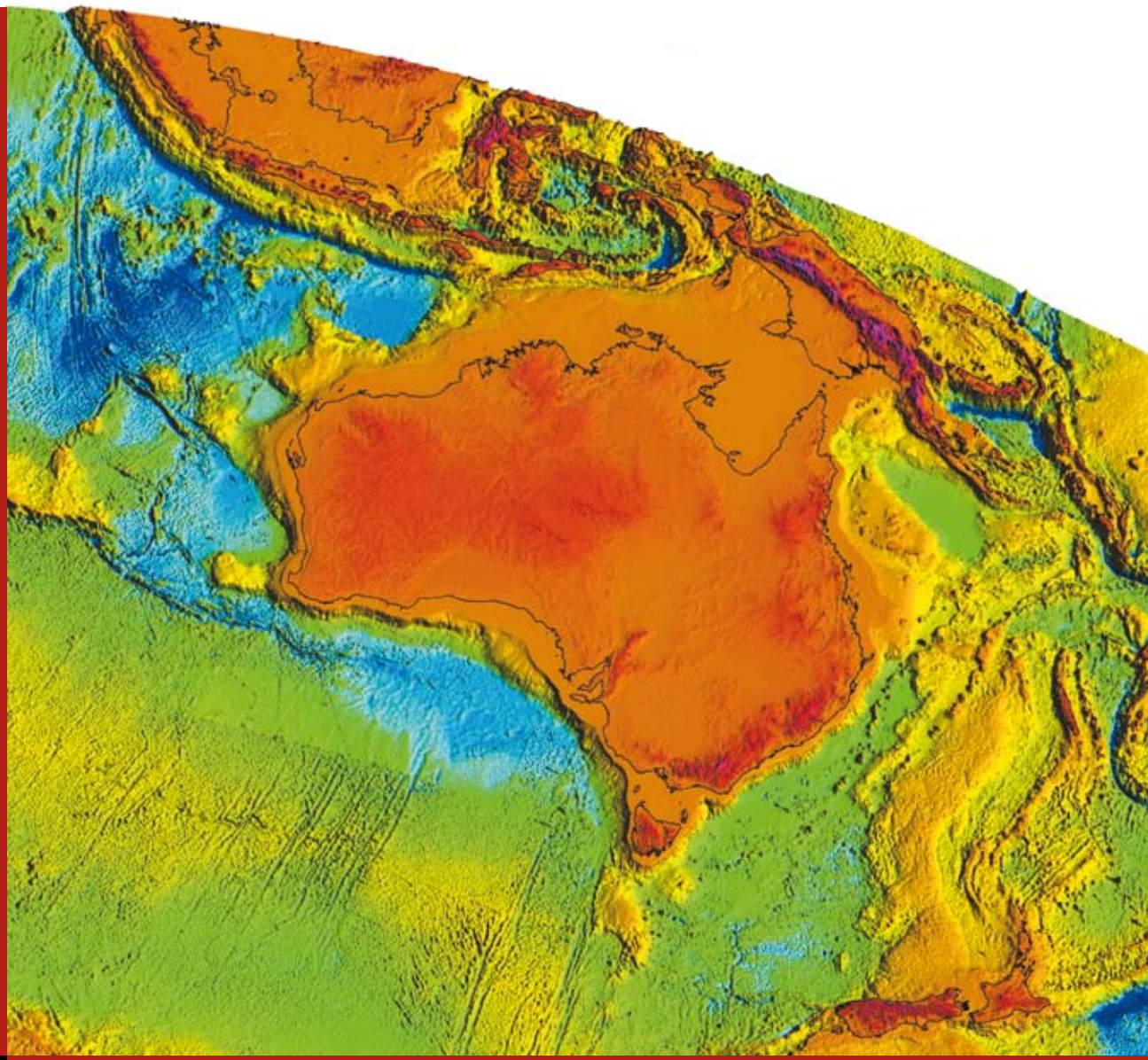

New SHRIMP U-Pb zircon ages from the eastern Lachlan Orogen, New South Wales, July 2008–June 2009

GEOSCIENCE AUSTRALIA
RECORD 2010/31

by

S. Bodorkos[1]
C. J. Simpson[2]
O. D. Thomas[3]
S. J. Trigg[3]
P. L. Blevin[2]
L. M. Campbell[3]
L. J. Deyssing[3]
J. A. Fitzherbert[2]

Australian Government
Geoscience Australia

Industry & Investment
Geological Survey of New South Wales

1. Onshore Energy and Minerals Division, Geoscience Australia, GPO Box 378, Canberra ACT 2601
2. Regional Mapping and Exploration Geoscience, Geological Survey of New South Wales, Industry and Investment NSW, 516 High St, Maitland NSW 2310
3. Regional Mapping and Exploration Geoscience, Geological Survey of New South Wales, Industry and Investment NSW, 161 Kite St, Orange NSW 2800

Department of Resources, Energy and Tourism
Minister for Resources and Energy: The Hon. Martin Ferguson, AM MP
Secretary: Mr Drew Clarke

Geoscience Australia
Chief Executive Officer: Dr Chris Pigram

ISSN 1448-2177
ISBN 978-1-921781-31-5 (Hardcopy)
ISBN 978-1-921781-30-8 (Web)

GeoCat # 70290

Bibliographic reference: Bodorkos, S., Simpson, C. J., Thomas, O. D., Trigg, S. J., Blevin, P. L., Campbell, L. M., Deyssing, L. J. and Fitzherbert, J. A., 2010. New SHRIMP U-Pb zircon ages from the eastern Lachlan Orogen, New South Wales, July 2008–June 2009. Geoscience Australia Record 2010/31, 100p.

Contents

List of Figures

List of Tables

Summary

This Record presents new zircon U-Pb geochronological data, obtained via Sensitive High Resolution Ion Micro Probe (SHRIMP) from 14 samples of volcanic and plutonic igneous rocks of the eastern Lachlan Orogen, New South Wales. These data were generated under the auspices of the National Geoscience Accord, as part of the collaborative Geochronology Project between the Geological Survey of New South Wales (GSNSW) and Geoscience Australia (GA), during the reporting period July 2008–June 2009.

Six samples were analysed from BRAIDWOOD[1] (northeastern CANBERRA), a total of seven from MOSS VALE and BURRAGORANG (southwestern and northwestern WOLLONGONG, respectively), and one from BOOROWA (northwestern GOULBURN). The results are summarised in Table i.

Table i. Summary of sample identifiers, locations, stratigraphic units and results (magmatic crystallisation ages and associated 95% confidence limits) for the GSNSW–GA Geochronology Project 2008–09 (eastern Lachlan Orogen). Single-quotes denote informal names.

GSNSW SiteID	GA SampleNo	Easting	Northing	Stratigraphic name	$^{238}U/^{206}Pb$ age (Ma)
Braidwood 1:100 000 sheet (MGA94 Zone 55), all SiteIDs prefixed '8827'					
JAF0837	1974958	729428	6087379	Lockhart Igneous Complex ('leucogranite phase')	424.4 ± 3.2
JAF0672	1974959	728845	6088322	Lockhart Igneous Complex ('tonalite phase')	428.5 ± 3.1
ODT1152	1974960	731961	6117253	Woodlawn Volcanics	423.3 ± 2.6
JAF0300	1974961	753831	6097409	Braidwood Granodiorite ('northern phase')	411.3 ± 2.6
JAF0193	1949548	739710	6071307	Long Flat Volcanics: Kain Porphyry Member	414.1 ± 2.8
CJS0070	1989476	748261	6101147	Long Flat Volcanics: Croppies Gunyah Rhyolite	414.0 ± 2.5
Moss Vale and Burragorang 1:100 000 sheets (MGA94 Zone 56), all SiteIDs prefixed '8928'					
LMC0363	1985433	232317	6127455	Touga Granite	325.5 ± 2.6
LMC0365	1985435	261660	6134041	Bundundah Granite	324.4 ± 3.2
LMC0364	1985434	240217	6131145	Tullyangela Granite	382.4 ± 3.0
LMC0073	1985436	264684	6141055	Yalwal Volcanics: Grassy Gully Rhyolite Member	384.5 ± 4.4
LMC0002	1985440	229670	6165305	Pleasant Hill Granite	412.6 ± 2.2
LMC0368	1985439	226345	6149354	Tangerang Formation: Kerillon Tuff Member	412.7 ± 2.2
LMC0366	1985437	263980	6182491	'Mount Gibraltar microsyenite'	—
Boorowa 1:100 000 sheet (MGA94 Zone 55), no prefix for SiteID					
WRP-046	1989773	761455	6075259	Rye Park Granite	431.4 ± 4.9

BRAIDWOOD

Three samples were sourced from the belt of Silurian igneous rocks along the western edge of BRAIDWOOD, and were aimed at establishing a chronology of magmatism for the plutonic Thurralilly Suite (which includes the mid-crustal, multiphase Lockhart Igneous Complex and the shallow-level Ellenden Granite) and evaluating its potential relationship to the Late Silurian supracrustal Mount Fairy Group, which includes the mineralised Woodlawn-Currawang bimodal volcanic succession. Two of the samples are from the Lockhart Igneous Complex, which comprises plutonic rocks ranging from olivine-bearing gabbro to leucogranite, that display a variety of magma mixing and mingling relationships (Fitzherbert *et al.*, in press). A weakly deformed porphyritic leucocratic granite (GSNSW 8827JAF0837, GA 1974958) and an enclave-bearing quartz-rich tonalite (GSNSW 8827JAF0672, GA 1974959) yielded magmatic crystallisation ages of 424.4 ± 3.2 Ma and

[1] Names with small capitals (e.g. BRAIDWOOD) refer to standard 1:100 000 map sheet areas; fully-capitalised names (e.g. CANBERRA) refer to standard 1:250 000 map sheet areas

428.5 ± 3.1 Ma respectively (all uncertainties are quoted at the 95% confidence level). The third sample (GSNSW 8827ODT1152, GA 1974960) is a coherent porphyritic rhyolite lava within the predominantly volcaniclastic lower part of the Woodlawn Volcanics succession, which yielded a magmatic crystallisation age of 423.3 ± 2.6 Ma.

The two Lockhart Igneous Complex dates are externally indistinguishable at the 95% confidence level (probability of equivalence = 0.07); however, the two samples were analysed during the same SHRIMP session, so the shared component of the uncertainties (associated with determining the session-specific mean value of the Temora-2 reference zircon) can be neglected for the purpose of evaluating the equivalence of the two magmatic crystallisation ages. Recomparing the two dates decreases their probability of equivalence to 0.03, and establishes that the leucogranite phase of Lockhart Igneous Complex is slightly younger than the tonalite phase at the 95% confidence level.

The magmatic crystallisation ages presented herein for the Lockhart Igneous Complex leucogranite and Woodlawn Volcanics are indistinguishable, and both are also indistinguishable from the 423.4 ± 3.3 Ma Ellenden Granite (Bodorkos and Simpson, 2008), and the 423.4 ± 2.5 Ma Woodlawn Volcanics on southern GOULBURN (Black, 2005). All four of these ages are slightly younger than the Lockhart Igneous Complex tonalite, and slightly older than the age of 419.2 ± 3.2 Ma obtained for a high-level intrusion within the upper Woodlawn Volcanics by Bodorkos and Simpson (2008).

The remaining three samples were sourced from the Long Flat Volcanics (within the Early Devonian Bindook Group) and the plutonic Braidwood Suite, which jointly dominate the west-central part of BRAIDWOOD. One sample is a crystal-rich, densely-welded rhyolitic ignimbrite from the Croppies Gunyah Rhyolite Member (GSNSW 8827CJS0070, GA 1989476) of the Long Flat Volcanics succession, and one is a dacitic, plagioclase-phyric subvolcanic rock from the Kain Porphyry Member (GSNSW 8827JAF0193, GA 1949548), which intrudes all supracrustal members of the Long Flat Volcanics. These two phases yielded magmatic crystallisation ages of 414.0 ± 2.5 Ma and 414.1 ± 2.8 Ma respectively. The third sample is a hornblende granodiorite from the northern extremity of the Braidwood Granodiorite (GSNSW 8827JAF0300, GA 1974961), which intrudes the Long Flat Volcanics, and which yielded a magmatic crystallisation age of 411.3 ± 2.6 Ma.

These three ages are indistinguishable from each other at the 95% confidence level, and all three are also indistinguishable from three previous ages obtained for units within the Long Flat Volcanics (413.4 ± 2.6 Ma Kadoona Dacite Member, 412.3 ± 2.3 Ma Toggannoggra Rhyolite Member, and 413.0 ± 2.4 Ma Manar Ignimbrite Member; Bodorkos and Simpson, 2008), so the apparent age reversal between the Kain Porphyry Member and the supracrustal units of the Long Flat Volcanics it intrudes is not significant with respect to the uncertainties associated with each of the dates. The three new ages are also indistinguishable from two previous determinations on the 'western' and 'eastern' phases of the Braidwood Granodiorite (410.8 ± 3.2 Ma and 410.2 ± 3.1 Ma respectively; Bodorkos and Simpson, 2008), as well as one on the leucogranite phase of the nearby Boro Granite (411.5 ± 3.1 Ma; Bodorkos and Simpson, 2008) of the Glenbog Suite (Fitzherbert *et al.*, in press).

MOSS VALE–BURRAGORANG

Two of the seven MOSS VALE–BURRAGORANG samples were collected close to the western edge of MOSS VALE. One is a crystal-rich welded dacitic ignimbrite from the Kerillon Tuff Member (GSNSW 8928LMC0368, GA 1985439) of the Tangerang Formation (within the Early Devonian Bindook Group), which yielded a magmatic crystallisation age of 412.7 ± 2.2 Ma. The other is a coarse-grained granodiorite from the Pleasant Hill Granite (GSNSW 8928LMC0002, GA 1985440) of the plutonic Arthursleigh Suite, which intrudes the Bindook Group, and it yielded a magmatic crystallisation age of 412.6 ± 2.2 Ma.

These two ages are indistinguishable from each other, and both are also indistinguishable from other volcanic units within the Bindook Group previously dated on neighbouring GOULBURN, which include the 414.4 ± 2.9 Ma Barrallier Ignimbrite (Black, 2006), and the Newacres Ignimbrite Member of the Quialigo Volcanics, which has yielded SHRIMP zircon $^{238}U/^{206}Pb$ dates of 414.4 ± 2.9 Ma (Black, 2006), 411 ± 3 Ma and 409 ± 4 Ma (Wilde, 2002). At the 95% confidence level, the Pleasant Hill Granite age is marginally younger than that of the 416.7 ± 3.1 Ma Marulan Granite (Black, 2005), which is also part of the Arthursleigh Suite; however, the 412.6 ± 2.2 Ma age presented herein appears to better fit the interpreted intrusive relationship with the felsic volcanic rocks of the host Bindook Group.

The remaining four MOSS VALE samples were sourced from the southern part of the sheet, and targeted Late Devonian volcanic rocks, and ungrouped plutonic rocks of assumed Carboniferous age. One sample is a near-aphyric rhyolite from the Grassy Gully Rhyolite Member (GSNSW 8928LMC0073, GA 1985436), within the Late Devonian Yalwal Volcanics, which yielded a magmatic crystallisation age of 384.5 ± 4.4 Ma. The other three samples comprised melanocratic hornblende granodiorite of the Touga Granite (GSNSW 8928LMC0363, GA 1985433), leucocratic quartz- and feldspar-phyric microgranite from within the Bundundah Granite (GSNSW 8928LMC0365, GA 1985435), and clinopyroxene-hornblende quartz diorite of the Tullyangela Granite (GSNSW 8928LMC0364, GA 1985434). These plutons yielded magmatic crystallisation ages of 325.5 ± 2.6 Ma, 324.4 ± 3.2 Ma, and 382.4 ± 3.0 Ma respectively.

The most noteworthy of these four results is that of the Tullyangela Granite, which is not Carboniferous as previously supposed, but instead represents a plutonic time-equivalent of the Late Devonian Yalwal Volcanics, as its magmatic crystallisation age is indistinguishable from that of the Grassy Gully Rhyolite Member. The Middle Carboniferous ages for the Touga and Bundundah plutons are indistinguishable from each other, and are comparable to magmatic crystallisation ages obtained for Carboniferous granitic rocks on BATHURST (Pogson and Watkins, 1998) and DUBBO (Meakin and Morgan, 1999) some 200–300 km to the north-northwest.

The remaining sample is a fine-grained aegirine-bearing syenite from the informally-named 'Mount Gibraltar microsyenite' (GSNSW 8928LMC0366, GA 1985437), obtained within the township of Bowral on southern BURRAGORANG. It yielded very few zircons, and all of those analysed yielded pre-300 Ma dates. These are far older than the K-Ar date of ~178 Ma obtained by Evernden and Richards (1962), and they also exceed the maximum possible age of the microsyenite, dictated by the Triassic depositional age of the host Wianamatta Group sedimentary rocks of the Sydney Basin. Consequently, all of the analysed zircons are interpreted to be of inherited origin.

BOOROWA

The single sample from the southern edge of BOOROWA is the Rye Park Granite (GSNSW WRP-046, GA 1989773), a leucocratic medium-grained granite that hosts tungsten mineralisation, and is part of the Hovells Suite. The Rye Park Granite yielded a magmatic crystallisation age of 431.4 ± 4.9 Ma, which is indistinguishable from that of the 430 ± 6 Ma Bigga Granite (Wilde, 2001), also within the Hovells Suite. Both ages are also indistinguishable from those of the S-type Burrawinda Suite (427.8 ± 2.7 Ma Mulgowrie Granodiorite and 427.9 ± 3.0 Ma Winduella Tonalite) and the I-type Gunning Suite (428.6 ± 2.4 Ma Gunning Granite and 429.2 ± 2.3 Ma Cumberoona Tonalite) obtained by Bodorkos and Simpson (2008). These results establish the temporal equivalence of the Hovells, Burrawinda and Gunning Suites in west-central GOULBURN (Johnston *et al.*, 2001, 2004, in press; Thomas *et al.*, 2001).

Introduction

This Record contains new zircon U-Pb geochronological data obtained via Sensitive High-Resolution Ion Micro Probe (SHRIMP) from 14 samples of volcanic and plutonic igneous rocks of the eastern Lachlan Orogen and the Sydney Basin, New South Wales. These data were obtained during the reporting period July 2008–June 2009, under the auspices of the collaborative Geochronology Project between the Geological Survey of New South Wales (GSNSW) and Geoscience Australia (GA), which is part of the National Geoscience Accord.

The samples selected for analysis were obtained from four separate 1:100 000 map sheet areas (Figure 1):

- six from BRAIDWOOD (northeastern CANBERRA),
- six from MOSS VALE and one from BURRAGORANG (southwestern and northwestern WOLLONGONG respectively), and
- one from BOOROWA (northwestern GOULBURN).

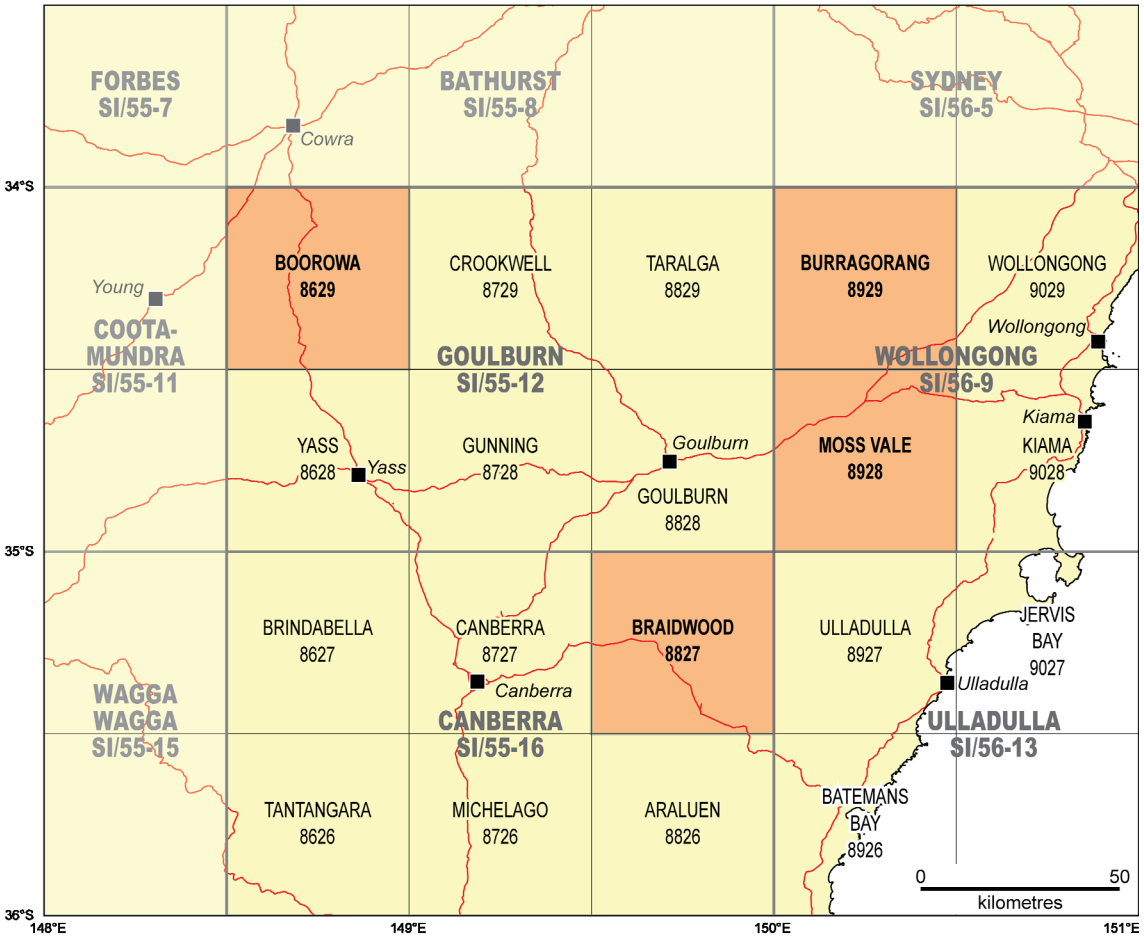

Figure 1. *Index map of southeastern NSW, derived from the Eastern Lachlan Orogen Geoscience Database (Glen et al., 2006) showing the 1:100 000 sheet areas from which samples were analysed. Grey text and lines denote the names and boundaries of 1:250 000 map sheet areas.*

The six BRAIDWOOD samples complement eight results previously reported by Bodorkos and Simpson (2008) for this map sheet (Figure 2), and provide additional support for second-edition remapping of the sheet by Fitzherbert *et al.* (in press), updating the first-edition map and explanatory notes by Felton and Huleatt (1976).

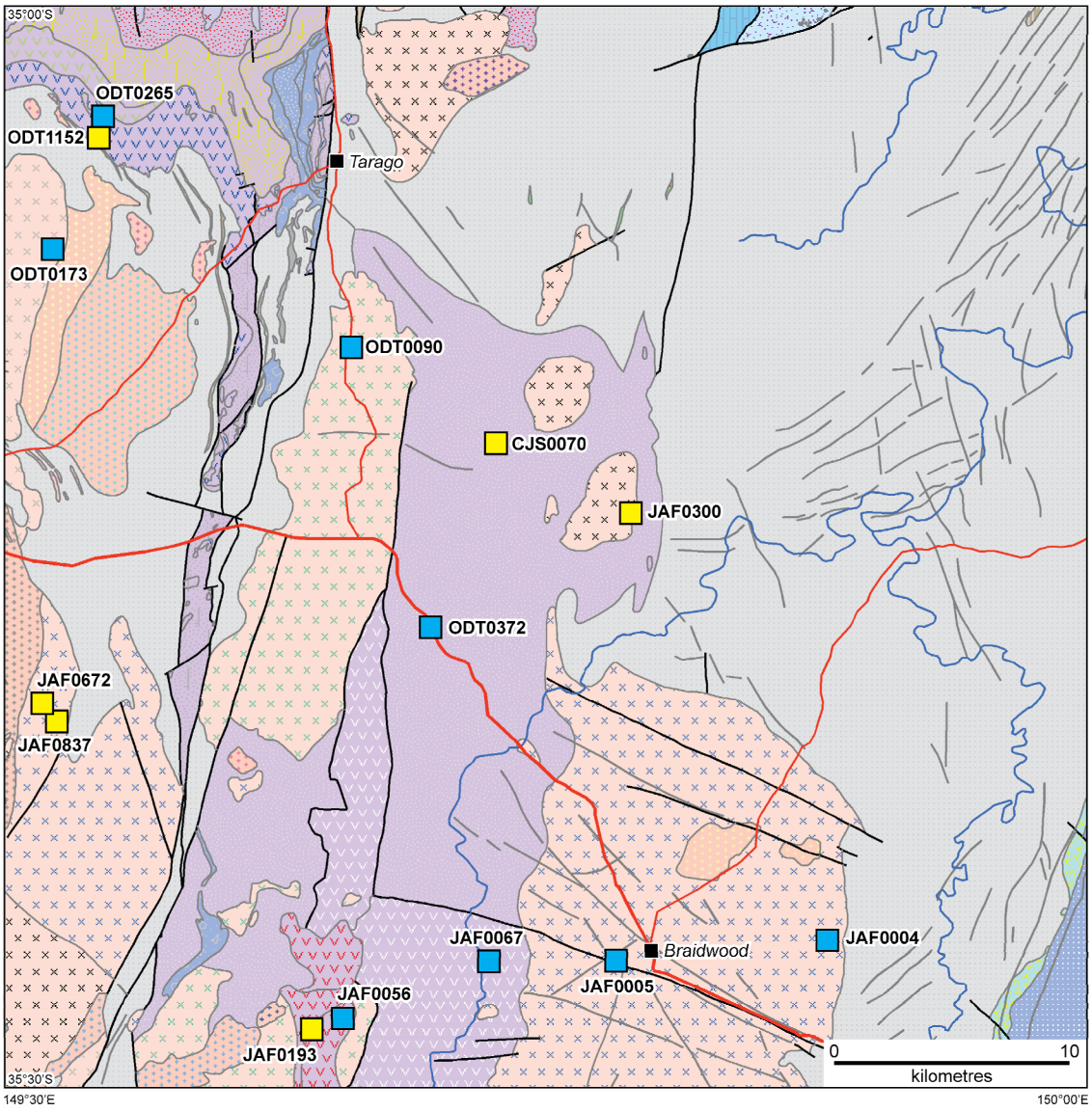

Figure 2. *Braidwood 1:100 000 sheet area, showing the locations of analysed samples documented in this Record (yellow squares) and those documented by Bodorkos and Simpson (2008; blue squares). Sites are labelled with GSNSW SiteIDs, minus the common prefix '8827'. Background is basement geology ('formation/pluton' level) derived from Glen et al. (2006).*

Similarly, the seven samples from MOSS VALE and BURRAGORANG were analysed in support of ongoing mapping of MOSS VALE by Trigg and Campbell (in prep.), with particular respect to its southern and western regions where basement rocks of the eastern Lachlan Orogen are exposed (Figure 3). This map (Trigg and Campbell, in prep.) will revise, update and extend the special 1:100 000 Southern Coalfields geological map (Moffitt, 1999), which focused specifically on the

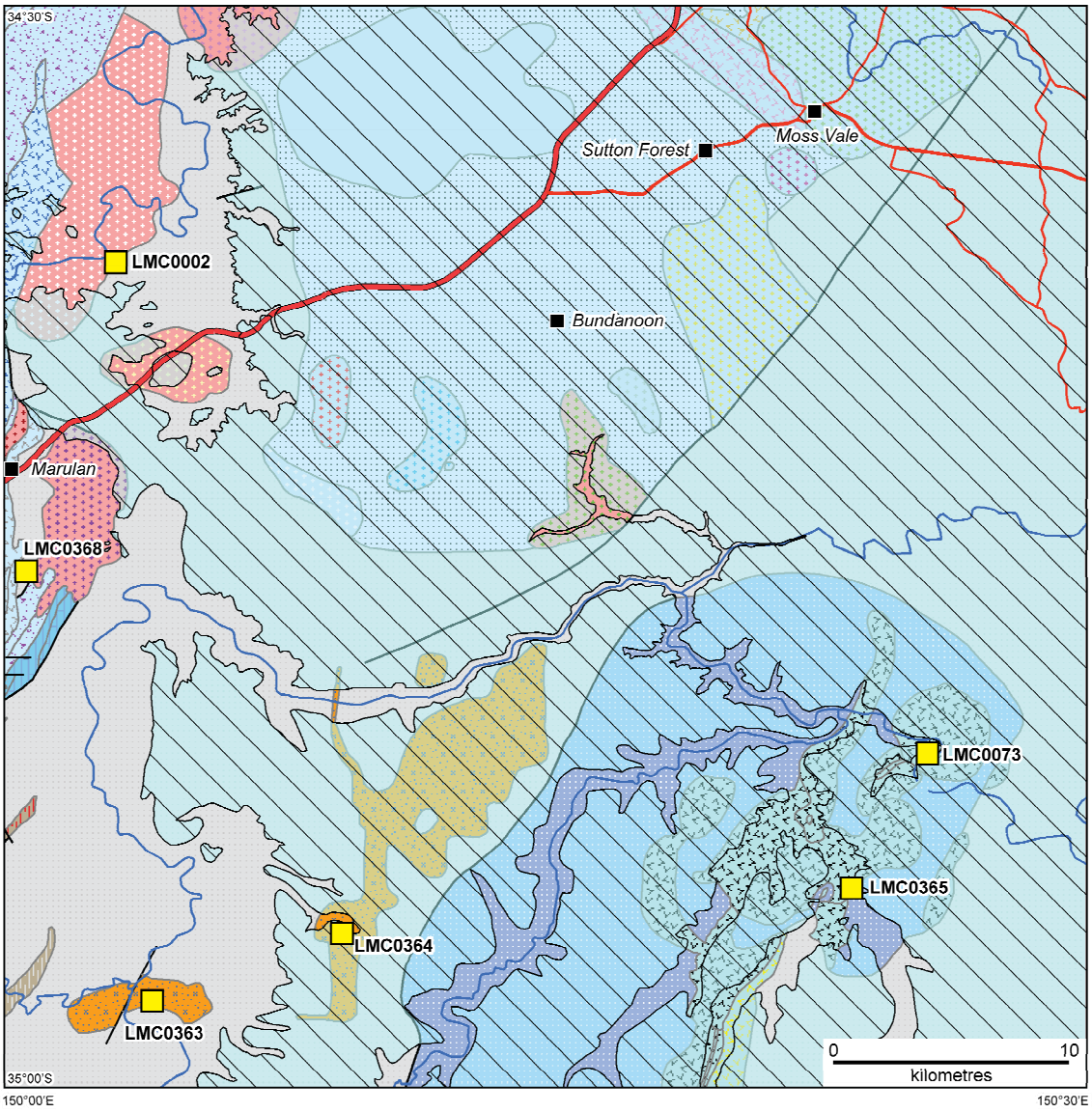

Figure 3. *Moss Vale 1:100 000 sheet area, showing the locations of analysed samples documented in this Record (yellow squares). Sites are labelled with GSNSW SiteIDs, minus the common prefix '8928'. Background is basement geology ('formation/pluton' level) derived from Glen et al. (2006). Diagonal stipple and pale blue colour denotes the extent of Sydney Basin cover, rendered partially transparent in order to highlight the interpreted basement geology.*

Sydney Basin, and also the second-edition geological map of WOLLONGONG (Rose, 1966). The U-Pb SHRIMP zircon geochronology program documented herein is integrated with existing determinations on neighbouring GOULBURN to the west (Wilde, 2002; Black, 2005, 2006).

The remaining sample, from BOOROWA, was chosen to test intrusive relationships between granite suites inferred by Johnston *et al.* (2001, 2004, in press) and Thomas *et al.* (2001) in the west-central GOULBURN region, and complements existing U-Pb SHRIMP zircon data obtained by Wilde (2001) and Bodorkos and Simpson (2008).

This Record describes the analysed samples, presents a summary of the data obtained from them, and briefly discusses their geochronological interpretation. The broader geological implications of the data will be published elsewhere. The complete analytical data files are stored in the Geoscience Australia geochronology database OZCHRON (www.ga.gov.au).

ACKNOWLEDGEMENTS

This SHRIMP zircon U-Pb analytical program was conducted using high quality zircon separates, mounts, photographs and cathodoluminescence images professionally and skilfully prepared by Chris Foudoulis, Steve Ridgway, Emma Chisholm and David DiBugnara of Geoscience Australia's Mineral Separation Laboratory. Patrick Burke, Keith Sircombe and Les Sullivan provided valuable technical support and assistance in optimising analytical conditions during data acquisition. Narelle Neumann and Andrew Cross (Geoscience Australia) provided formal reviews of this Record.

Analytical Procedures

SAMPLE PROCESSING

The locations of field sites were determined using hand-held GPS units with accuracies of about 50 metres, and are referred to the Geocentric Datum of Australia 1994 (GDA94). Co-ordinates are reported as decimal latitude and longitude, and as Map Grid of Australia eastings and northings (MGA94; Zones 55 and 56 as appropriate). Site locations are labelled using the relevant identifiers in each of the corporate databases: SITES SiteID for GSNSW, and FIELDSITES SampleNo for GA.

Sampling involved the splitting of boulders via sledgehammer to access fresh rock, followed by fragmentation of the sample into fist-sized fragments at the field site in order to remove weathering rinds and minimize the risk of contamination. Most samples weighed 10–30 kg. In the Mineral Separation Laboratory at Geoscience Australia, each sample was pulverised (to 2–5 cm pieces) using a pre-cleaned hydraulic splitter, ultrasonically washed in water, and dried under heat lamps. Samples were then crushed using a Rocklabs Boyd crusher, and milled using a Rocklabs continuous ring mill.

Mineral-density separation was undertaken using a Wilfley table, with multiple iterations employed in order to reduce the sample to about 1–2% of its post-milling weight. Strongly paramagnetic grains were successively removed from this heavy fraction using a ferrous magnet and a rare-earth element magnet, before the remainder underwent a series of magnetic separations using a Frantz isodynamic separator. This typically involved 8–10 separations in total, with adjustments (firstly to the magnet current, and secondly to the horizontal tilt of the ramp) aimed at the sequential removal of minerals with progressively weaker paramagnetism. Where available, 200–300 zircon crystals were hand-picked for each sample, commencing with grains in the least magnetic fraction, and progressing to successively more magnetic fractions in samples with low zircon yield. For all of the samples reported herein, the primary geochronological focus is the determination of a magmatic crystallisation age, so zircon selection during hand-picking was biased towards the least magnetic, clearest crystals, but without any discrimination based on the external morphologies of the grains.

Hand-picked mineral separates were mounted in epoxy (with three to five samples per mount), together with about 100 grains of the $^{238}U/^{206}Pb$ reference zircon Temora-2 (Black *et al.*, 2004), about 40 grains of the $^{207}Pb/^{206}Pb$ reference zircon OG1 (Stern *et al.*, 2009), and a fragment of the uranium concentration standard zircon SL13 (Claouè-Long *et al.*, 1995). Each mount was polished to expose longitudinal sections of the grains, photographed in transmitted light and reflected light, and coated with a thin film of carbon, prior to cathodoluminescence (CL) imaging using the JEOL JSM-6490LV scanning electron microscope (SEM), located within the SHRIMP Laboratory at Geoscience Australia.

The carbon coats were then removed using ethanol, and the mounts were ultrasonically cleaned using petroleum spirit and a 10% Extran solution, and triple-rinsed in quartz-distilled water. Mounts were dried overnight in an oven at 30 °C, coated with 15 nm of high-purity (99.999%) gold, and loaded into the high-vacuum sample lock of the SHRIMP at least 24 hours prior to commencement of the analytical session, to ensure that outgassing of the newly-cured epoxy was complete, prior to lowering mounts into the source chamber of the SHRIMP for analysis.

ZIRCON DATA ACQUISITION AND REDUCTION

SHRIMP analyses were undertaken on the SHRIMP-IIe instrument housed in the SHRIMP Laboratory at Geoscience Australia, using procedures developed and documented by Compston *et al.* (1984), Williams and Claesson (1987), Nelson (1997), and Williams (1998).

A 20–30 μm-diameter primary beam of O_2^- ions at 10 keV, purified by means of a Wein filter to minimise the presence of OH^- species, was employed to sputter secondary ions from the surface of the target zircons. The total ion current measured at the mount surface was typically between 1.5 and 4.0 nA. Secondary ions were accelerated to 10 keV, energy-filtered by passage through a double-focusing cylindrical 85° electrostatic analyser with a turning radius of 1.27 m, and mass-filtered using a 72.5° magnet sector with a turning radius of 1 m. Before each analysis, the surface of the analysis site was pre-cleaned by rastering of the primary beam for 3–5 minutes, in order to reduce the amount of common Pb on the mount surface. Ion currents of the relevant secondary species were then determined by switching the magnetic field to direct the secondary ion beam into an electron multiplier. Data acquisition involved cycling the magnetic field six times per analysis through a run-table comprising the following ten nominal mass-stations and counting times: $^{196}Zr_2O$ (2 s), ^{204}Pb (20 s), background 204.1 (20 s), ^{206}Pb (15 s), ^{207}Pb (40 s, except for session 90093, which used 30 s), ^{208}Pb (5 s), ^{238}U (5 s), ^{248}ThO (2 s), ^{254}UO (2 s), and $^{270}UO_2$ (2 s). Session-specific analytical conditions are detailed in the next section.

Analyses were collected in 'round-robin' fashion, with the analytical sequence comprising one measurement from each sample on the mount, in turn. In general, one measurement of a Temora-2 reference zircon was made after every third or fourth sample analysis, and one measurement of an OG1 reference zircon was made after every second or third Temora-2 analysis.

In this Record, labels for individual SHRIMP analyses (as shown in Tables 2–15) take the form X.Y.Z, where X is the 'grain number' (usually assigned sequentially within a sample, at the time of analysis), Y is the 'spot number' within grain X (used to distinguish between spots at different locations within the same grain), and Z is the 'replicate number' within spot Y (used to distinguish between multiple analyses at the same location in the same grain). Nowhere in this Record have multiple analyses been made at the same location in the same grain, so Z is 1 for all analyses.

Data reduction used SQUID 1.13b (October 2005 revision of Ludwig, 2002) and Isoplot 3.70 (April 2008 revision of Ludwig, 2003), with $^{238}U/^{206}Pb$ ratios calibrated using the Temora-2 reference zircon ($^{238}U/^{206}Pb$ age = 416.8 Ma; Black *et al.*, 2004), $^{207}Pb/^{206}Pb$ ratios monitored using the OG1 reference zircon ($^{207}Pb/^{206}Pb$ age = 3465.4 Ma; Stern *et al.*, 2009), and U concentrations calibrated using the SL13 reference zircon (238 ppm U; Claouè-Long *et al.*, 1995). The usage of decay constants followed the recommendations of Steiger and Jäger (1977).

Sample data were calibrated to the $^{238}U/^{206}Pb$ reference zircon using a power-law relationship (Claouè-Long *et al.*, 1995) of the form:

$$[^{206}Pb^+/^{238}U^+] = A \times [(^{238}U^{16}O)^+/^{238}U^+]^B \quad [1]$$

where A and B are session-dependent constants. The canonical value of B is 2.0, but its session-specific apparent value was determined independently (via calculation of the slope of the robust regression of $\ln[^{206}Pb^+/^{238}U^+]$ against $\ln[(^{238}U^{16}O)^+/^{238}U^+]$) in order to inform the decision regarding the most applicable calibration for the session. Session-specific details of this procedure are included in the next section.

After pre-cleaning of the analysis site via rastering of the primary beam, the isotopic composition of common Pb in the calibration standards was assumed to be of geological origin, so default common-Pb corrections for Temora-2 analyses were based on the isotopic composition calculated using the single-stage Pb isotopic evolution model of Stacey and Kramers (1975) at 416.8 Ma (i.e. $^{206}Pb/^{204}Pb$ = 18.053; $^{207}Pb/^{206}Pb$ = 0.864; $^{208}Pb/^{206}Pb$ = 2.097) in conjunction with measured ^{204}Pb. Common-Pb

corrections for samples were based on measured ^{204}Pb and an isotopic composition calculated using the Pb isotopic evolution model of Stacey and Kramers (1975), and a time corresponding to a preliminary $^{238}U/^{206}Pb$ age calculated using the default common-Pb compositions. The result of this calculation is expressed in Tables 2–15 as common ^{206}Pb as a percentage of total measured ^{206}Pb. All isotopic ratios and dates cited in the Tables and text are corrected for common Pb.

Dates derived from the pooling of multiple individual analyses are error-weighted means unless otherwise specified, and the uncertainties of weighted means and robust means (Tukey's biweight mean: Hoaglin *et al.*, 1983) are quoted at the 95% confidence level unless otherwise indicated. Medians are quoted with non-parametric uncertainties associated with medians are also quoted at a confidence level of about 95% (Rock *et al.*, 1987). All algorithms were utilised via the implementation of Ludwig (2003).

Discordance is a measure of the internal agreement of the dates derived from the independent $^{207}Pb/^{206}Pb$ and $^{238}U/^{206}Pb$ isotopic systems within a single analysis. In zircons of Mesoproterozoic and older age, discordance values for single analyses (and discordance patterns within a population of analyses) can provide important information about the timing and extent of radiogenic Pb loss (see Sircombe *et al.* (2007) for a more detailed discussion), and are usually a valuable indicator of 'geological' data quality. The comparison is less useful in SHRIMP analyses of post-1000 Ma zircons, because the poor counting statistics associated with $^{207}Pb/^{206}Pb$ determinations in these young grains usually result in uncertainties large enough to obscure the 'true' agreement or otherwise of the two isotopic systems. Nevertheless, the comparison has been performed throughout this Record, using the equation:

$$\text{Disc. (\%)} = 100 \times [(^{207}Pb/^{206}Pb \text{ date}) - (^{238}U/^{206}Pb \text{ date})] / (^{238}U/^{206}Pb \text{ date}) \quad [2]$$

The analysis-specific results of Equation [2] are reported in Tables 2–15.

SESSION-SPECIFIC CALIBRATIONS AND DATA REDUCTION

The data reported herein were obtained over the course of four separate analytical sessions, each with its own calibration characteristics and data reduction parameters (Table 1). Each session is described separately below.

Session 90021: Mount GA6078, 4–9 March 2009

This session encompassed the analysis of five samples:

- GSNSW 8827JAF0837 (GA 1974958): Lockhart Igneous Complex ('leucogranite phase')
- GSNSW 8827JAF0672 (GA 1974959): Lockhart Igneous Complex ('tonalite phase')
- GSNSW 8827ODT1152 (GA 1974960): Woodlawn Volcanics
- GSNSW 8827JAF0300 (GA 1974961): Braidwood Granodiorite ('northern phase')
- GSNSW 8827JAF0193 (GA 1949548): Long Flat Volcanics: Kain Porphyry Member

A total of 53 analyses of the $^{238}U/^{206}Pb$ reference zircon Temora-2 were obtained during session 90021, but one analysis defined a gross outlier relative to the rest of the data. That analysis was adversely affected by instrumental instability, and is excluded from further consideration.

The remaining 52 analyses display little dispersion in $\ln[(^{238}U^{16}O)^+/^{238}U^+]$ (Figure 4), so the slope of the array is not well defined (1.90 ± 0.33), nor is it significantly different to 2.0. Consequently, the canonical value of 2.0 was adopted as the calibration exponent B (Equation [1]). All 52 analyses comprise a well-defined calibration (Figure 5): the weighted mean $^{238}U/^{206}Pb$ value has an internal

Table 1. Summary of session-specific metadata, parameters obtained from analyses of $^{238}U/^{206}Pb$ and $^{207}Pb/^{206}Pb$ reference zircons, and samples analysed.

SESSION NUMBER:	90021	90064	90068	90093
Mount:	GA6078	GA6094	GA6095	GA6101
Session date:	4–9 Mar 2009	7–10 Jul 2009	22–24 Jul 2009	3–5 Oct 2009
Calibration batch no:	1 of 1	1 of 1	1 of 1	1 of 1
$^{238}U/^{206}Pb$ reference zircon: Temora-2 (416.8 ± 1.3 Ma; Black et al., 2004)				
Analyses used:	52 of 53	31 of 31	26 of 26	41 of 42
$^{238}U/^{206}Pb$ uncertainty (2σ):	0.38%	0.52%	0.82%	0.38%
$^{238}U/^{206}Pb$ reproducibility (2σ):	2.17%	2.40%	3.64%	1.61%
$^{207}Pb/^{206}Pb$ date (95% confidence):	397 ± 23 Ma	381 ± 31 Ma	389 ± 33 Ma	397 ± 33 Ma
^{204}Pb overcount correction applied:	No	No	No	No
$^{207}Pb/^{206}Pb$ reference zircon: OG1 (3465.4 ± 0.6 Ma; Stern et al., 2009)				
Analyses used:	24 of 24	15 of 15	14 of 14	No analyses
$^{207}Pb/^{206}Pb$ date (95% confidence):	3467.2 ± 1.8 Ma	3467.5 ± 2.2 Ma	3469.4 ± 2.6 Ma	—
Mass fractionation correction factor:	—	—	1.00254	—
Uncertainty in correction factor (2σ):	—	—	0.17%	—
Mass fractionation correction applied:	No	No	No	—
Number of samples analysed:	5	4	2	3
GSNSW SiteID (GA SampleNo):	8827JAF0837 (1974958)	8928LMC0363 (1985433)	8928LMC0073 (1985436)	8928LMC0002 (1985440)
	8827JAF0672 (1974959)	8928LMC0365 (1985435)	WRP-046 (1989773)	8928LMC0368 (1985439)
	8827ODT1152 (1974960)	8928LMC0364 (1985434)		8827CJS0070 (1989476)
	8827JAF0300 (1974961)	8928LMC0366 (1985437)		
	8827JAF0193 (1949548)			

uncertainty of 0.38% (2σ), and $^{238}U/^{206}Pb$ reproducibility is 2.17% (2σ). The former value is included in the uncertainty of each weighted mean $^{238}U/^{206}Pb$ date calculated from this session; the latter value is included (at the 1σ level) in the uncertainty associated with $^{238}U/^{206}Pb$ for each individual analysis in this session.

The possibility of overcounts at mass ^{204}Pb was monitored by reference to the robust mean of the 52 $^{207}Pb/^{206}Pb$ dates determined for Temora-2 (397 ± 23 Ma). This result does not differ significantly from its reference value (416.8 ± 1.3 Ma; Black *et al.*, 2004) at the 95% confidence level, and ^{204}Pb overcounts based on measured ^{207}Pb and measured ^{208}Pb both yielded robust mean values indistinguishable from zero (+0.013 ± 0.014 and +0.008 ± 0.018 counts per second, respectively), so no correction was necessary.

In addition, a total of 24 analyses of the $^{207}Pb/^{206}Pb$ reference zircon OG1 were obtained during session 90021 (Figure 6). The weighted mean of all 24 $^{207}Pb/^{206}Pb$ dates is 3467.2 ± 1.8 Ma (MSWD = 0.81), and this result is indistinguishable from the OG1 reference value (3465.4 ± 0.6 Ma; Stern *et al.*, 2009), so no correction for instrumental fractionation of $^{207}Pb/^{206}Pb$ was applied.

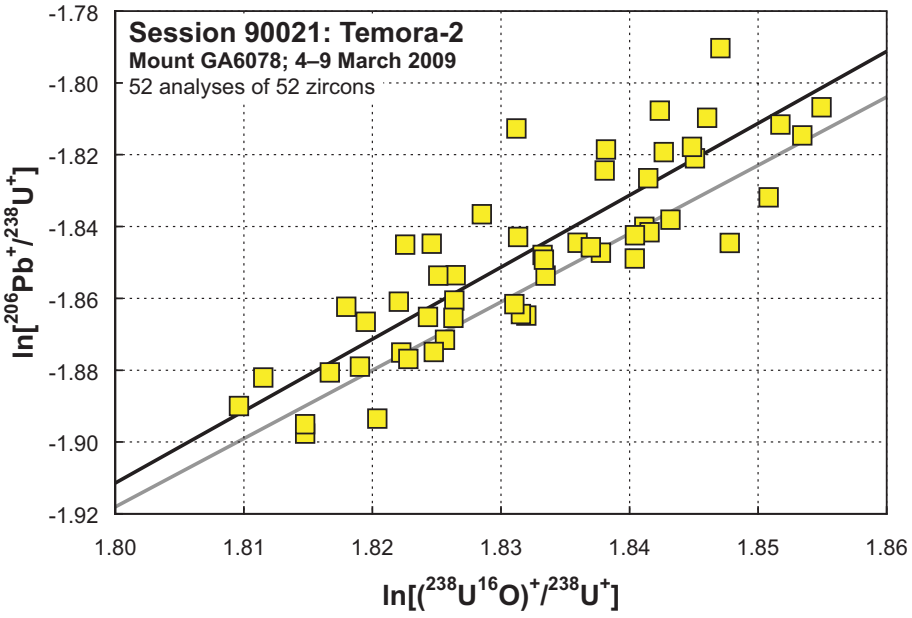

Figure 4. *Robust regressions of $ln[^{206}Pb^{+}/^{238}U^{+}]$ against $ln[(^{238}U^{16}O)^{+}/^{238}U^{+}]$ for Temora-2 data obtained during session 90021. Heavy black line: regression with slope 2.0; heavy grey line: regression fitted to all measurements (slope = 1.90 ± 0.33). The former was used for the calibration. Yellow fill: analyses used in the determination of $^{238}U/^{206}Pb$ uncertainty and reproducibility (Figure 5).*

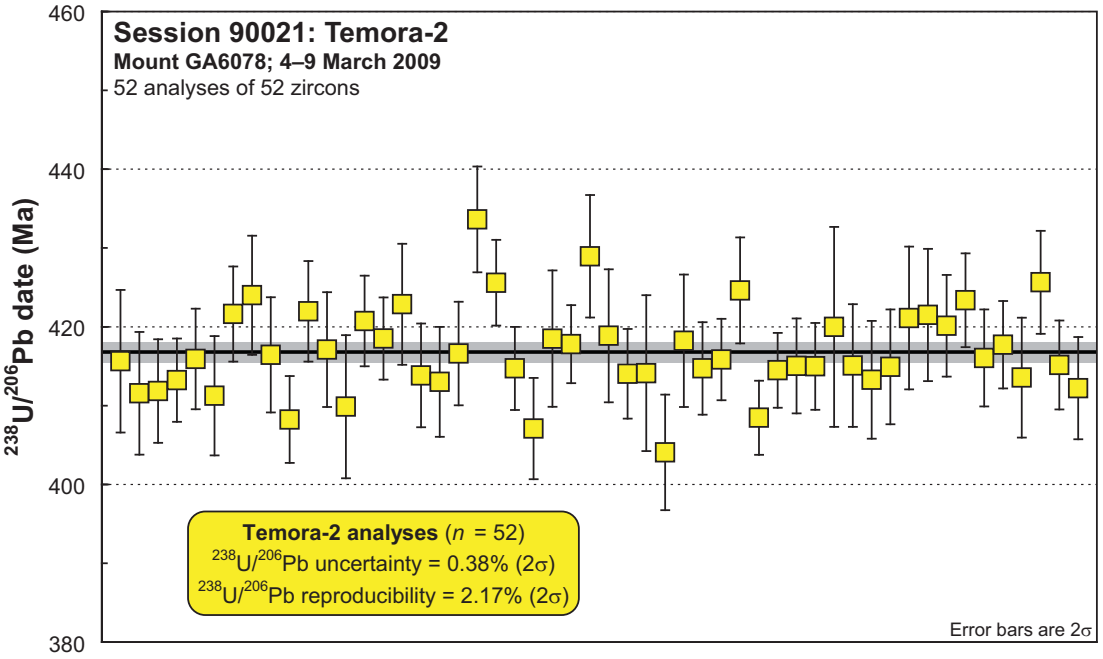

Figure 5. *SHRIMP $^{238}U/^{206}Pb$ dates on Temora-2 during session 90021, in order of acquisition. Yellow fill: analyses used in the determination of $^{238}U/^{206}Pb$ uncertainty and reproducibility. Heavy black line and grey band: reference $^{238}U/^{206}Pb$ age and its 2σ uncertainty, respectively.*

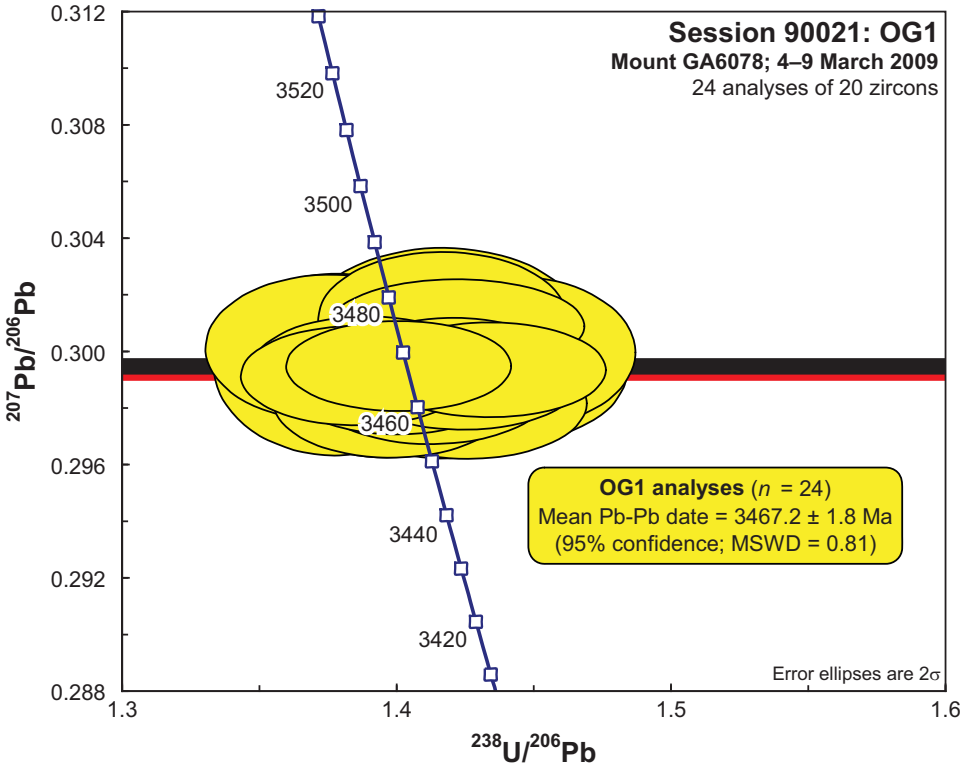

Figure 6. *SHRIMP U-Pb analyses of OG1 during session 90021, on a Tera-Wasserburg concordia diagram. Yellow fill: analyses used in the weighted mean $^{207}Pb/^{206}Pb$ date. Black band: 95% confidence envelope of weighted mean $^{207}Pb/^{206}Pb$ value measured this session (0.29941 ± 0.00035); red band: 2σ envelope of reference $^{207}Pb/^{206}Pb$ value (0.29907 ± 0.00011; Stern et al., 2009).*

Session 90064: Mount GA6094, 7–10 July 2009

This session encompassed the analysis of four samples:

- GSNSW 8928LMC0363 (GA 1985433): Touga Granite
- GSNSW 8928LMC0365 (GA 1985435): Bundundah Granite
- GSNSW 8928LMC0364 (GA 1985434): Tullyangela Granite
- GSNSW 8928LMC0366 (GA 1985437): 'Mount Gibraltar microsyenite'

A total of 31 analyses of the $^{238}U/^{206}Pb$ reference zircon Temora-2 were obtained during session 90064, and display little dispersion in $\ln[(^{238}U^{16}O)^+/^{238}U^+]$ (Figure 7), so the slope of the array is not well defined (2.16 +0.45/-0.32), nor is it significantly different to 2.0. Consequently, the canonical value of 2.0 was adopted as the calibration exponent B (Equation [1]). All 31 analyses comprise a well-defined calibration (Figure 8): the weighted mean $^{238}U/^{206}Pb$ value has an internal uncertainty of 0.52% (2σ), and $^{238}U/^{206}Pb$ reproducibility is 2.40% (2σ). The former value is included in the uncertainty of each weighted mean $^{238}U/^{206}Pb$ date calculated from this session; the latter value is included (at the 1σ level) in the uncertainty associated with $^{238}U/^{206}Pb$ for each individual analysis in this session.

The possibility of overcounts at mass ^{204}Pb was monitored by reference to the robust mean of the 31 $^{207}Pb/^{206}Pb$ dates determined for Temora-2 (381 ± 31 Ma). This result was slightly younger than its reference value (416.8 ± 1.3 Ma; Black *et al.*, 2004) at the 95% confidence level, and raised the possibility that ^{204}Pb was distinguishably 'overcounted' during the session. This idea was supported

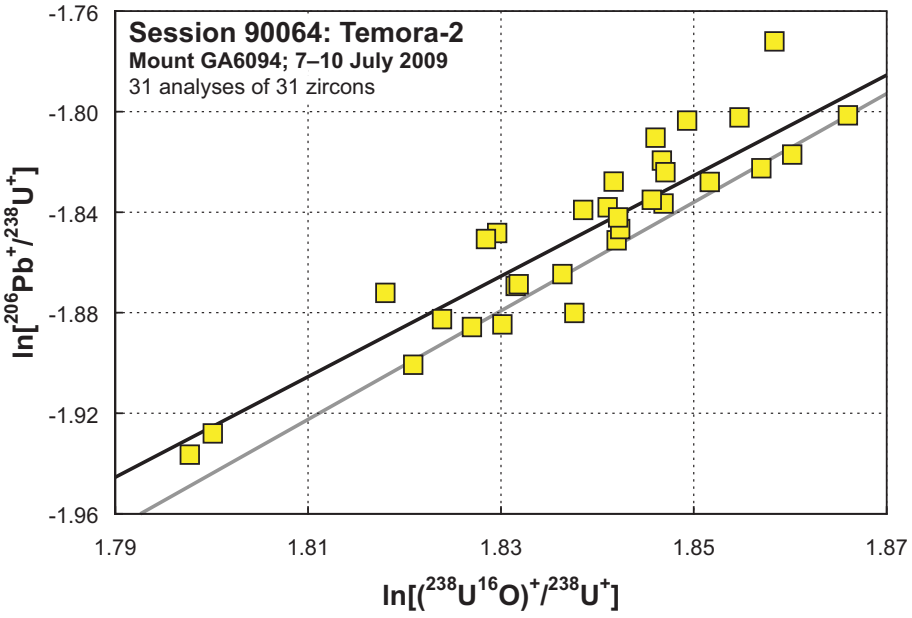

Figure 7. *Robust regressions of $ln[^{206}Pb^{+}/^{238}U^{+}]$ against $ln[(^{238}U^{16}O)^{+}/^{238}U^{+}]$ for Temora-2 data obtained during session 90064. Heavy black line: regression with slope 2.0; heavy grey line: regression fitted to all measurements (slope = 2.16 +0.45/-0.32). The former was used for the calibration. Yellow fill: analyses used in the determination of $^{238}U/^{206}Pb$ uncertainty and reproducibility (Figure 8).*

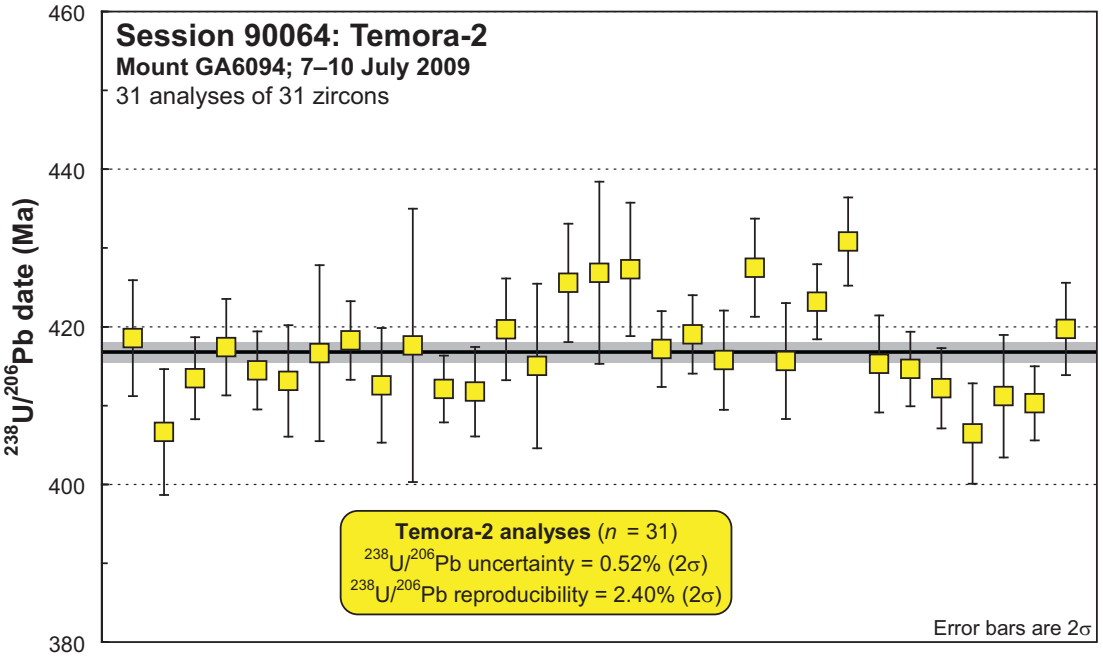

Figure 8. *SHRIMP $^{238}U/^{206}Pb$ dates on Temora-2 during session 90064, in order of acquisition. Yellow fill: analyses used in the determination of $^{238}U/^{206}Pb$ uncertainty and reproducibility. Heavy black line and grey band: reference $^{238}U/^{206}Pb$ age and its 2σ uncertainty, respectively.*

by estimated ^{204}Pb overcounts based on measured ^{207}Pb (+0.028 ± 0.024 counts per second), but not those based on measured ^{208}Pb (+0.014 ± 0.028 counts per second). In the absence of unequivocal evidence for overcounting at mass ^{204}Pb, no correction was applied.

In addition, a total of 15 analyses of the ^{207}Pb/^{206}Pb reference zircon OG1 were obtained during session 90064 (Figure 9). The weighted mean of all 15 ^{207}Pb/^{206}Pb dates is 3467.5 ± 2.2 Ma (MSWD = 0.64), and this result is indistinguishable from the OG1 reference value (3465.4 ± 0.6 Ma; Stern *et al.*, 2009), so no correction for instrumental fractionation of ^{207}Pb/^{206}Pb was applied.

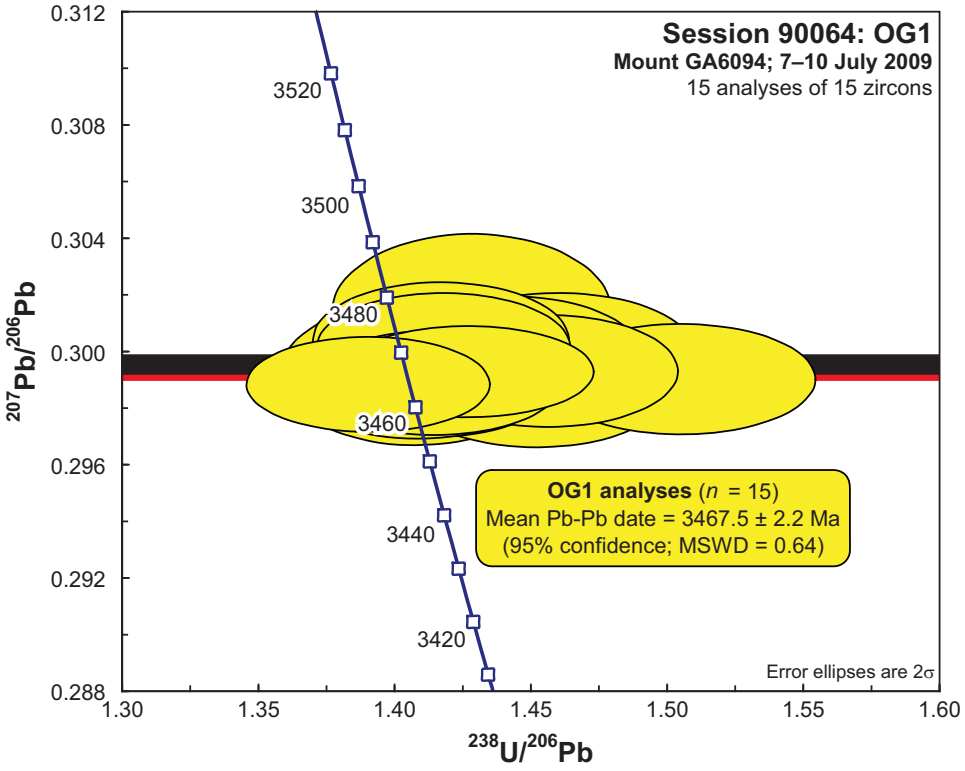

Figure 9. *SHRIMP U-Pb analyses of OG1 during session 90064, on a Tera-Wasserburg concordia diagram. Yellow fill: analyses used in the weighted mean ^{207}Pb/^{206}Pb date. Black band: 95% confidence envelope of weighted mean ^{207}Pb/^{206}Pb value measured this session (0.29948 ± 0.00042); red band: 2σ envelope of reference ^{207}Pb/^{206}Pb value (0.29907 ± 0.00011; Stern et al., 2009).*

Session 90068: Mount GA6095, 22–24 July 2009

This session encompassed the analysis of two samples:

- GSNSW 8928LMC0073 (GA 1985436): Yalwal Volcanics: Grassy Gully Rhyolite Member
- GSNSW WRP-046 (GA 1989773): Rye Park Granite

A total of 26 analyses of the ^{238}U/^{206}Pb reference zircon Temora-2 were obtained during session 90068, and display little dispersion in ln[(^{238}U^{16}O)$^{+}$/^{238}U^{+}] (Figure 10), so the slope of the array is not well defined (2.46 +0.70/-0.57), nor is it significantly different to 2.0. Consequently, the canonical value of 2.0 was adopted as the calibration exponent B (Equation [1]). All 26 analyses comprise a single calibration, albeit with moderate scatter in ^{238}U/^{206}Pb (Figure 11): the weighted mean ^{238}U/^{206}Pb value has an internal uncertainty of 0.82% (2σ), and ^{238}U/^{206}Pb reproducibility is 3.64% (2σ). The former value is included in the uncertainty of each weighted mean ^{238}U/^{206}Pb date

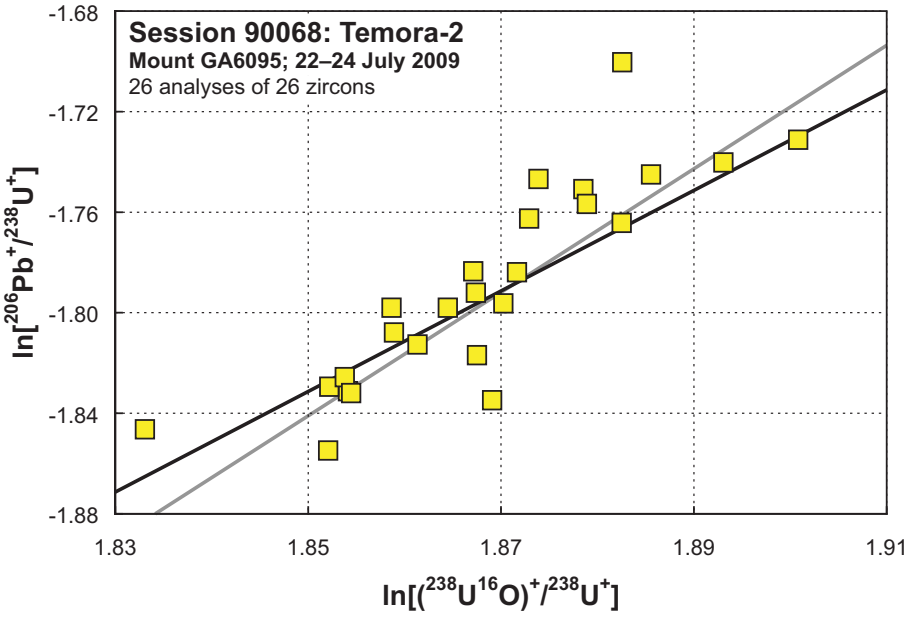

Figure 10. *Robust regressions of $ln[^{206}Pb^{+}/^{238}U^{+}]$ against $ln[(^{238}U^{16}O)^{+}/^{238}U^{+}]$ for Temora-2 data obtained during session 90068. Heavy black line: regression with slope 2.0; heavy grey line: regression fitted to all measurements (slope = 2.46 +0.70/-0.57). The former was used for the calibration. Yellow fill: analyses used in the determination of $^{238}U/^{206}Pb$ uncertainty and reproducibility (Figure 11).*

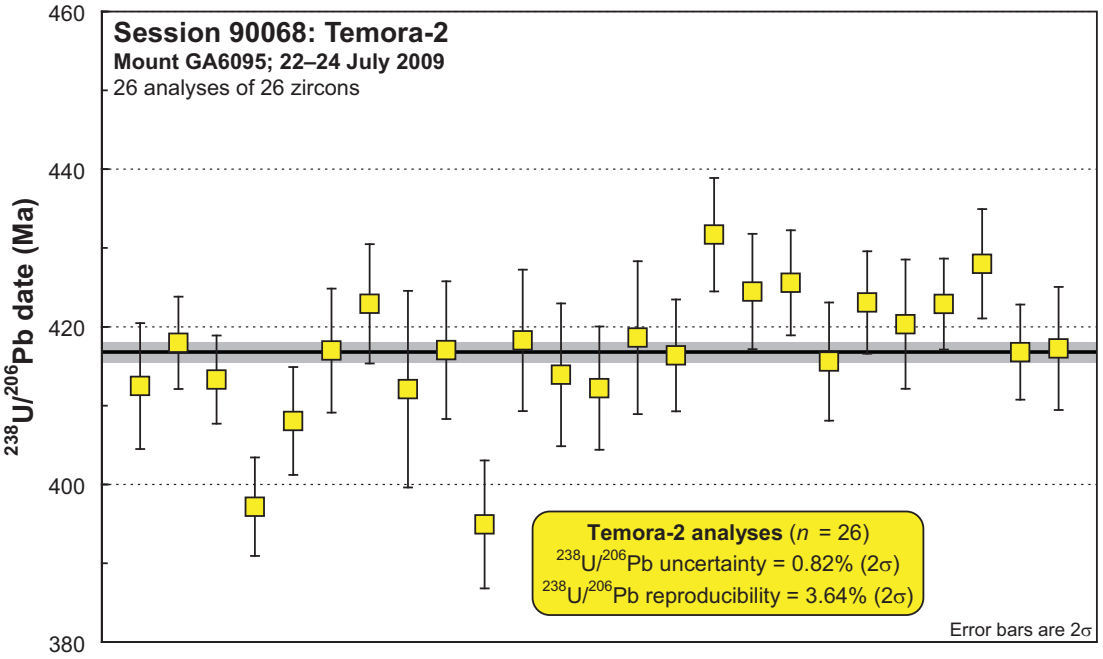

Figure 11. *SHRIMP U-Pb analyses of Temora-2 during session 90068, in order of acquisition. Yellow fill: analyses used in the determination of $^{238}U/^{206}Pb$ uncertainty and reproducibility. Heavy black line and grey band: reference $^{238}U/^{206}Pb$ age and its 2σ uncertainty, respectively.*

calculated from this session; the latter value is included (at the 1σ level) in the uncertainty associated with $^{238}U/^{206}Pb$ for each individual analysis in this session.

The possibility of overcounts at mass ^{204}Pb was monitored by reference to the robust mean of the 31 $^{207}Pb/^{206}Pb$ dates determined for Temora-2 (389 ± 33 Ma). This result does not differ significantly from its reference value (416.8 ± 1.3 Ma; Black *et al.*, 2004) at the 95% confidence level, and ^{204}Pb overcounts based on measured ^{207}Pb and measured ^{208}Pb both yielded robust mean values indistinguishable from zero (+0.012 ± 0.016 and +0.011 ± 0.021 counts per second, respectively), so no correction was necessary.

In addition, a total of 14 analyses of the $^{207}Pb/^{206}Pb$ reference zircon OG1 were obtained during session 90068 (Figure 12). The weighted mean of all 14 $^{207}Pb/^{206}Pb$ dates is 3469.4 ± 2.6 Ma (MSWD = 0.51), which is distinguishably older than the OG1 reference value (3465.4 ± 0.6 Ma; Stern *et al.*, 2009). The correction factor α defined by Stern *et al.* (2009), by which the measured $^{207}Pb/^{206}Pb$ should be divided, is 1.00254, and the associated uncertainty (which should be added in quadrature to the uncertainty of any weighted mean $^{207}Pb/^{206}Pb$ value calculated) is 0.17% (2σ). Note, however, that these corrections have not been applied to the $^{207}Pb/^{206}Pb$ data presented in Tables 11 and 15, because the magnitude of both the correction and its uncertainty are insignificant at the scale of individual analyses, and no weighted mean $^{207}Pb/^{206}Pb$ dates have been calculated from these data.

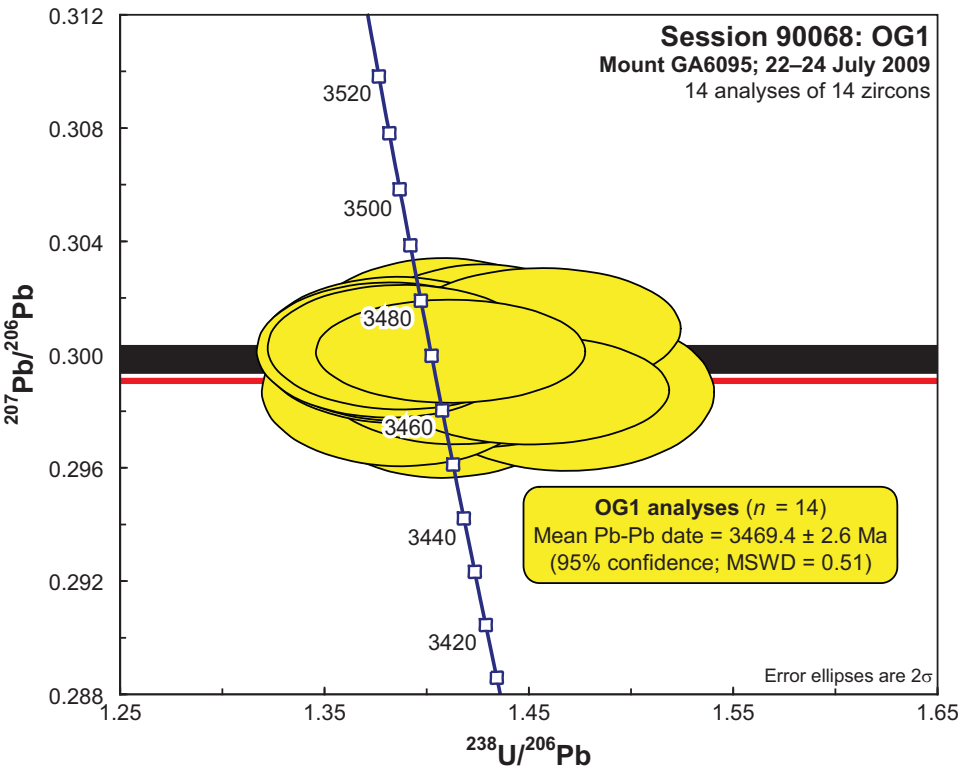

Figure 12. *SHRIMP U-Pb analyses of OG1 during session 90068, on a Tera-Wasserburg concordia diagram. Yellow fill: analyses used in the weighted mean $^{207}Pb/^{206}Pb$ date. Black band: 95% confidence envelope of weighted mean $^{207}Pb/^{206}Pb$ value measured this session (0.29983 ± 0.00051); red band: 2σ envelope of reference $^{207}Pb/^{206}Pb$ value (0.29907 ± 0.00011; Stern et al., 2009).*

Session 90093: Mount GA6101, 3–5 October 2009

This session encompassed the analysis of three samples:

- GSNSW 8928LMC0002 (GA 1985440): Pleasant Hill Granite
- GSNSW 8928LMC0368 (GA 1985439): Tangerang Formation: Kerillon Tuff Member
- GSNSW 8827CJS0070 (GA 1989476): Long Flat Volcanics: Croppies Gunyah Rhyolite Member

This session followed an attempt (session 90070, mount GA6095; 24–27 July 2009) to analyse these samples, which failed due to localised but irreparable damage to the mount surface. Data from session 90070 are not reported in this Record. Mount GA6101 contains a new aliquot of zircons from each sample: however, in order to maintain unique identifiers for SHRIMP analyses, consistency was retained between analysis labels assigned during the successful session and those assigned during the original, failed session. As a consequence, the grain numbers of all of the analyses in Tables 7, 12 and 13 is 32 or greater.

A total of 42 analyses of the $^{238}U/^{206}Pb$ reference zircon Temora-2 were obtained during session 90093, but one analysis defined a gross outlier relative to the rest of the data. That analysis was adversely affected by instrumental instability, and is excluded from further consideration.

The remaining 41 analyses display little dispersion in $\ln[(^{238}U^{16}O)^+/^{238}U^+]$ (Figure 13), so the slope of the array is not well defined (1.68 +0.33/-0.36), nor is it significantly different to 2.0. Consequently, the canonical value of 2.0 was adopted as the calibration exponent B (Equation [1]). All 41 analyses comprise a well-defined calibration (Figure 14): the weighted mean $^{238}U/^{206}Pb$ value has an internal uncertainty of 0.38% (2σ), and $^{238}U/^{206}Pb$ reproducibility is 1.61% (2σ). The former value is included in the uncertainty of each weighted mean $^{238}U/^{206}Pb$ date calculated from this session; the latter value is included (at the 1σ level) in the uncertainty associated with $^{238}U/^{206}Pb$ for each individual analysis in this session.

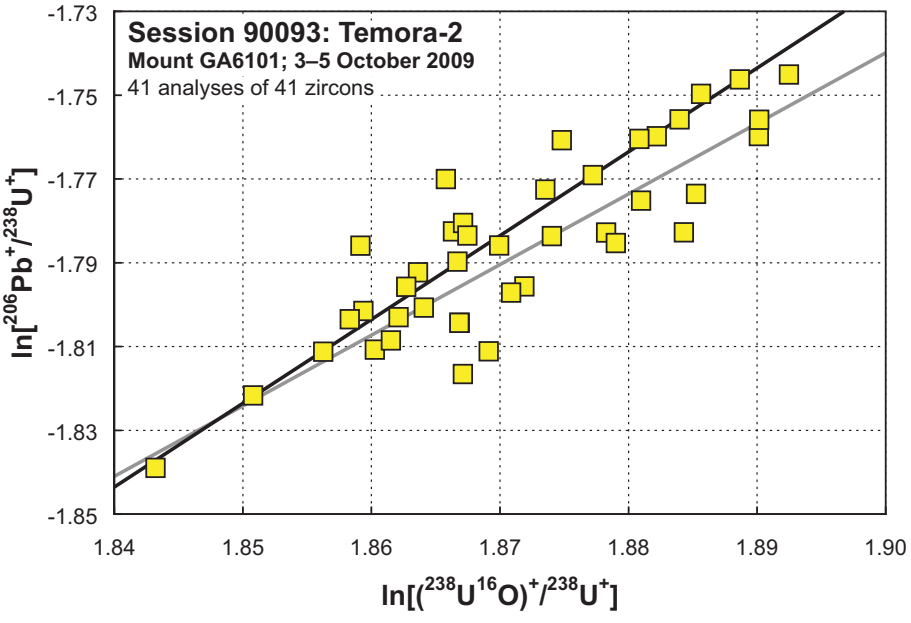

Figure 13. *Robust regressions of $\ln[^{206}Pb^+/^{238}U^+]$ against $\ln[(^{238}U^{16}O)^+/^{238}U^+]$ for Temora-2 data obtained during session 90093. Heavy black line: regression with slope 2.0; heavy grey line: regression fitted to all measurements (slope = 1.68 +0.33/-0.36). The former was used for the calibration. Yellow fill: analyses used in the determination of $^{238}U/^{206}Pb$ uncertainty and reproducibility (Figure 14).*

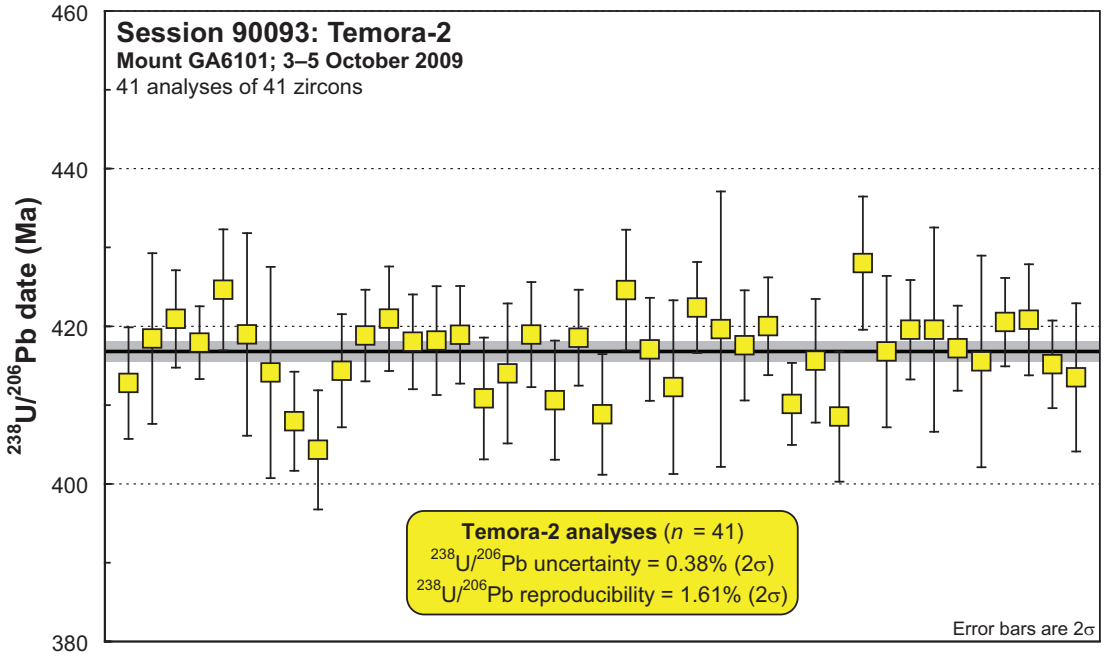

Figure 14. *SHRIMP $^{238}U/^{206}Pb$ dates on Temora-2 during session 90093, in order of acquisition. Yellow fill: analyses used in the determination of $^{238}U/^{206}Pb$ uncertainty and reproducibility. Heavy black line and grey band: reference $^{238}U/^{206}Pb$ age and its 2σ uncertainty, respectively.*

The possibility of overcounts at mass ^{204}Pb was monitored by reference to the robust mean of the 41 $^{207}Pb/^{206}Pb$ dates determined for Temora-2 (397 ± 33 Ma). This result does not differ significantly from its reference value (416.8 ± 1.3 Ma; Black *et al.*, 2004) at the 95% confidence level, and ^{204}Pb overcounts based on measured ^{207}Pb and measured ^{208}Pb both yielded robust mean values indistinguishable from zero (+0.013 ± 0.019 and -0.002 ± 0.023 counts per second, respectively), so no correction was necessary.

The $^{207}Pb/^{206}Pb$ reference zircon OG1 was not included in mount GA6101, so $^{207}Pb/^{206}Pb$ was not monitored during session 90093.

Braidwood 1:100 000 sheet area

THURRALILLY SUITE: LOCKHART IGNEOUS COMPLEX ('LEUCOGRANITE PHASE')

GA SAMPLENO:	**1974958**
GSNSW SITEID:	**8827JAF0837**
PARENT UNIT(S):	Thurralilly Suite
FORMAL NAME:	Lockhart Igneous Complex
INFORMAL NAME:	'leucogranite phase'
LITHOLOGY:	Weakly-deformed porphyritic leucocratic granite
PROVINCE:	Eastern Lachlan Orogen
1:250 000 SHEET:	CANBERRA (SI/55-16)
1:100 000 SHEET:	BRAIDWOOD (8827)
LOCATION (GDA94):	35.330519 °S, 149.524154 °E
LOCATION (MGA94):	Zone 55, 729428 mE, 6087379 mN
ANALYTICAL SESSION NO(S):	90021 (see Table 1 for parameters derived from concurrent measurements of $^{238}U/^{206}Pb$ and $^{207}Pb/^{206}Pb$ reference zircons)
INTERPRETED AGE:	**424.4 ± 3.2 Ma** (95% confidence; 26 analyses of 26 zircons)
GEOLOGICAL ATTRIBUTION:	Magmatic crystallisation
ISOTOPIC RATIO(S) USED:	$^{238}U/^{206}Pb$ (^{204}Pb-corrected)

Sampling Details

This sample was taken from some low slabs and boulders on the southern verge of Ingledow Road, about 500 m northwest of Ingledow homestead.

Relationships and Rationale for Dating

The unit sampled is a medium-grained and weakly deformed porphyritic leucocratic granite within the Lockhart Igneous Complex (Felton and Huleatt, 1976), which is part of the Thurralilly Suite in the eastern Lachlan Orogen (Fitzherbert *et al.*, in press). The Lockhart Igneous Complex intrudes Ordovician turbiditic sedimentary rocks of the Adaminaby Group, and comprises plutonic rocks ranging from olivine-bearing gabbro to leucogranite, which display a variety of magma mixing and mingling relationships (Fitzherbert *et al.*, in press).

This sample was selected for SHRIMP analysis in order to test the hypothesis that plutons of the Lockhart Igneous Complex are lower-crustal equivalents of, and therefore broadly contemporaneous with, the Ellenden Granite (423.4 ± 3.3 Ma; Bodorkos and Simpson, 2008) and the Woodlawn Volcanics, which have previously yielded SHRIMP zircon $^{238}U/^{206}Pb$ ages of 423.4 ± 2.5 Ma (Black, 2005) and 419.2 ± 3.2 Ma (Bodorkos and Simpson, 2008).

The aim was to obtain a magmatic crystallisation age for this homogeneous leucogranite phase of the Lockhart Igneous Complex, for comparison with a nearby foliated tonalite phase (GSNSW 8827JAF0672, GA 1974959; this volume), and new data constraining magmatic crystallisation of the Woodlawn Volcanics (GSNSW 8827ODT1152, GA 1974960; this volume).

Petrography

This sample is a medium- to coarse-grained, weakly deformed porphyritic leucocratic granite. Coarse-grained (3–5 mm) phases comprise about 30% of the rock, and are composed of 10% quartz, 15% plagioclase, 5% K-feldspar, and minor clusters and stringers of biotite and muscovite (Figure 15). These are set in an even-grained (0.03–0.05 mm) mosaic of recrystallised quartz and feldspar, with minor development of fine-grained granophyric texture evident near the margins of some larger crystals. Primary quartz was probably coarse-grained and embayed, but now occurs as deformed lenses up to 5 mm in length, oriented parallel to the tectonic foliation (Figure 15). These lenses feature extensive subgrain development, and partial recrystallisation into fine-grained polygonal aggregates. Plagioclase forms euhedral to subhedral and mainly undeformed crystals of predominantly andesine composition ($An_{29–36}$) that are up to 3.5 mm long, as well as aggregates of smaller crystals. K-feldspar is perthitic and occurs as undeformed, subhedral grains up to 3 mm in length. Biotite (which is fine-grained, greenish and partly replaced by chlorite) is associated with fine-grained muscovite, forming small, discontinuous aggregates that define the foliation. Accessory minerals include euhedral zircon, and fine-grained opaque oxide minerals commonly featuring narrow rims of fine-grained titanite.

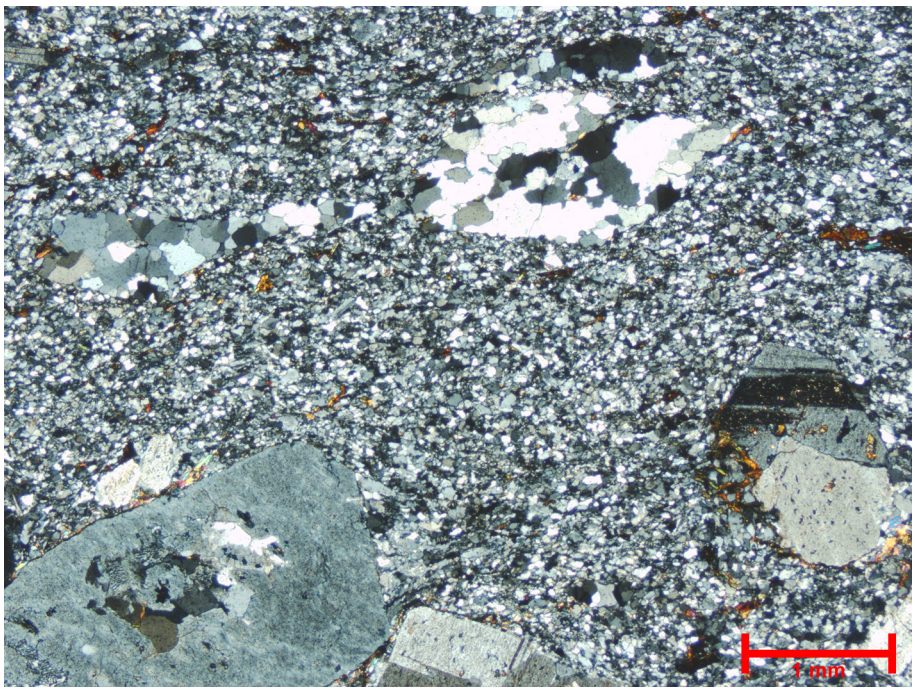

Figure 15: *Representative photomicrograph (in cross-polarised light) of the 'leucogranite phase' of the Lockhart Igneous Complex (GSNSW 8827JAF0837, GA 1974958). Its weakly deformed, porphyritic texture contains large crystals of aligned recrystallised quartz (top centre), plagioclase (lower right) and K-feldspar (lower left) within a recrystallised mosaic of quartz and feldspar. Mica trails define the foliation.*

Zircon Description

Zircons from this sample range from euhedral to anhedral, with external morphologies ranging from rounded and anhedral grains, through euhedral prisms with pyramidal terminations, to elongate crystals. Aspect ratios (length/width) are 1–5 and vary widely, and long axes are 50–270 µm (Figure 16). In transmitted light, two main zircon types are evident. The dominant population is euhedral to subhedral, mostly transparent and colourless to pale pink or pale yellow, and often hosts abundant

inclusions of dark-coloured minerals. The subordinate population is mostly subhedral to anhedral or rounded, translucent rather than transparent, and hosts few inclusions.

Cathodoluminescence (CL) images reveal characteristic emission patterns for each of the populations identified in transmitted light. Euhedral zircons are characterised by moderate to high CL emission, and predominantly high-contrast concentric oscillatory zoning parallel to the crystal faces, or broad banding parallel to the long axes. These zoning patterns are typical of magmatic zircon. The subhedral to anhedral grains show a wide range of CL emission intensities and zoning patterns. Some crystals feature oscillatory zoning truncated by the grain margin, or disconformable contacts where cores are overgrown by rim zircon with uniform CL emission (Figure 16). The heterogeneity of this population is consistent with an inherited origin.

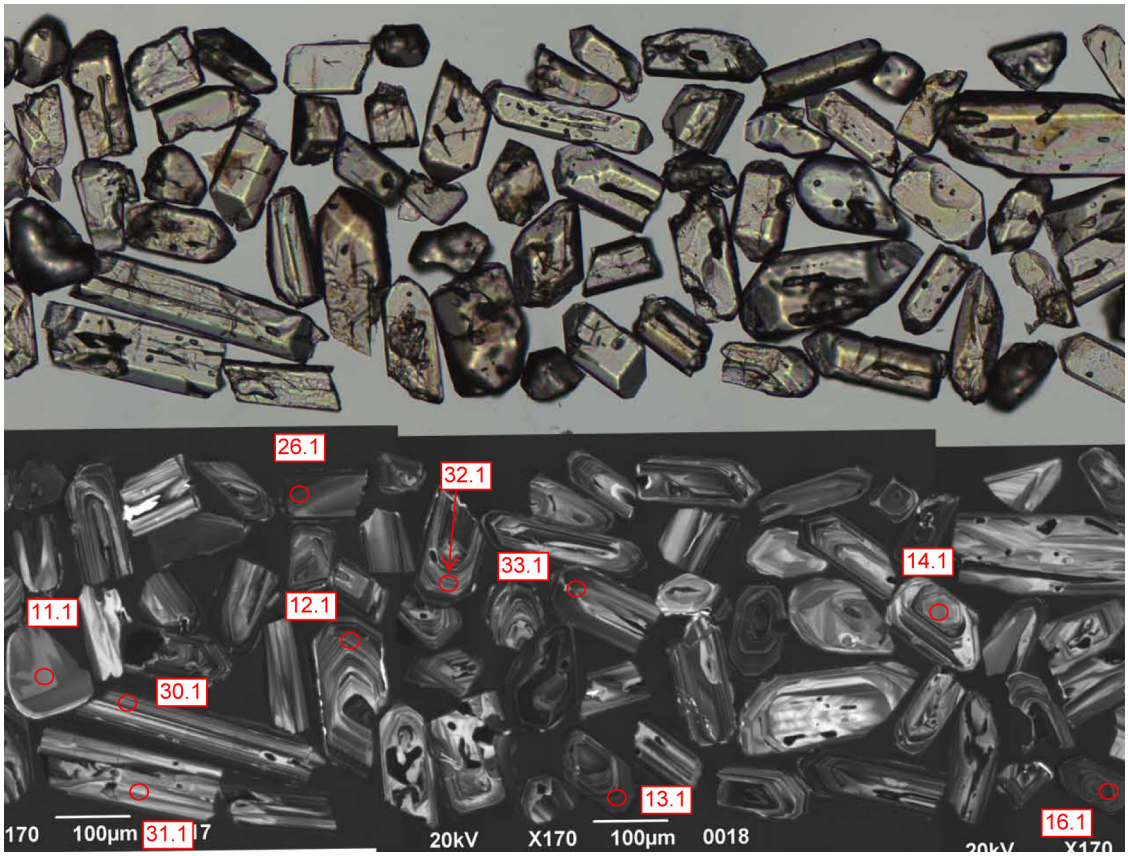

Figure 16: *Representative zircons from the 'leucogranite phase' of the Lockhart Igneous Complex (GSNSW 8827JAF0837, GA 1974958). Transmitted-light image is shown in the upper half; cathodoluminescence image in the lower half. SHRIMP analysis sites are indicated, and labelled with grain and spot number.*

U-Pb Isotopic Results

Forty-one analyses were obtained from 41 individual zircons, and the results are presented in Figure 17 and Table 2. The analysed zircons are characterised by low to moderate U contents, with some exceptions (57–1058 ppm, median 195 ppm), and varied Th/U (0.26–1.31, median 0.77).

One analysis (8.1.1; green fill in Figure 17) yielded a spuriously low common Pb content ($^{206}Pb_c$ < -1%), and is interpreted as being inaccurately corrected for common Pb. Consequently, its $^{238}U/^{206}Pb$ date is unreliable, and this analysis is not considered further.

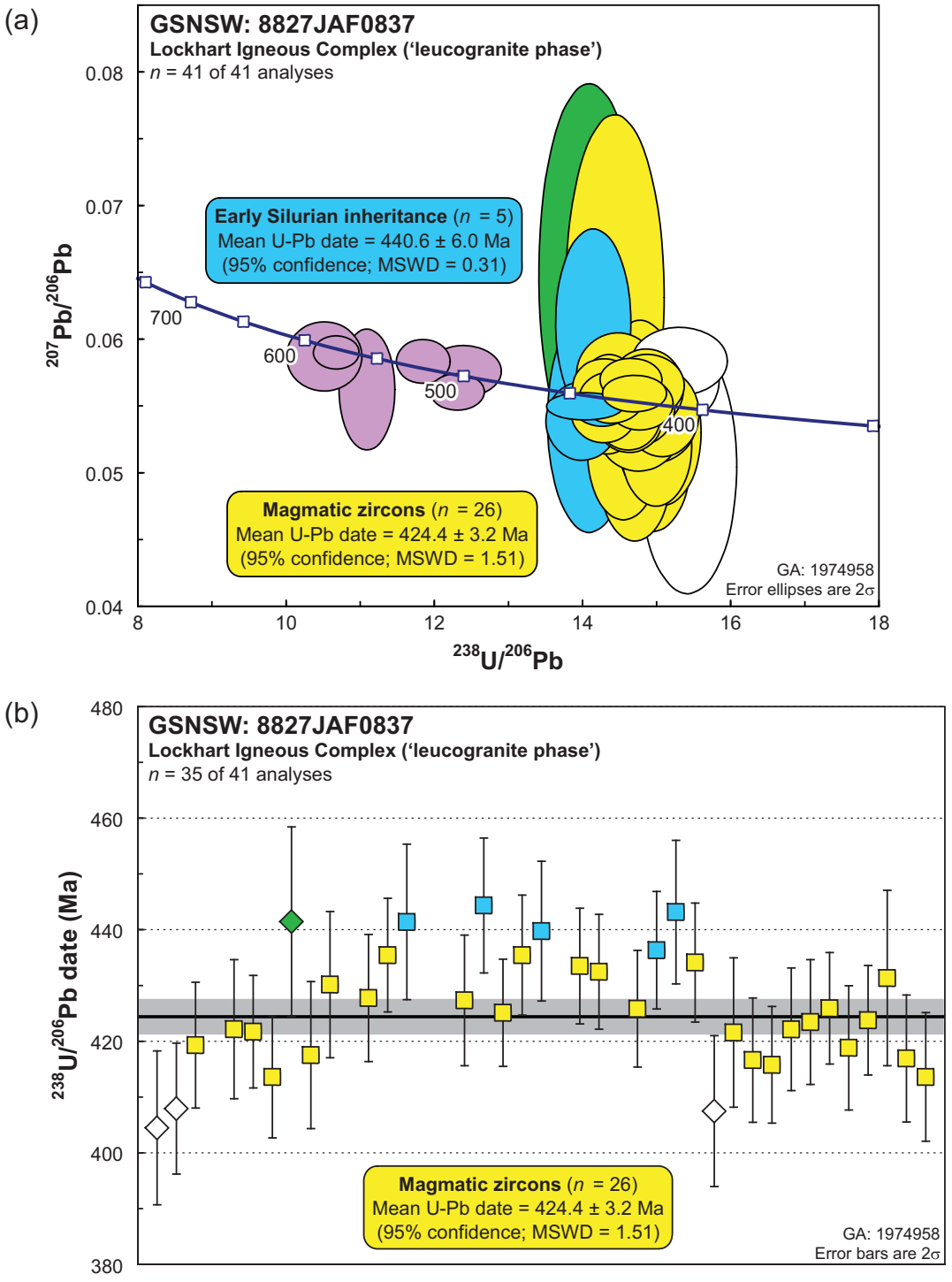

Figure 17: *SHRIMP U-Pb data for zircons from the 'leucogranite phase' of the Lockhart Igneous Complex (GSNSW 8827JAF0837, GA 1974958). (a) Tera-Wasserburg concordia diagram; (b) $^{238}U/^{206}Pb$ dates in order of acquisition (six analyses with pre-480 Ma dates are not shown). Yellow fill: magmatic zircons; blue fill: Early Silurian inheritance; pink fill: Neoproterozoic–Cambrian inheritance; white fill: affected by loss of radiogenic Pb; green fill: not considered due to spurious negative $^{206}Pb_c$. Heavy black line and grey band: weighted mean $^{238}U/^{206}Pb$ date and its 95% confidence interval, respectively.*

The remaining 40 analyses have uniformly low $^{206}Pb_c$ (maximum 0.76%, median 0.09%), and can be divided into four groups (Table 2):

- 26 analyses of 26 zircons (Group 1; yellow fill in Figure 17) with individual $^{238}U/^{206}Pb$ dates between c. 435 Ma and c. 414 Ma, which yielded a weighted mean date of 424.4 ± 3.2 Ma (MSWD = 1.51),
- five analyses of five zircons (Group 2; blue fill in Figure 17) with individual $^{238}U/^{206}Pb$ dates between c. 444 Ma and c. 436 Ma, which yielded a weighted mean date of 440.6 ± 6.0 Ma (MSWD = 0.31),
- six analyses of six zircons (Group 3; pink fill in Figure 17) with individual $^{238}U/^{206}Pb$ dates between c. 585 Ma and c. 500 Ma, and
- three analyses of three zircons (Group 4; white fill in Figure 17) with individual $^{238}U/^{206}Pb$ dates between c. 408 Ma and c. 405 Ma.

Geochronological Interpretation

The weighted mean date of 424.4 ± 3.2 Ma obtained from the 26 analyses in Group 1 is indistinguishable from the median $^{238}U/^{206}Pb$ date for the same 26 analyses (423.6 +3.7/-2.0 Ma), and the absence of significant asymmetry in the uncertainties associated with the latter suggests that Group 1 represents a single population of analyses with an approximately normal distribution. Consequently, the weighted mean $^{238}U/^{206}Pb$ date of 424.4 ± 3.2 Ma is interpreted as the best estimate of the age of magmatic crystallisation of the leucogranite phase of the Lockhart Igneous Complex.

The weighted mean $^{238}U/^{206}Pb$ date of 440.6 ± 6.0 Ma obtained from the five analyses in Group 2 is interpreted to reflect inheritance from one or more sources containing Early Silurian zircons. Similarly, the six analyses in Group 3 are interpreted as inherited individuals of Neoproterozoic to Cambrian age. The three analyses in Group 4 are slightly younger than the main magmatic population defined by Group 1, and are interpreted to have been affected by post-crystallisation loss of radiogenic Pb.

The magmatic crystallisation age of 424.4 ± 3.2 Ma for the leucogranite phase of the Lockhart Igneous Complex appears to be indistinguishable (at the 95% confidence level) from that of the nearby tonalite phase (428.5 ± 3.1 Ma, this volume; probability of equivalence = 0.07), and that of the Woodlawn Volcanics to the north (423.3 ± 2.6 Ma, this volume; probability of equivalence = 0.59). However, the fact that these three samples were analysed concurrently within SHRIMP session 90021 (see Introduction) means that the (shared) component of each uncertainty, associated with determining the session-specific mean value of the Temora-2 reference zircon (2σ = 0.38%; Figure 5), can be neglected for the specific purpose of evaluating the equivalence of each pair of magmatic crystallisation ages. Recomparing each pair of weighted mean ages in this fashion establishes that the magmatic crystallisation age of the leucogranite phase of Lockhart Igneous Complex remains indistinguishable from that of the Woodlawn Volcanics (probability of equivalence = 0.43), but is slightly younger than that of the tonalite phase of Lockhart Igneous Complex (probability of equivalence = 0.03) at the 95% confidence level.

In broader comparison with existing SHRIMP zircon $^{238}U/^{206}Pb$ dates, the magmatic crystallisation age of 424.4 ± 3.2 Ma for the leucogranite phase of the Lockhart Igneous Complex is indistinguishable from those of the 423.4 ± 3.3 Ma Ellenden Granite (Bodorkos and Simpson, 2008) and the (423.4 ± 2.5 Ma) Woodlawn Volcanics on southern GOULBURN (Black, 2005), but is slightly older than that of the high-level intrusion within the Woodlawn Volcanics on northwestern BRAIDWOOD (419.2 ± 3.2 Ma; Bodorkos and Simpson, 2008).

Table 2: SHRIMP U-Pb zircon data from the 'leucogranite phase' of the Lockhart Igneous Complex (GSNSW 8827JAF0837, GA 1974958). All dates are $^{238}U/^{206}Pb$ unless otherwise indicated.

Sess. no.	Grain.area .replicate	$^{206}Pb_c$ (%)	U (ppm)	Th (ppm)	$^{232}Th/^{238}U$	$^{238}U/^{206}Pb$	±1σ (%)	$^{207}Pb/^{206}Pb$	±1σ (%)	Date (Ma)	±1σ (Ma)	Disc. (%)
Group 3: Neoproterozoic–Cambrian inherited individuals (n = 6)												
90021	15.1.1	0.07	145	150	1.07	10.532	1.97	0.05880	1.79	584.7	11.0	-4
90021	4.1.1	-0.06	531	133	0.26	10.693	1.17	0.05913	0.85	576.3	6.5	-1
90021	11.1.1	0.38	137	145	1.10	11.104	1.38	0.05637	3.26	555.9	7.3	-16
90021	22.1.1	-0.04	309	336	1.12	11.867	1.24	0.05846	1.15	521.5	6.2	5
90021	25.1.1	0.00	391	220	0.58	12.325	1.20	0.05618	0.98	502.9	5.8	-9
90021	16.1.1	0.10	377	454	1.24	12.409	1.68	0.05772	1.36	499.6	8.1	4
Group 2: Early Silurian inherited component (n = 5)												
90021	18.1.1	0.08	145	53	0.38	14.014	1.41	0.05402	2.20	444.3	6.0	-16
90021	28.1.1	0.04	1057	997	0.97	14.052	1.50	0.05511	0.76	443.2	6.4	-6
90021	14.1.1	0.41	84	99	1.22	14.110	1.63	0.05409	6.31	441.4	7.0	-15
90021	21.1.1	-0.68	128	91	0.74	14.165	1.47	0.06133	4.66	439.7	6.3	48
90021	27.1.1	0.06	308	211	0.71	14.280	1.25	0.05566	1.49	436.3	5.3	1
Group 1: Magmatic zircons (n = 26)												
90021	20.1.1	0.09	257	128	0.51	14.310	1.28	0.05464	1.68	435.4	5.4	-9
90021	13.1.1	-0.16	426	250	0.61	14.310	1.21	0.05653	1.53	435.4	5.1	9
90021	29.1.1	0.22	293	255	0.90	14.355	1.27	0.05472	2.36	434.1	5.3	-8
90021	23.1.1	0.76	352	153	0.45	14.377	1.24	0.05543	2.61	433.5	5.2	-1
90021	24.1.1	0.05	351	190	0.56	14.412	1.23	0.05575	1.39	432.5	5.1	2
90021	39.1.1	-0.76	56	39	0.71	14.451	1.88	0.06322	8.78	431.3	7.9	66
90021	10.1.1	-0.03	85	68	0.82	14.492	1.57	0.05733	2.31	430.2	6.6	17
90021	12.1.1	0.54	212	171	0.83	14.576	1.38	0.05183	4.09	427.8	5.7	-35
90021	17.1.1	0.08	139	146	1.09	14.591	1.42	0.05483	2.22	427.3	5.9	-5
90021	36.1.1	0.17	411	216	0.54	14.641	1.21	0.05433	1.84	425.9	5.0	-10
90021	26.1.1	0.12	343	306	0.92	14.644	1.27	0.05423	1.91	425.8	5.2	-11
90021	19.1.1	-0.14	678	554	0.84	14.670	1.17	0.05707	1.14	425.1	4.8	16
90021	38.1.1	-0.01	446	222	0.51	14.718	1.20	0.05605	0.99	423.8	4.9	7
90021	35.1.1	0.57	177	168	0.98	14.730	1.36	0.05042	4.33	423.4	5.6	-49
90021	5.1.1	0.24	330	189	0.59	14.776	1.52	0.05331	2.31	422.2	6.2	-19
90021	34.1.1	0.09	179	164	0.95	14.776	1.35	0.05506	2.10	422.1	5.5	-2
90021	6.1.1	0.09	325	335	1.07	14.792	1.23	0.05532	1.44	421.7	5.0	1
90021	31.1.1	0.41	77	47	0.63	14.797	1.64	0.05357	6.06	421.6	6.7	-16
90021	3.1.1	-0.18	139	97	0.72	14.880	1.39	0.05645	2.12	419.3	5.6	12
90021	37.1.1	-0.05	146	174	1.23	14.897	1.37	0.05667	1.67	418.8	5.6	14
90021	9.1.1	0.20	293	372	1.31	14.945	1.63	0.05369	2.15	417.5	6.6	-14
90021	40.1.1	0.53	140	103	0.76	14.968	1.41	0.05131	4.37	416.9	5.7	-39
90021	32.1.1	0.40	155	112	0.75	14.979	1.38	0.05307	3.73	416.6	5.6	-20
90021	33.1.1	0.47	230	121	0.55	15.010	1.30	0.05214	3.48	415.8	5.2	-30
90021	41.1.1	0.45	129	63	0.51	15.091	1.44	0.05317	4.15	413.6	5.8	-19
90021	7.1.1	0.16	162	159	1.01	15.092	1.36	0.05461	2.42	413.6	5.5	-4
Group 4: Affected by loss of radiogenic Pb (n = 3)												
90021	2.1.1	-0.07	101	76	0.78	15.309	1.48	0.05699	2.23	407.9	5.9	20
90021	30.1.1	0.00	136	116	0.88	15.326	1.71	0.05846	1.76	407.5	6.8	34
90021	1.1.1	0.68	74	51	0.71	15.443	1.76	0.05061	7.62	404.5	6.9	-45
Not considered, due to spurious negative $^{206}Pb_c$ (< -1%; n = 1)												
90021	8.1.1	-1.05	47	27	0.59	14.109	1.99	0.06492	8.94	441.4	8.5	75

THURRALILLY SUITE: LOCKHART IGNEOUS COMPLEX ('TONALITE PHASE')

GA SAMPLENO:	**1974959**
GSNSW SITEID:	**8827JAF0672**
PARENT UNIT(S):	Thurralilly Suite
FORMAL NAME:	Lockhart Igneous Complex
INFORMAL NAME:	'tonalite phase'
LITHOLOGY:	Medium-grained, strongly-foliated quartz-rich tonalite
PROVINCE:	Eastern Lachlan Orogen
1:250 000 SHEET:	CANBERRA (SI/55-16)
1:100 000 SHEET:	BRAIDWOOD (8827)
LOCATION (GDA94):	35.322158 °S, 149.517482 °E
LOCATION (MGA94):	Zone 55, 728845 mE, 6088322 mN
ANALYTICAL SESSION NO(S):	90021 (see Table 1 for parameters derived from concurrent measurements of $^{238}U/^{206}Pb$ and $^{207}Pb/^{206}Pb$ reference zircons)
INTERPRETED AGE:	**428.5 ± 3.1 Ma** (95% confidence; 22 analyses of 22 zircons)
GEOLOGICAL ATTRIBUTION:	Magmatic crystallisation
ISOTOPIC RATIO(S) USED:	$^{238}U/^{206}Pb$ (^{204}Pb-corrected)

Sampling Details

This sample was taken from an outcrop near, and on the western side of, a north-south trending fenceline on the eastern slope of a prominent hill about 800 m north of Ingledow Road and about 1 km northeast of Lockhart homestead.

Relationships and Rationale for Dating

The unit sampled is a medium-grained and strongly foliated quartz-rich tonalite within the Lockhart Igneous Complex (Felton and Huleatt, 1976), which is part of the Thurralilly Suite in the eastern Lachlan Orogen (Fitzherbert *et al.*, in press). The Lockhart Igneous Complex intrudes Ordovician turbiditic sedimentary rocks of the Adaminaby Group, and comprises plutonic rocks ranging from olivine-bearing gabbro to leucogranite, which display a variety of magma mixing and mingling relationships (Fitzherbert *et al.*, in press).

This sample was selected for SHRIMP analysis in order to test the hypothesis that plutons of the Lockhart Igneous Complex are lower-crustal equivalents of, and therefore broadly contemporaneous with, the 423.4 ± 3.3 Ma Ellenden Granite (Bodorkos and Simpson, 2008) and the Woodlawn Volcanics, which have previously yielded SHRIMP zircon $^{238}U/^{206}Pb$ ages of 423.4 ± 2.5 Ma (Black, 2005) and 419.2 ± 3.2 Ma (Bodorkos and Simpson, 2008).

The aim was to obtain a magmatic crystallisation age for this foliated tonalite phase of the Lockhart Igneous Complex, for comparison with a nearby homogeneous leucogranite phase (GSNSW 8827JAF0837, GA 1974958; this volume), and new data constraining magmatic crystallisation of the Woodlawn Volcanics (GSNSW 8827ODT1152, GA 1974960; this volume).

Petrography

This sample is a fine- to medium-grained, inequigranular quartz-rich tonalite that is strongly foliated but retains a weak, relic porphyritic texture primarily imparted by quartz crystals up to 5 mm in length. The rock comprises 45% quartz, 40% plagioclase, 10% biotite, 5% K-feldspar, and accessory

allanite, opaque oxide minerals, and zircon (Figure 18). Quartz forms large, highly strained crystals elongated parallel to the tectonic foliation, and partly recrystallised around their margins. Quartz also forms finer-grained recrystallised patches between the larger minerals. Plagioclase occurs as euhedral, equant to stubby crystals up to 2.5 mm in length. Biotite is golden-tan in colour, and occurs mainly as small (up to 0.5 mm) decussate crystals within aggregates aligned parallel to the tectonic foliation (Figure 18). K-feldspar forms rare, small and irregular interstitial grains, some of which are rimmed by myrmekite. Biotite and K-feldspar are both intergrown with patches of finer-grained recrystallised quartz. Pale greenish brown, metamict allanite is a conspicuous accessory mineral, along with fine-grained probable magnetite. Plagioclase is commonly partly replaced by granular epidote and muscovite, but the rock is otherwise unaltered.

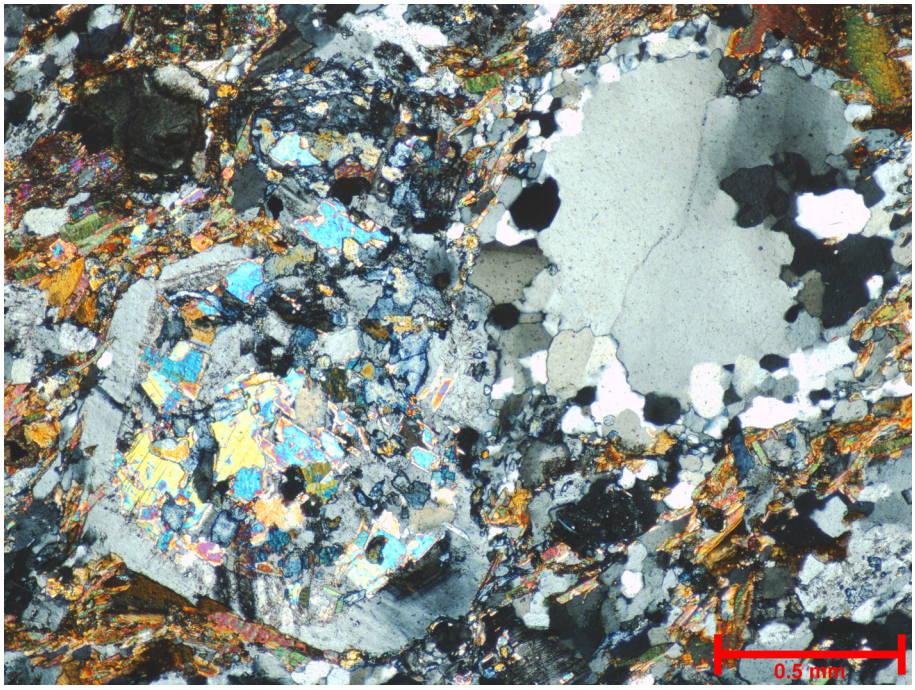

Figure 18: *Representative photomicrograph (in cross-polarised light) of the 'tonalite phase' of the Lockhart Igneous Complex (GSNSW 8827JAF0672, GA 1974959). Tonalite comprises euhedral, epidote- and muscovite-replaced plagioclase (left), partly recrystallised quartz (upper left) and a foliation defined by brown biotite. A small dark crystal of metamict allanite (top left) is also evident.*

Zircon Description

Zircons from this sample range from euhedral to anhedral, with external morphologies ranging from rounded and anhedral grains to euhedral prismatic crystals. Aspect ratios (length/width) are 1–4, and the grains are large, with long axes 100–500 µm (Figure 19). In transmitted light, two main zircon types are evident. The dominant population is euhedral, mostly transparent and colourless to pale pink, and rarely hosts inclusions of any kind. The subordinate population is mostly subhedral to anhedral, pale to medium-brown, and translucent or faintly mottled. Many of these grains host abundant inclusions of dark-coloured minerals, and cracking or pitting are both common.

Cathodoluminescence (CL) images reveal emission patterns that vary widely within each of the populations identified in transmitted light. Euhedral zircons are characterised by moderate to high CL emission, but zoning patterns include broad, low-contrast concentric and sector zoning in high-CL grains, finer oscillatory zoning with moderate contrast parallel to the crystal faces, and rarer

broad banding parallel to the long axes (Figure 19). These zoning patterns are typical of magmatic zircon. The subhedral to anhedral grains show a wide range of CL emission intensities and zoning patterns. Many crystals host a concentrically-zoned core with low to moderate CL emission, which is usually disconformably overgrown by a rim of structureless zircon, although the oscillatory zoning is sometimes truncated by the grain margin directly (Figure 19). The heterogeneity of this population is consistent with an inherited origin.

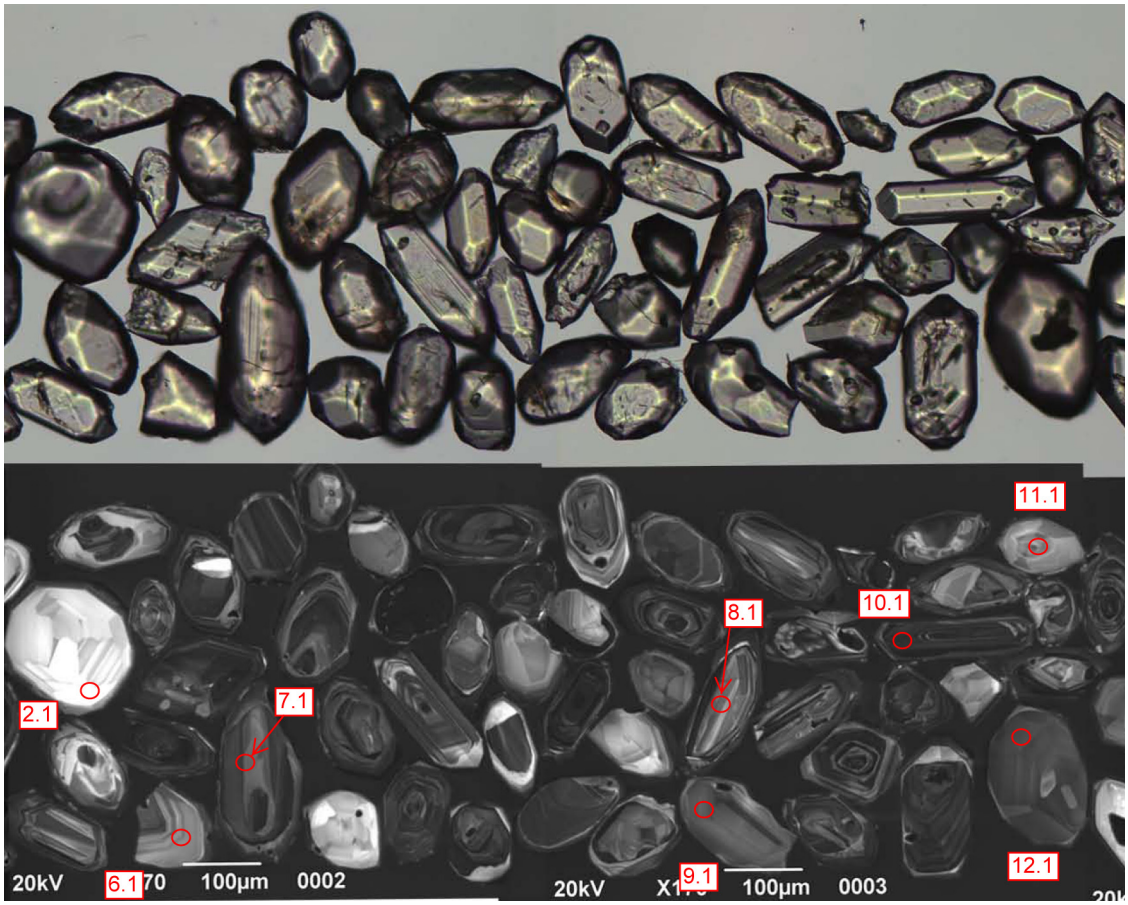

Figure 19: *Representative zircons from the 'tonalite phase' of the Lockhart Igneous Complex (GSNSW 8827JAF0672, GA 1974959). Transmitted-light image is shown in the upper half; cathodoluminescence image in the lower half. SHRIMP analysis sites are indicated, and labelled with grain and spot number.*

U-Pb Isotopic Results

Thirty-one analyses were obtained from 30 individual zircons (with grain 25 analysed twice), and the results are presented in Figure 20, and Table 3. The analysed zircons are characterised by predominantly low to moderate U contents (41–636 ppm, median 185 ppm), whereas Th/U varies widely (0.12–2.12, median 0.47).

One analysis (23.1.1; not shown in Figure 20) was adversely affected by instrumental instability during data acquisition, and is not considered further. Another analysis (25.1.1; red fill in Figure 20) yielded a high common Pb content ($^{206}Pb_c$ > 2%), and is interpreted to have been affected by loss of radiogenic Pb during one or more events of unknown age. Consequently, its $^{238}U/^{206}Pb$ date is unreliable, and this analysis is not considered further.

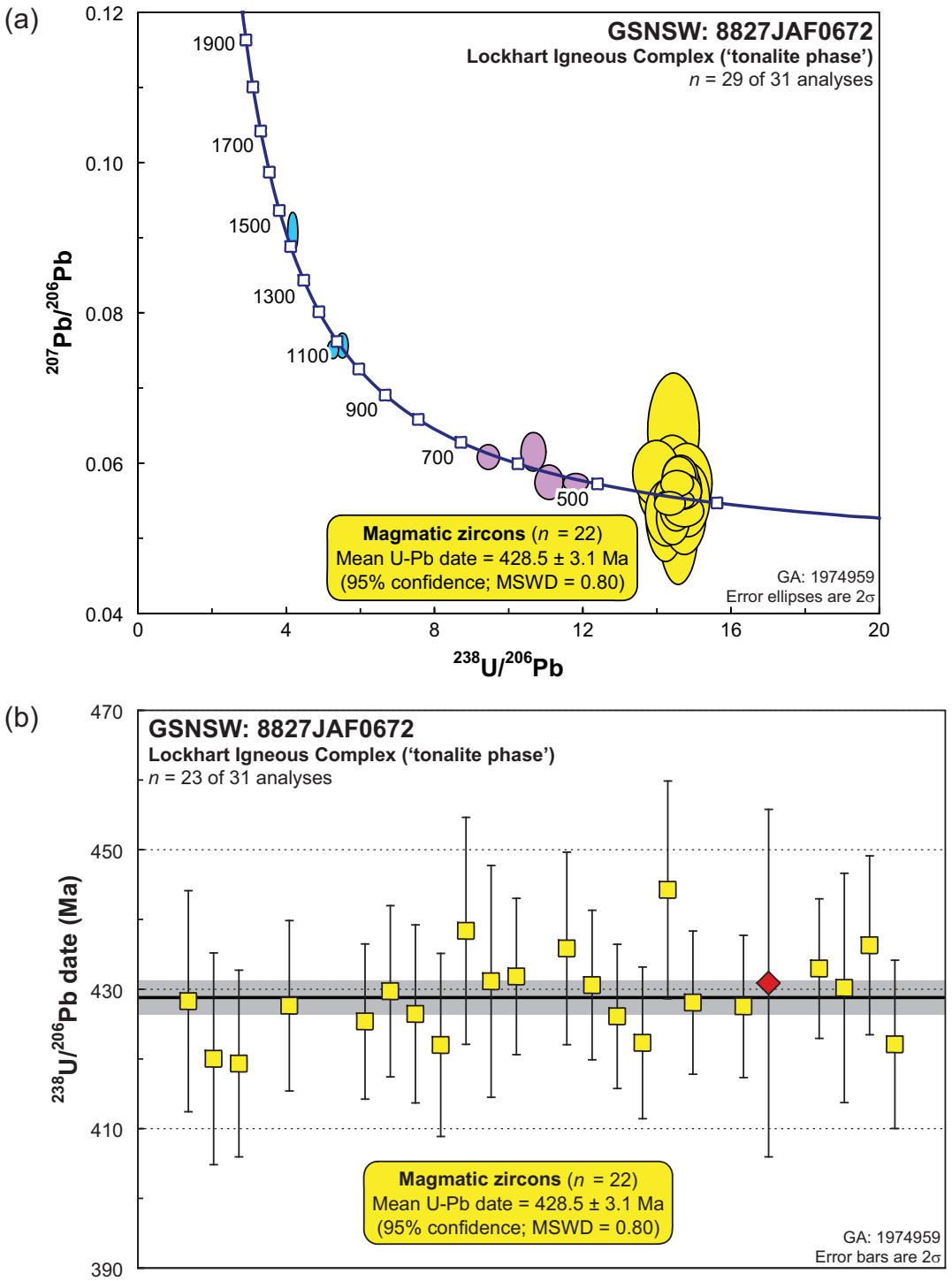

Figure 20: *SHRIMP U-Pb data for zircons from the 'tonalite phase' of the Lockhart Igneous Complex (GSNSW 8827JAF0672, GA 1974959). One analysis affected by instrumental instability (23.1.1) is not shown in either panel. (a) Tera-Wasserburg concordia diagram (analysis 25.1.1, with a very large uncertainty on $^{207}Pb/^{206}Pb$, is not shown); (b) $^{238}U/^{206}Pb$ dates in order of acquisition (seven analyses with pre-470 Ma dates are not shown). Yellow fill: magmatic zircons; pink fill: Neoproterozoic–Cambrian inheritance; blue fill: Mesoproterozoic inheritance; red fill: not considered due to high $^{206}Pb_c$. Heavy black line and grey band: weighted mean $^{238}U/^{206}Pb$ date and its 95% confidence interval, respectively.*

The remaining 29 analyses have uniformly low $^{206}Pb_c$ (maximum 0.53%, median 0.05%), and can be divided into three groups (Table 3):

- 22 analyses of 22 zircons (Group 1; yellow fill in Figure 20) with individual $^{238}U/^{206}Pb$ dates between c. 444 Ma and c. 419 Ma, which yielded a weighted mean $^{238}U/^{206}Pb$ date of 428.5 ± 3.1 Ma (MSWD = 0.80),
- four analyses of four zircons (Group 2; pink fill in Figure 20) with individual $^{238}U/^{206}Pb$ dates between c. 646 Ma and c. 522 Ma, and
- three analyses of three zircons (Group 3; blue fill in Figure 20) with individual $^{207}Pb/^{206}Pb$ dates between c. 1442 Ma and c. 1077 Ma.

Geochronological Interpretation

The weighted mean date of 428.5 ± 3.1 Ma obtained from the 22 analyses in Group 1 is indistinguishable from the median $^{238}U/^{206}Pb$ date for the same 22 analyses (428.2 +2.9/-2.1 Ma), and the absence of significant asymmetry in the uncertainties associated with the latter suggests that Group 1 represents a single population of analyses with an approximately normal distribution. Consequently, the weighted mean $^{238}U/^{206}Pb$ date of 428.5 ± 3.1 Ma is interpreted as the best estimate of the age of magmatic crystallisation of the tonalite phase of the Lockhart Igneous Complex.

The four analyses in Group 2 are interpreted as inherited individuals of Neoproterozoic to Cambrian age, and the three analyses in Group 3 are similarly interpreted as inherited individuals of Mesoproterozoic age.

The magmatic crystallisation age of 428.5 ± 3.1 Ma for the tonalite phase of the Lockhart Igneous Complex is distinctly older than that of the Woodlawn Volcanics to the north (423.3 ± 2.6 Ma, this volume; probability of equivalence = 0.01), but appears to be indistinguishable (at the 95% confidence level) from that of the nearby leucogranite phase (424.4 ± 3.2 Ma, this volume; probability of equivalence = 0.07). However, the fact that the two Lockhart Igneous Complex samples were analysed concurrently within SHRIMP session 90021 (see Introduction) means that the (shared) component of each uncertainty, associated with determining the session-specific mean value of the Temora-2 reference zircon (2σ = 0.38%; Figure 5), can be neglected for the specific purpose of evaluating the equivalence of the two magmatic crystallisation ages. Recomparing the pair of weighted mean ages in this fashion establishes that the magmatic crystallisation age of the tonalite phase of Lockhart Igneous Complex is indeed slightly older than that of the leucogranite phase (probability of equivalence = 0.03) at the 95% confidence level.

In broader comparison with existing SHRIMP zircon data, the magmatic crystallisation age of 428.5 ± 3.1 Ma for the tonalite phase of the Lockhart Igneous Complex is distinguishably older than those of the 423.4 ± 3.3 Ma Ellenden Granite (Bodorkos and Simpson, 2008), the 423.7 ± 2.5 Ma Woodlawn Volcanics on southern GOULBURN (Black, 2005), and the high-level intrusion within the Woodlawn Volcanics on northwestern BRAIDWOOD (419.2 ± 3.2 Ma; Bodorkos and Simpson, 2008).

Table 3: SHRIMP U-Pb zircon data from the 'tonalite phase' of the Lockhart Igneous Complex (GSNSW 8827JAF0672, GA 1974959). All dates are $^{238}U/^{206}Pb$ unless otherwise indicated.

Sess. no.	Grain.area .replicate	$^{206}Pb_c$ (%)	U (ppm)	Th (ppm)	$^{232}Th/^{238}U$	$^{238}U/^{206}Pb$	±1σ (%)	$^{207}Pb/^{206}Pb$	±1σ (%)	Date (Ma)	±1σ (Ma)	Disc. (%)
Group 3: Mesoproterozoic inherited individuals (n = 3; $^{207}Pb/^{206}Pb$ dates tabulated)												
90021	8.1.1	0.18	91	86	0.98	4.203	1.42	0.09078	1.20	1442	23	5
90021	25.2.1	0.03	370	169	0.47	5.293	1.19	0.07531	0.64	1077	13	-3
90021	1.1.1	0.15	215	149	0.72	5.546	1.23	0.07580	0.89	1090	18	2
Group 2: Neoproterozoic–Cambrian inherited individuals (n = 4)												
90021	5.1.1	0.03	241	59	0.25	9.486	1.28	0.06110	1.12	646.1	7.9	0
90021	30.1.1	-0.12	171	351	2.12	10.708	1.32	0.06178	1.69	575.6	7.3	16
90021	7.1.1	0.02	127	14	0.12	11.132	1.40	0.05775	1.62	554.5	7.4	-6
90021	16.1.1	0.03	636	404	0.66	11.849	1.16	0.05774	0.85	522.3	5.8	0
Group 1: Magmatic zircons (n = 22)												
90021	21.1.1	-0.15	64	43	0.69	14.016	1.82	0.05899	3.00	444.3	7.8	28
90021	13.1.1	0.00	44	17	0.40	14.211	1.92	0.05654	3.29	438.4	8.1	8
90021	28.1.1	0.49	109	47	0.44	14.281	1.52	0.05335	4.63	436.3	6.4	-21
90021	17.1.1	0.31	231	102	0.46	14.296	1.64	0.05373	3.34	435.8	6.9	-18
90021	26.1.1	0.09	474	223	0.49	14.395	1.20	0.05494	1.18	433.0	5.0	-5
90021	15.1.1	0.06	185	84	0.47	14.434	1.34	0.05606	1.79	431.8	5.6	5
90021	14.1.1	-0.37	41	21	0.53	14.458	1.99	0.05808	4.14	431.1	8.3	24
90021	18.1.1	0.32	257	204	0.82	14.477	1.29	0.05300	2.73	430.6	5.4	-24
90021	27.1.1	-0.71	44	21	0.49	14.491	1.98	0.06457	4.80	430.2	8.2	77
90021	10.1.1	0.02	501	338	0.70	14.508	1.48	0.05545	0.97	429.7	6.1	0
90021	2.1.1	-0.11	48	19	0.41	14.557	1.91	0.05667	3.10	428.3	7.9	12
90021	22.1.1	0.29	357	310	0.90	14.565	1.24	0.05413	2.13	428.1	5.1	-12
90021	6.1.1	0.06	107	32	0.31	14.581	1.48	0.05562	2.22	427.6	6.1	2
90021	24.1.1	0.02	352	280	0.82	14.584	1.23	0.05757	1.22	427.5	5.1	20
90021	11.1.1	0.53	107	49	0.47	14.622	1.55	0.05264	6.52	426.5	6.4	-27
90021	19.1.1	-0.22	305	166	0.56	14.634	1.25	0.05837	1.95	426.1	5.2	28
90021	9.1.1	-0.12	173	100	0.60	14.661	1.35	0.05844	1.99	425.4	5.6	28
90021	20.1.1	0.05	196	68	0.36	14.770	1.33	0.05651	1.67	422.3	5.4	12
90021	29.1.1	0.05	244	92	0.39	14.778	1.48	0.05396	1.55	422.1	6.0	-13
90021	12.1.1	0.33	198	86	0.45	14.781	1.61	0.05326	3.85	422.0	6.6	-19
90021	3.1.1	0.15	45	20	0.45	14.853	1.87	0.05762	3.76	420.0	7.6	23
90021	4.1.1	0.18	71	31	0.46	14.878	1.65	0.05548	3.62	419.3	6.7	3
Not considered, due to high $^{206}Pb_c$ (> 2%; n = 1)												
90021	25.1.1	2.79	23	8	0.35	14.467	2.99	0.05938	26.45	430.9	12.5	35
Not considered, due to instrumental instability (n = 1)												
90021	23.1.1	0.01	444	302	0.70	14.670	4.04	0.05497	1.04	425.1	16.6	-3

MOUNT FAIRY GROUP: WOODLAWN VOLCANICS

GA SAMPLENO:	**1974960**
GSNSW SITEID:	**8827ODT1152**
PARENT UNIT(S):	Mount Fairy Group
FORMAL NAME:	Woodlawn Volcanics
INFORMAL NAME:	–
LITHOLOGY:	Coherent porphyritic rhyolite
PROVINCE:	Eastern Lachlan Orogen
1:250 000 SHEET:	CANBERRA (SI/55-16)
1:100 000 SHEET:	BRAIDWOOD (8827)
LOCATION (GDA94):	35.060823 °S, 149.543590 °E
LOCATION (MGA94):	Zone 55, 731961 mE, 6117253 mN
ANALYTICAL SESSION NO(S):	90021 (see Table 1 for parameters derived from concurrent measurements of $^{238}U/^{206}Pb$ and $^{207}Pb/^{206}Pb$ reference zircons)
INTERPRETED AGE:	**423.3 ± 2.6 Ma** (95% confidence; 38 analyses of 38 zircons)
GEOLOGICAL ATTRIBUTION:	Magmatic crystallisation
ISOTOPIC RATIO(S) USED:	$^{238}U/^{206}Pb$ (^{204}Pb-corrected)

Sampling Details

This sample was taken from an outcrop on the northern bank of a small creek, about 1 km west of the Woodlawn mine site.

Relationships and Rationale for Dating

The unit sampled is a coherent porphyritic rhyolite that is interpreted as an eruptive layer within the predominantly volcaniclastic lower part of the Woodlawn Volcanics, which is part of the Mount Fairy Group in the eastern Lachlan Orogen (Felton and Huleatt, 1976; Fitzherbert *et al.*, in press). This rhyolite stratigraphically and structurally underlies a nearby high-level rhyolitic intrusion that yielded a SHRIMP zircon $^{238}U/^{206}Pb$ date of 419.2 ± 3.2 Ma (Bodorkos and Simpson, 2008), and is tentatively interpreted as a lateral equivalent of the 423.4 ± 2.5 Ma Woodlawn Volcanics (Black, 2005) on southern GOULBURN (Thomas *et al.*, 2002).

This sample was selected for SHRIMP analysis in order to test the hypothesis that the Woodlawn Volcanics and the related 423.4 ± 3.3 Ma Ellenden Granite (Bodorkos and Simpson, 2008) of southern GOULBURN and northwestern BRAIDWOOD (Thomas *et al.*, 2002; Fitzherbert *et al.*, in press) are upper-crustal equivalents of, and therefore broadly contemporaneous with, the Lockhart Igneous Complex of southwestern BRAIDWOOD (Fitzherbert *et al.*, in press). The Lockhart Igneous Complex comprises plutonic rocks ranging from olivine-bearing gabbro to leucogranite, which display a variety of magma mixing and mingling relationships; however, the igneous crystallisation history is not well constrained.

The aim was to obtain a magmatic crystallisation age for the lower part of the Woodlawn Volcanics on northwestern BRAIDWOOD, for comparison with the existing data described above. The age will also be compared with new data from the homogeneous leucogranite phase (GSNSW 8827JAF0837, GA 1974958; this volume) and the foliated tonalite phase (GSNSW 8827JAF0672, GA 1974959; this volume) of the Lockhart Igneous Complex.

Petrography

This sample is a weakly deformed, porphyritic rhyolite lava which contains euhedral to subhedral phenocrysts of quartz, perthitic K-feldspar, plagioclase and minor biotite within a finely micropoikilitic groundmass (Figure 21). Phenocrysts up to 3 mm in length comprise about 30% of the rock, and are composed of 12% quartz (as embayed, hexagonal-shaped crystals), 10% plagioclase (as tabular laths of oligoclase composition ($An_{25–28}$), although some crystals have albitic rims), 8% perthitic K-feldspar, and 1–2% straw- to tan-coloured biotite. Accessory minerals include zircon, opaque oxide minerals, and a single crystal of zoned brown allanite. The sample also contains two aggregates of fine-grained recrystallised quartz, biotite and feldspar, each about 1 mm in diameter, which possibly represent volcanic clasts.

The micropoikilitic texture in the groundmass indicates it was originally glass and this, together with the mainly euhedral nature of the phenocrysts, suggests a magmatic (rather than volcaniclastic) mode of emplacement for this rock. Biotite phenocrysts are widely altered to chlorite, and the groundmass has been affected by sericite-iron oxide alteration.

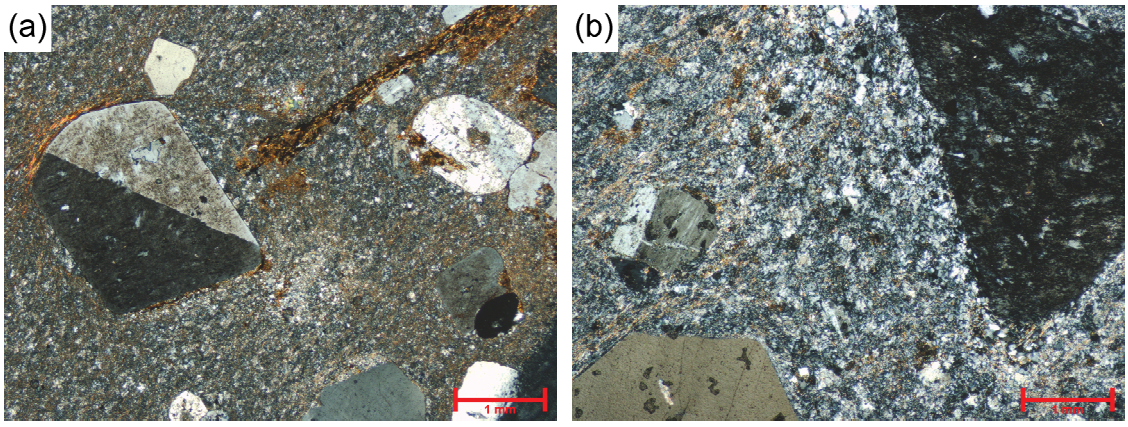

Figure 21: *Representative photomicrographs (in cross-polarised light) of the Woodlawn Volcanics (GSNSW 8827ODT1152, GA 1974960). (a) Coherent porphyritic rhyolite containing phenocrysts of K-feldspar (left), plagioclase (top right), quartz (base), and trace biotite (top right) in a massive, micropoikilitic felsic groundmass. (b) Felsic groundmass between phenocrysts of perthitic K-feldspar (top right), plagioclase (left) and quartz (lower left).*

Zircon Description

Zircons from this sample are mostly euhedral, with subordinate subhedral and anhedral grain fragments, and rare elongate crystals. Aspect ratios (length/width) are 1–6 (but mostly less than 4), and long axes are 40–350 µm (Figure 22). In transmitted light, most grains are pale- to medium-brown and transparent to translucent, although a significant number are mottled, and some are opaque. Inclusions of dark-coloured minerals are relatively common, and many grains feature cracking and brown staining in their central regions, consistent with incipient metamictisation.

Cathodoluminescence (CL) images reveal predominantly low CL emission, and a sub-population with moderate CL emission and concentric oscillatory zoning was targeted for dating. Most of the darker-CL crystals also feature low-contrast, ill-defined concentric zoning and banding (Figure 22), consistent with damage to the crystal lattices during metamictisation and/or alteration. Some crystals contain internal domains of high CL emission, but these are typically sharply and disconformably truncated by oscillatory-zoned overgrowths, and thus probably reflect inheritance.

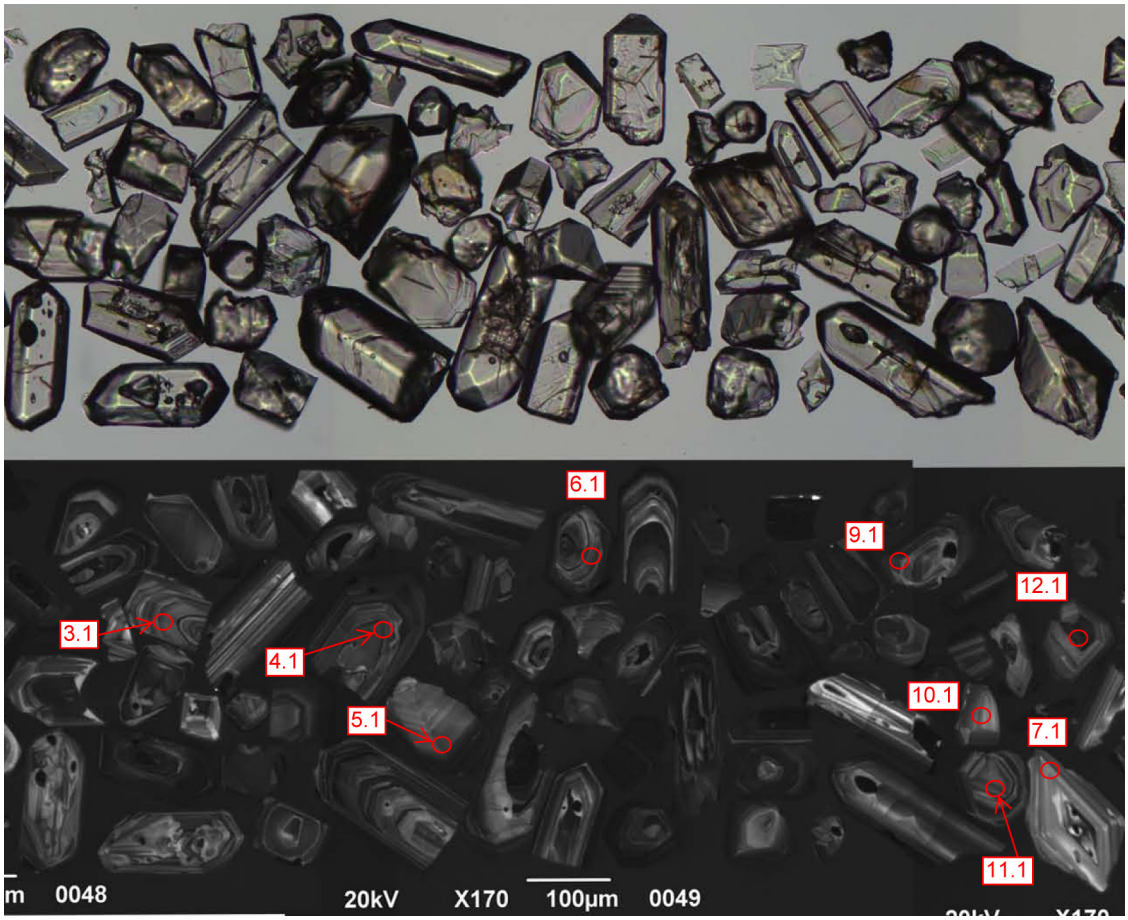

Figure 22: *Representative zircons from the Woodlawn Volcanics (GSNSW 8827ODT1152, GA 1974960). Transmitted-light image is shown in the upper half; cathodoluminescence image in the lower half. SHRIMP analysis sites are indicated, and labelled with grain and spot number.*

U-Pb Isotopic Results

Forty-nine analyses were obtained from 49 individual zircons, and the results are presented in Table 4 and Figure 23. The analysed zircons are characterised by predominantly moderate U contents (56–556 ppm, median 271 ppm), and moderate Th/U (0.32–1.14, median 0.57).

One analysis (44.1.1; not shown in Figure 23) was adversely affected by instrumental instability during data acquisition, and is not considered further. A further five analyses (2.1.1, 17.1.1, 27.1.1, 31.1.1 and 37.1.1; red fill in Figure 23) yielded high common Pb contents ($^{206}Pb_c$ > 1.5%), and are interpreted to have been affected by loss of radiogenic Pb during one or more events of unknown age. Their $^{238}U/^{206}Pb$ dates are unreliable, and these analyses are not considered further.

The remaining 43 analyses have uniformly low $^{206}Pb_c$ (maximum 0.51%, median 0.07%), and can be divided into four groups (Table 4):

- 38 analyses of 38 zircons (Group 1; yellow fill in Figure 23) with individual $^{238}U/^{206}Pb$ dates between c. 435 Ma and c. 409 Ma, which yielded a weighted mean date of 423.3 ± 2.6 Ma (MSWD = 1.27),
- three analyses of three zircons (Group 2; blue fill in Figure 23) with individual $^{238}U/^{206}Pb$ dates between c. 462 Ma and c. 449 Ma, which yielded a weighted mean date of 457.8 ± 6.4 Ma (MSWD = 1.10),

- a single analysis (Group 3; pink fill in Figure 23) with a $^{207}Pb/^{206}Pb$ date of 985 ± 84 Ma (2σ), and
- a single analysis (Group 4; white fill in Figure 23) with a $^{238}U/^{206}Pb$ date of 407 ± 10 Ma (2σ).

Geochronological Interpretation

The weighted mean date of 423.3 ± 2.6 Ma obtained from the 38 analyses in Group 1 is indistinguishable from the median $^{238}U/^{206}Pb$ date for the same 38 analyses (422.5 +3.1/-2.5 Ma), and the absence of significant asymmetry in the uncertainties associated with the latter suggests that Group 1 represents a single population of analyses with an approximately normal distribution. Consequently, the weighted mean $^{238}U/^{206}Pb$ date of 423.3 ± 2.6 Ma is interpreted as the best estimate of the age of magmatic crystallisation of the lower part of the Woodlawn Volcanics.

The weighted mean $^{238}U/^{206}Pb$ date of 457.8 ± 6.4 Ma obtained from the three analyses in Group 2 is interpreted to reflect inheritance from one or more sources containing Ordovician zircons. The single analysis in Group 3 is interpreted as an inherited individual of Proterozoic age that has been affected by at least one ancient episode of radiogenic Pb loss, possibly during incorporation into its current host rhyolite. The single analysis in Group 4 is very slightly younger than the main magmatic population defined by Group 1, and is interpreted to have been affected by minor post-crystallisation loss of radiogenic Pb.

The magmatic crystallisation age of 423.3 ± 2.6 Ma for this sample of the Woodlawn Volcanics is distinctly younger than that of the tonalite phase of the Lockhart Igneous Complex (428.5 ± 3.1 Ma, this volume; probability of equivalence = 0.01), but is indistinguishable (at the 95% confidence level) from that of the leucogranite phase of the Lockhart Igneous Complex (424.4 ± 3.2 Ma, this volume). In broader comparison with existing SHRIMP zircon $^{238}U/^{206}Pb$ dates, the magmatic crystallisation age of 423.3 ± 2.6 Ma for this sample of the Woodlawn Volcanics is indistinguishable from those of the 423.4 ± 3.3 Ma Ellenden Granite (Bodorkos and Simpson, 2008) and the 423.4 ± 2.5 Ma Woodlawn Volcanics on southern GOULBURN (Black, 2005), but is slightly older than that of the nearby high-level rhyolitic intrusion within the Woodlawn Volcanics on northwestern BRAIDWOOD (419.2 ± 3.2 Ma; Bodorkos and Simpson, 2008).

Table 4: SHRIMP U-Pb zircon data from the Woodlawn Volcanics (GSNSW 8827ODT1152, GA 1974960). All dates are $^{238}U/^{206}Pb$ unless otherwise indicated.

Sess. no.	Grain.area .replicate	$^{206}Pb_c$ (%)	U (ppm)	Th (ppm)	$^{232}Th/^{238}U$	$^{238}U/^{206}Pb$	±1σ (%)	$^{207}Pb/^{206}Pb$	±1σ (%)	Date (Ma)	±1σ (Ma)	Disc. (%)
Group 3: Proterozoic inherited individual (n = 1; $^{207}Pb/^{206}Pb$ date tabulated)												
90021	36.1.1	-0.22	107	51	0.49	12.840	1.46	0.07197	2.06	985	84	104
Group 2: Ordovician inherited component (n = 3)												
90021	4.1.1	0.00	271	84	0.32	13.466	1.25	0.05701	1.22	461.8	5.6	7
90021	15.1.1	-0.13	382	166	0.45	13.538	1.23	0.05631	1.18	459.4	5.5	1
90021	33.1.1	0.10	400	246	0.64	13.869	1.63	0.05530	1.41	448.8	7.1	-5
Group 1: Magmatic zircons (n = 38)												
90021	11.1.1	-0.01	232	125	0.56	14.331	1.27	0.05609	1.34	434.8	5.4	5
90021	45.1.1	-0.02	406	256	0.65	14.390	1.21	0.05601	1.04	433.1	5.1	5
90021	10.1.1	-0.44	111	45	0.42	14.396	1.46	0.06247	2.89	432.9	6.1	59
90021	28.1.1	0.07	449	274	0.63	14.479	1.19	0.05547	1.17	430.5	4.9	0
90021	30.1.1	-0.21	286	161	0.58	14.481	1.25	0.05750	1.78	430.5	5.2	19
90021	19.1.1	-0.05	486	155	0.33	14.523	1.18	0.05623	1.08	429.3	4.9	8
90021	25.1.1	-0.10	482	339	0.73	14.535	1.18	0.05606	1.16	428.9	4.9	6
90021	12.1.1	0.39	518	506	1.01	14.544	1.18	0.05424	2.57	428.7	4.9	-11

Sess. no.	Grain.area .replicate	$^{206}Pb_c$ (%)	U (ppm)	Th (ppm)	$^{232}Th/^{238}U$	$^{238}U/^{206}Pb$	±1σ (%)	$^{207}Pb/^{206}Pb$	±1σ (%)	Date (Ma)	±1σ (Ma)	Disc. (%)
90021	23.1.1	0.08	554	375	0.70	14.550	1.17	0.05525	1.17	428.5	4.9	-1
90021	6.1.1	-0.21	303	224	0.77	14.577	1.24	0.05676	1.82	427.7	5.1	13
90021	29.1.1	0.16	188	68	0.37	14.578	1.32	0.05398	2.32	427.7	5.4	-13
90021	18.1.1	-0.22	223	99	0.46	14.628	1.28	0.05858	2.30	426.3	5.3	29
90021	35.1.1	0.05	534	385	0.74	14.650	1.18	0.05476	1.15	425.7	4.8	-5
90021	3.1.1	0.11	229	111	0.50	14.657	1.30	0.05418	2.13	425.5	5.4	-11
90021	43.1.1	0.27	259	147	0.59	14.665	1.30	0.05219	2.28	425.2	5.3	-31
90021	7.1.1	-0.11	71	45	0.64	14.685	1.61	0.05736	2.46	424.7	6.6	19
90021	41.1.1	0.32	293	145	0.51	14.716	1.25	0.05270	2.32	423.8	5.1	-25
90021	1.1.1	0.14	211	96	0.47	14.738	1.31	0.05479	2.39	423.2	5.4	-5
90021	9.1.1	0.11	243	128	0.55	14.750	1.27	0.05325	2.16	422.9	5.2	-20
90021	26.1.1	0.22	354	200	0.58	14.775	1.22	0.05374	2.13	422.2	5.0	-15
90021	48.1.1	0.39	56	33	0.62	14.782	1.98	0.05135	7.15	422.0	8.1	-39
90021	42.1.1	0.04	254	187	0.76	14.783	1.28	0.05646	1.44	422.0	5.2	11
90021	40.1.1	0.12	221	104	0.49	14.789	1.29	0.05507	2.28	421.8	5.3	-2
90021	38.1.1	0.00	271	299	1.14	14.802	1.25	0.05626	1.24	421.4	5.1	10
90021	5.1.1	0.08	225	82	0.38	14.838	1.28	0.05595	1.79	420.4	5.2	7
90021	39.1.1	-0.26	276	177	0.66	14.852	1.26	0.05687	2.37	420.1	5.1	16
90021	22.1.1	0.41	193	135	0.72	14.865	1.71	0.05236	3.47	419.7	7.0	-28
90021	14.1.1	0.51	553	441	0.82	14.879	1.17	0.05581	1.60	419.3	4.8	6
90021	49.1.1	0.14	342	167	0.50	14.907	1.56	0.05560	2.19	418.6	6.3	4
90021	20.1.1	-0.07	358	197	0.57	14.914	1.21	0.05611	1.17	418.4	4.9	9
90021	21.1.1	-0.04	335	150	0.46	14.917	1.22	0.05641	1.11	418.3	4.9	12
90021	46.1.1	0.10	280	119	0.44	14.926	1.30	0.05390	1.72	418.0	5.3	-12
90021	32.1.1	0.17	208	133	0.66	14.941	1.30	0.05447	2.25	417.6	5.3	-6
90021	34.1.1	0.13	152	68	0.46	14.986	1.38	0.05527	2.59	416.4	5.6	2
90021	24.1.1	0.00	279	155	0.57	15.060	1.24	0.05672	1.20	414.4	5.0	16
90021	47.1.1	0.16	202	134	0.69	15.094	1.39	0.05476	2.45	413.5	5.6	-3
90021	8.1.1	0.05	475	212	0.46	15.168	1.77	0.05581	1.22	411.6	7.0	8
90021	13.1.1	0.10	146	65	0.46	15.275	1.36	0.05472	2.29	408.8	5.4	-2
Group 4: Affected by loss of radiogenic Pb (n = 1)												
90021	16.1.1	-0.02	230	136	0.61	15.342	1.26	0.05602	1.35	407.1	5.0	11
Not considered, due to high $^{206}Pb_c$ (> 1.5%; n = 5)												
90021	27.1.1	21.85	137	70	0.53	14.297	2.21	0.05854	24.74	435.8	9.3	26
90021	37.1.1	4.74	346	151	0.45	14.650	1.31	0.05540	9.38	425.7	5.4	1
90021	31.1.1	1.51	427	231	0.56	16.035	1.20	0.05577	3.04	390.0	4.6	14
90021	2.1.1	30.05	432	291	0.70	16.186	2.48	0.03773	49.81	386.4	9.3	-230
90021	17.1.1	27.84	340	294	0.90	16.334	15.84	—	—	383.1	58.9	—
Not considered, due to instrumental instability (n = 1)												
90021	44.1.1	-0.02	252	105	0.43	15.443	1.54	0.05574	1.46	404.5	6.0	9

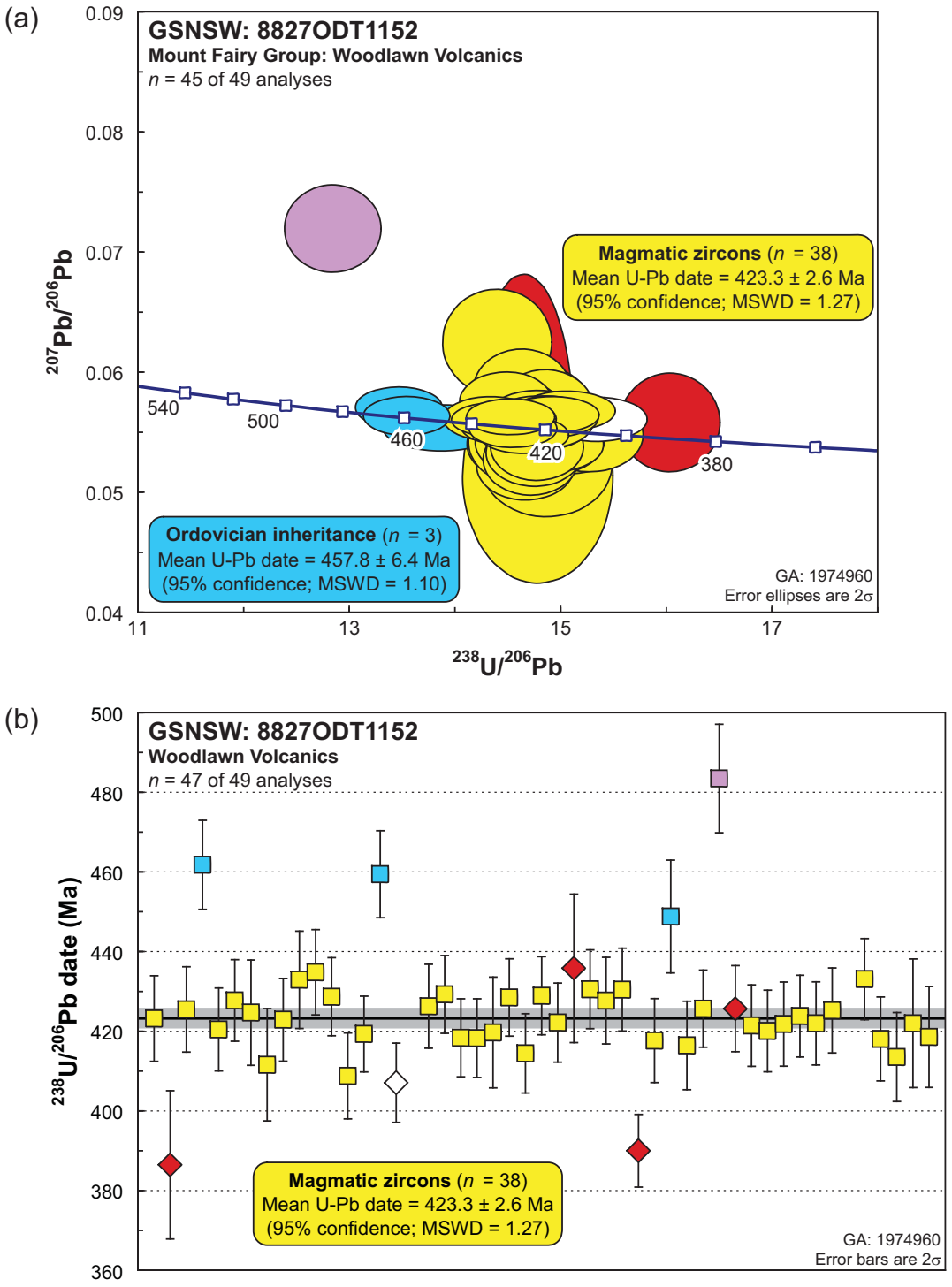

Figure 23: *SHRIMP U-Pb data for zircons from the Woodlawn Volcanics (GSNSW 8827ODT1152, GA 1974960). Two analyses are not shown in either panel: one (44.1.1) affected by instrumental instability and one (17.1.1) with very large uncertainties. (a) Tera-Wasserburg concordia diagram (analyses 2.1.1 and 27.1.1, with very large uncertainties on $^{207}Pb/^{206}Pb$, are not shown); (b) $^{238}U/^{206}Pb$ dates in order of acquisition. Yellow fill: magmatic zircons; blue fill: Ordovician inheritance; pink fill: Proterozoic inheritance. Heavy black line and grey band: weighted mean $^{238}U/^{206}Pb$ date and its 95% confidence interval, respectively.*

BRAIDWOOD SUITE: BRAIDWOOD GRANODIORITE ('NORTHERN PHASE')

GA SAMPLENO:	**1974961**
GSNSW SITEID:	**8827JAF0300**
PARENT UNIT(S)	Braidwood Suite
FORMAL NAME:	Braidwood Granodiorite
INFORMAL NAME:	('northern phase')
LITHOLOGY:	Hornblende-biotite granodiorite
PROVINCE:	Eastern Lachlan Orogen
1:250 000 SHEET:	CANBERRA (SI/55-16)
1:100 000 SHEET:	BRAIDWOOD (8827)
LOCATION (GDA94):	35.234284 °S, 149.789262 °E
LOCATION (MGA94):	Zone 55, 753831 mE, 6097409 mN
ANALYTICAL SESSION NO(S):	90021 (see Table 1 for parameters derived from concurrent measurements of $^{238}U/^{206}Pb$ and $^{207}Pb/^{206}Pb$ reference zircons)
INTERPRETED AGE:	**411.3 ± 2.6 Ma** (95% confidence; 27 analyses of 27 zircons)
GEOLOGICAL ATTRIBUTION:	Magmatic crystallisation
ISOTOPIC RATIO(S) USED:	$^{238}U/^{206}Pb$ (^{204}Pb-corrected)

Sampling Details

This sample was taken from some low, fresh boulders on the western verge of Mayfield Road, about 4 km south of the locality of Mayfield.

Relationships and Rationale for Dating

The unit sampled is a massive, equigranular hornblende granodiorite proximal to the northern edge of the Braidwood Granodiorite, which is part of the Braidwood Suite in the eastern Lachlan Orogen (Felton and Huleatt, 1976; Fitzherbert *et al.*, in press). The Braidwood Granodiorite intrudes the Long Flat Volcanics, which are part of the Early Devonian Bindook Group, and locally include the 413.4 ± 2.6 Ma Kadoona Dacite Member, the 413.0 ± 2.3 Ma Manar Ignimbrite Member, and the 412.3 ± 2.3 Ma Toggannoggra Rhyolite Member (Bodorkos and Simpson, 2008; Fitzherbert *et al.*, in press).

Previous geochronology on the Braidwood Granodiorite includes SHRIMP zircon $^{238}U/^{206}Pb$ dates of 410.8 ± 3.2 Ma for its hornblende-phyric 'western phase' and 410.2 ± 3.1 Ma for its equigranular 'eastern phase' (Bodorkos and Simpson, 2008). Both dates are slightly older than an unpublished preliminary SHRIMP zircon $^{238}U/^{206}Pb$ date of 402 ± 6 Ma cited by McQueen (2003), and only partially overlap with data obtained elsewhere by other radiometric techniques. Wyborn and Owen (1986) reported K-Ar biotite ages of 415 ± 4 Ma and 412 ± 4 Ma, K-Ar hornblende ages of 403 ± 4 Ma and 401 ± 6 Ma, and a biotite–whole rock Rb-Sr pair with an age of 399 ± 6 Ma, all from unaltered rocks. McQueen and Perkins (1995) obtained K-Ar sericite ages of 411 ± 5 Ma and 406 ± 4 Ma from intensely altered granodiorite hosting gold mineralisation at Dargues Reef, along the western margin of the pluton.

The aim was to obtain an additional magmatic crystallisation age, in order to establish whether zircon ages for magmatic crystallisation of the Braidwood Granodiorite are distinguishably older than existing K-Ar and Rb-Sr dates (Wyborn and Owen, 1986; McQueen and Perkins, 1995), which should record lower-temperature processes. The age will also be compared with new data from the

Long Flat Volcanics, from the Croppies Gunyah Rhyolite Member (GSNSW 8827CJS0070, GA 1989476, this volume) and the Kain Porphyry Member (GSNSW 8827JAF0193, GA 1949548, this volume).

Petrography

This sample is a massive, medium-grained, equigranular hornblende granodiorite with an average grainsize of 2–4 mm (Figure 24). It comprises 40% plagioclase, 30% quartz, 15% K-feldspar, 8% hornblende, 5% biotite, 1% relict clinopyroxene, 1% opaque oxide minerals (probably magnetite), and accessory zircon, apatite and titanite. Plagioclase forms euhedral crystals of andesine composition ($An_{35–48}$) up to 4.5 mm in length, with finely sericitised and epidotised cores and clear outer rims. Quartz occurs as aggregates of large grains (up to 6 mm in diameter) and smaller anhedral consertal crystals, and occasionally hosts small inclusions of plagioclase, K-feldspar and ferromagnesian minerals. K-feldspar is perthitic and interstitial to weakly micropoikilitic in form, hosting small inclusions of quartz. Hornblende forms isolated crystals up to 2 mm in length, but more commonly occurs in aggregates with biotite and granular opaque oxide minerals (probably magnetite; Figure 24). Some of the aggregate-hosted hornblende crystals contain irregular cores of relict clinopyroxene, with which minor secondary actinolite is associated. Biotite is tan to chocolate-brown in colour, and is essentially unaltered, with minimal chlorite development.

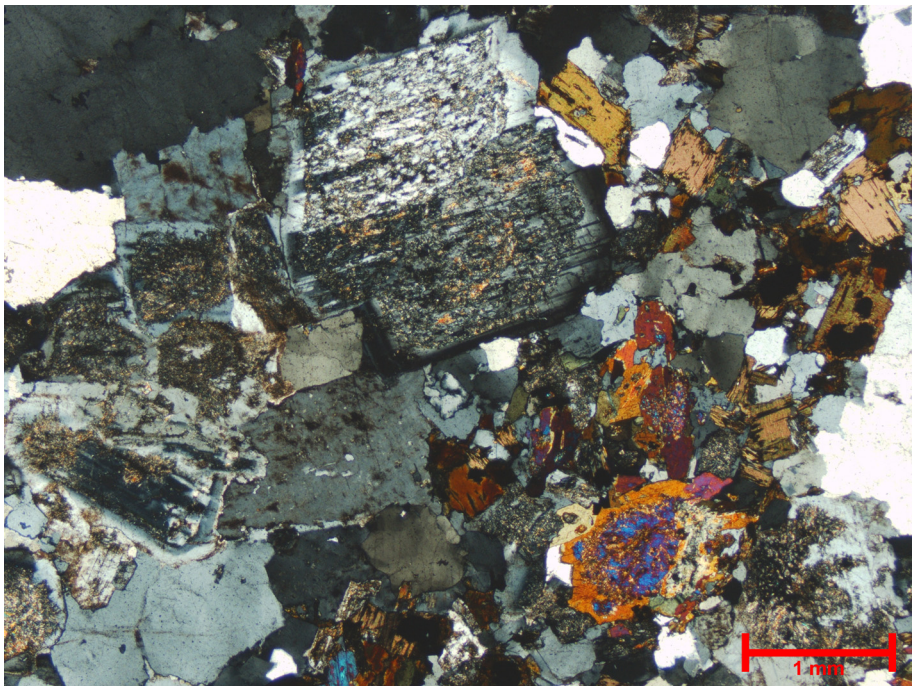

Figure 24: *Representative photomicrograph (in cross-polarised light) of the 'northern phase' of the Braidwood Granodiorite (GSNSW 8827JAF0300, GA 1974961). Granodiorite comprises plagioclase (upper centre), quartz (left, right margins), K-feldspar (lower centre), and an aggregate of ferromagnesian minerals comprising biotite (top right), hornblende (lower right), and magnetite. The orange-coloured hornblende (lower right) contains a blue-coloured core, which is relic clinopyroxene.*

Zircon Description

Zircons from this sample are euhedral to subhedral, and stubby to prismatic. Elongate crystals are rare, aspect ratios (length/width) are 1–4 (but mostly less than 3), and long axes are 70–300 µm. In

transmitted light, the grains are transparent to translucent and mostly colourless to pale yellow. Many crystals host abundant inclusions of other minerals, and some host fluid inclusions as well.

Cathodoluminescence (CL) images reveal a dominant population of zircons with relatively uniform, moderate to high CL emission (Figure 25). These grains are characterised by low- to moderate-contrast oscillatory zoning parallel to the external crystal faces, a pattern typical of magmatic zircon. Inherited cores are also identifiable in the CL images (grain 9.1 in Figure 25), and are most obvious where their CL emission is low and the fine-scale oscillatory zoning is low-contrast. Interfaces between the cores and their oscillatory-zoned magmatic overgrowths are typically sharp, and most display pronounced disconformity (Figure 25).

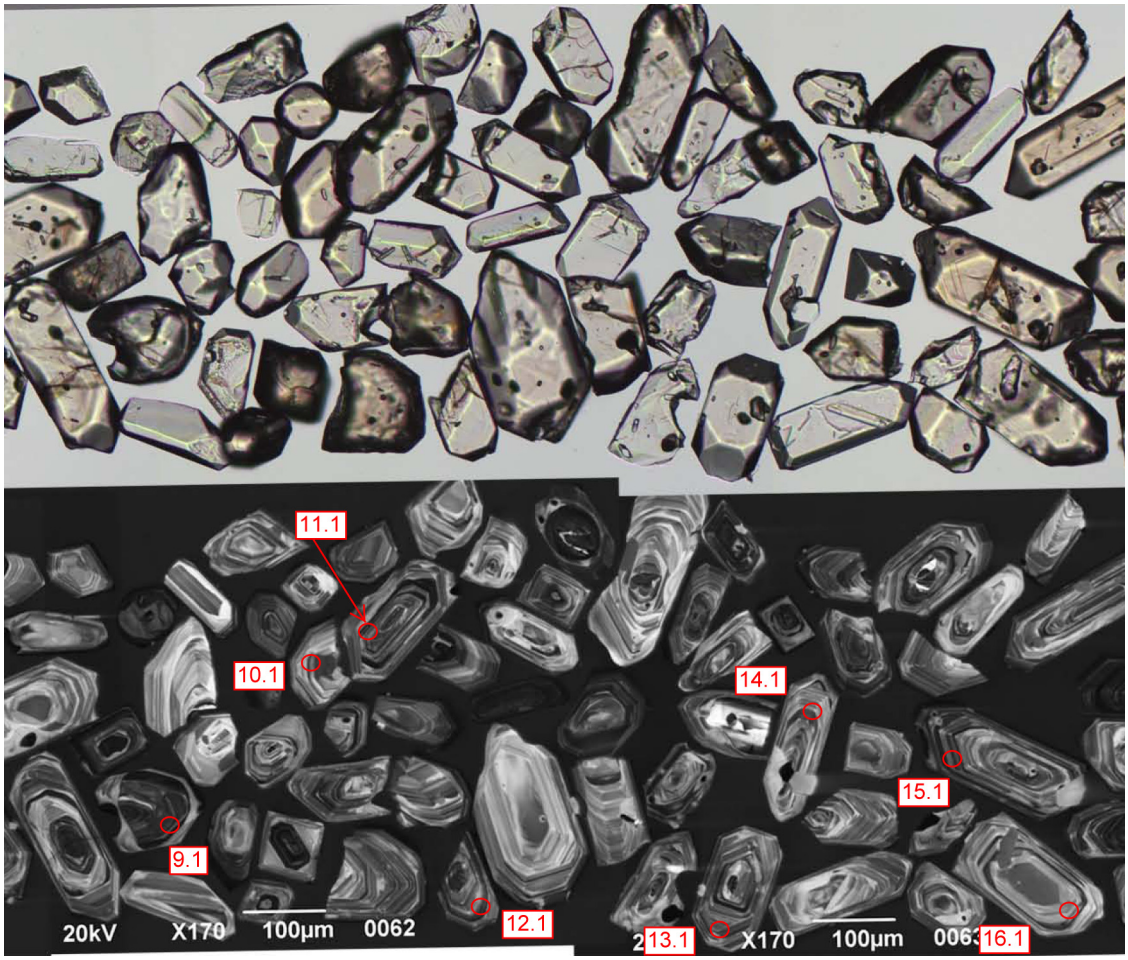

Figure 25: *Representative zircons from the 'northern phase' of the Braidwood Granodiorite (GSNSW 8827JAF0300, GA 1974961). Transmitted-light image is shown in the upper half; cathodoluminescence image in the lower half. SHRIMP analysis sites are indicated, and labelled with grain and spot number.*

U-Pb Isotopic Results

Twenty-nine analyses were obtained from 29 individual zircons, and the results are presented in Figure 26 and Table 5. Most zircons yielded a relatively narrow range of low to moderate U contents (104–323 ppm, median 174 ppm) and moderate to high Th/U (0.57–0.95, median 0.68), although the single core analysed yielded a significantly higher U content (403 ppm), and lower Th/U (0.18).

One analysis (18.1.1; green fill in Figure 26) yielded a spuriously low common Pb content ($^{206}Pb_c$ < -1%), and is interpreted as being inaccurately corrected for common Pb. Consequently, its $^{238}U/^{206}Pb$ date is unreliable, and it is not considered further.

The remaining 28 analyses have uniformly low $^{206}Pb_c$ (maximum 0.65%, median 0.15%), and can be divided into two groups (Table 5):

- 27 analyses of 27 zircons (Group 1; yellow fill in Figure 26) with individual $^{238}U/^{206}Pb$ dates between c. 423 Ma and c. 397 Ma, which yielded a weighted mean date of 411.3 ± 2.6 Ma (MSWD = 0.91), and
- a single analysis (Group 2; pink fill in Figure 26) with a $^{238}U/^{206}Pb$ date of 1047 ± 96 Ma (2σ).

Geochronological Interpretation

The weighted mean date of 411.3 ± 2.6 Ma obtained from the 27 analyses in Group 1 is indistinguishable from the median $^{238}U/^{206}Pb$ date for the same 27 analyses (410.8 +2.3/-1.0 Ma), and the absence of significant asymmetry in the uncertainties associated with the latter suggests that Group 1 represents a single population of analyses with an approximately normal distribution.

Consequently, the weighted mean $^{238}U/^{206}Pb$ date of 411.3 ± 2.6 Ma is interpreted as the best estimate of the age of magmatic crystallisation of the northern phase of the Braidwood Granodiorite. The single analysis in Group 2 is interpreted to reflect Mesoproterozoic inheritance.

The magmatic crystallisation age of 411.3 ± 2.6 Ma obtained for this northern phase of the Braidwood Granodiorite is indistinguishable from both the 410.8 ± 3.2 Ma 'western phase' and 410.2 ± 3.1 Ma 'eastern phase' (Bodorkos and Simpson, 2008) of the pluton. All the pre-410 Ma biotite and sericite K-Ar ages (Wyborn and Owen, 1986; McQueen and Perkins, 1995) are within uncertainty of the zircon ages, but the presence of a second cluster of K-Ar and Rb-Sr ages between c. 405 Ma and c. 400 Ma suggests that it is this latter group that gives the most accurate indication of when the Braidwood Granodiorite cooled through the relevant closure temperatures (typically 400 ±100 °C), with the older K-Ar ages potentially affected by the presence of minor excess argon.

In broader comparison with existing SHRIMP zircon $^{238}U/^{206}Pb$ dates, the magmatic crystallisation age of 411.3 ± 2.6 Ma obtained for this northern phase of the Braidwood Granodiorite is indistinguishable from all of the units dated in the Long Flat Volcanics, including the 414.1 ± 2.8 Ma Kain Porphyry Member (GSNSW 8827JAF0193, GA 1949548; this volume) and the 414.0 ± 2.5 Ma Croppies Gunyah Rhyolite Member (GSNSW 8827CJS0070, GA 1989476; this volume), but also encompassing the 413.4 ± 2.6 Ma Kadoona Dacite Member, the 413.0 ± 2.3 Ma Manar Ignimbrite Member, and the 412.3 ± 2.3 Ma Toggannoggra Rhyolite Member (Bodorkos and Simpson, 2008).

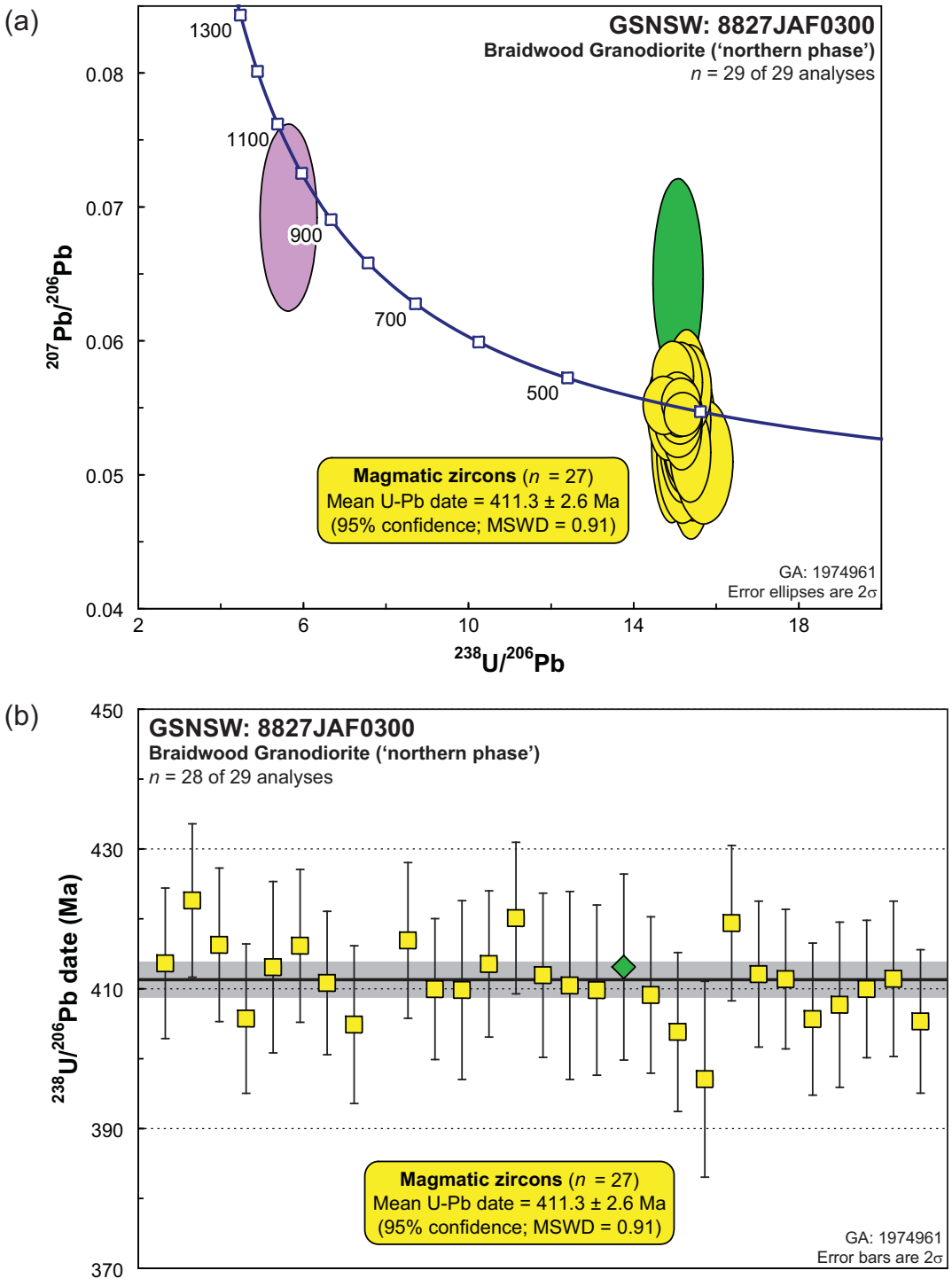

Figure 26: *SHRIMP U-Pb data for zircons from the 'northern phase' of the Braidwood Granodiorite (GSNSW 8827JAF0300, GA 1974961). (a) Tera-Wasserburg concordia diagram; (b) $^{238}U/^{206}Pb$ dates in order of acquisition (one analysis with a pre-450 Ma date is not shown). Yellow fill: magmatic zircons, pink fill: Proterozoic inheritance, green fill: not considered due to spurious negative $^{206}Pb_c$. Heavy black line and grey band: weighted mean $^{238}U/^{206}Pb$ date and its 95% confidence interval, respectively.*

Table 5: SHRIMP U-Pb zircon data from the 'northern phase' of the Braidwood Granodiorite (GSNSW 8827JAF0300; GA 1974961). All dates are $^{238}U/^{206}Pb$ unless otherwise indicated.

Sess. no.	Grain.area .replicate	$^{206}Pb_c$ (%)	U (ppm)	Th (ppm)	$^{232}Th/^{238}U$	$^{238}U/^{206}Pb$	±1σ (%)	$^{207}Pb/^{206}Pb$	±1σ (%)	Date (Ma)	±1σ (Ma)	Disc. (%)
Group 2: Proterozoic inherited individual (n = 1)												
90021	9.1.1	-0.02	415	71	0.18	5.668	4.98	0.06926	4.10	1047	48	-13
Group 1: Magmatic zircons (n = 27)												
90021	2.1.1	0.05	208	135	0.67	14.759	1.34	0.05531	1.60	422.6	5.5	1
90021	14.1.1	0.17	204	133	0.68	14.850	1.33	0.05473	2.61	420.1	5.4	-5
90021	22.1.1	0.15	170	112	0.68	14.876	1.37	0.05530	2.60	419.4	5.6	1
90021	10.1.1	0.38	177	159	0.93	14.967	1.38	0.05248	4.56	416.9	5.6	-27
90021	3.1.1	-0.14	160	102	0.66	14.991	1.36	0.05750	1.84	416.3	5.5	23
90021	6.1.1	-0.25	166	107	0.67	14.996	1.36	0.05633	2.37	416.1	5.5	12
90021	1.1.1	0.03	172	127	0.76	15.090	1.34	0.05551	1.68	413.6	5.4	5
90021	13.1.1	-0.20	228	134	0.61	15.094	1.31	0.05556	2.63	413.5	5.2	5
90021	5.1.1	0.18	226	138	0.63	15.111	1.53	0.05425	2.11	413.1	6.1	-8
90021	23.1.1	-0.06	212	152	0.74	15.148	1.31	0.05529	1.71	412.1	5.2	3
90021	15.1.1	0.13	282	179	0.66	15.155	1.47	0.05477	1.72	411.9	5.9	-2
90021	28.1.1	-0.12	148	105	0.73	15.174	1.39	0.05703	2.14	411.4	5.6	20
90021	24.1.1	0.03	310	284	0.95	15.176	1.25	0.05550	1.34	411.4	5.0	5
90021	7.1.1	0.16	240	174	0.75	15.197	1.29	0.05378	2.48	410.8	5.1	-12
90021	16.1.1	0.51	145	98	0.70	15.211	1.69	0.05173	4.10	410.5	6.7	-33
90021	27.1.1	0.01	323	244	0.78	15.230	1.24	0.05464	1.20	410.0	4.9	-3
90021	11.1.1	0.28	303	227	0.77	15.230	1.27	0.05308	2.99	410.0	5.0	-19
90021	12.1.1	0.17	194	117	0.62	15.235	1.61	0.05428	2.95	409.8	6.4	-7
90021	17.1.1	0.20	104	74	0.73	15.236	1.53	0.05291	3.73	409.8	6.1	-21
90021	19.1.1	0.19	151	89	0.61	15.262	1.41	0.05293	3.29	409.1	5.6	-20
90021	26.1.1	0.27	138	117	0.88	15.316	1.50	0.05539	4.09	407.7	5.9	5
90021	4.1.1	0.15	164	98	0.61	15.394	1.36	0.05420	2.78	405.7	5.3	-6
90021	25.1.1	-0.18	161	111	0.71	15.397	1.38	0.05651	2.41	405.7	5.4	16
90021	29.1.1	0.46	233	128	0.57	15.410	1.30	0.05184	2.91	405.3	5.1	-31
90021	8.1.1	0.65	132	82	0.65	15.428	1.44	0.05154	4.86	404.9	5.6	-35
90021	20.1.1	0.47	130	86	0.69	15.469	1.45	0.05279	4.68	403.8	5.7	-21
90021	21.1.1	0.61	189	120	0.66	15.741	1.82	0.05114	3.70	397.1	7.0	-38
Not considered, due to spurious negative $^{206}Pb_c$ (< -1%; n = 1)												
90021	18.1.1	-1.18	80	51	0.66	15.110	1.66	0.06467	4.71	413.1	6.7	85

BINDOOK GROUP: LONG FLAT VOLCANICS: KAIN PORPHYRY MEMBER

GA SAMPLENO:	**1949548**
GSNSW SITEID:	**8827JAF0193**
PARENT UNIT(S)	Bindook Group: Long Flat Volcanics
FORMAL NAME:	Kain Porphyry Member
INFORMAL NAME:	–
LITHOLOGY:	Crystal-rich porphyritic dacite
PROVINCE:	Eastern Lachlan Orogen
1:250 000 SHEET:	CANBERRA (SI/55-16)
1:100 000 SHEET:	BRAIDWOOD (8827)
LOCATION (GDA94):	35.472870 °S, 149.641893 °E
LOCATION (MGA94):	Zone 55, 739710 mE, 6071307 mN
ANALYTICAL SESSION NO(S):	90021 (see Table 1 for parameters derived from concurrent measurements of $^{238}U/^{206}Pb$ and $^{207}Pb/^{206}Pb$ reference zircons)
INTERPRETED AGE:	**414.1 ± 2.8 Ma** (95% confidence; 27 analyses of 27 zircons)
GEOLOGICAL ATTRIBUTION:	Magmatic crystallisation
ISOTOPIC RATIO(S) USED:	$^{238}U/^{206}Pb$ (^{204}Pb-corrected)

Sampling Details

This sample was taken from some large boulders beside the Bombay fire trail, about 400 m southeast of its intersection with the Cascades fire trail, and about 5 km south-southwest of the locality of Bombay.

Relationships and Rationale for Dating

The unit sampled is a massive, medium-grained porphyritic dacite of the Kain Porphyry Member (Wyborn and Owen, 1986), which is part of the Long Flat Volcanics, within the Early Devonian Bindook Group in the eastern Lachlan Orogen (Felton and Huleatt, 1976; Wyborn and Owen, 1986; Fitzherbert *et al.*, in press).

The Kain Porphyry Member is interpreted as a subvolcanic unit intruding the eruptive components of the Long Flat Volcanics, which locally comprise the 413.4 ± 2.6 Ma Kadoona Dacite Member, the 412.3 ± 2.3 Ma Toggannoggra Rhyolite Member, the 413.0 ± 2.3 Ma Manar Ignimbrite Member (Bodorkos and Simpson, 2008) and the Croppies Gunyah Rhyolite Member (GSNSW 8827CJS0070, GA 1989476; this volume). The Long Flat Volcanics are intruded by the Braidwood Granodiorite of the Braidwood Suite (GSNSW 8827JAF0300, GA 1974961; this volume), which has previously yielded SHRIMP zircon $^{238}U/^{206}Pb$ dates of 410.8 ± 3.2 Ma and 410.2 ± 3.1 Ma, and the 411.5 ± 3.1 Ma Boro Granite of the Glenbog Suite (Bodorkos and Simpson, 2008; Fitzherbert *et al.*, in press).

The aim was to obtain a magmatic crystallisation age, in order to determine whether there is any resolvable age difference between the subvolcanic Kain Porphyry Member and the eruptive units of ther Long Flat Volcanics that it intrudes. The age obtained will also be compared with new data from the Croppies Gunyah Rhyolite Member of the Long Flat Volcanics (GSNSW 8827CJS0070, GA 1989476; this volume) and the 'northern' phase of the Braidwood Granodiorite (GSNSW 8827JAF0300, GA 1974961; this volume).

Petrography

This sample is a massive, medium-grained, crystal-rich porphyritic dacite that is strongly altered. Phenocrysts up to 5 mm in length comprise about 50% of the rock, and are composed of 30% plagioclase, 15% quartz, 5% altered ferromagnesian minerals, and accessory magnetite (Figure 27). Plagioclase forms subhedral grains that have been completely sericitised, with only very faint twinning and zoning still evident. Quartz is strongly embayed, and some grains have undergone in situ fracturing. Ferromagnesian grains may originally have been amphibole and/or biotite, but have been entirely replaced by intergrown chlorite, epidote, actinolite and titanite. The groundmass is a microcrystalline quartzofeldspathic aggregate which retains a finely micropoikilitic texture (indicative of 'snowflake' devitrification) in its least-altered areas.

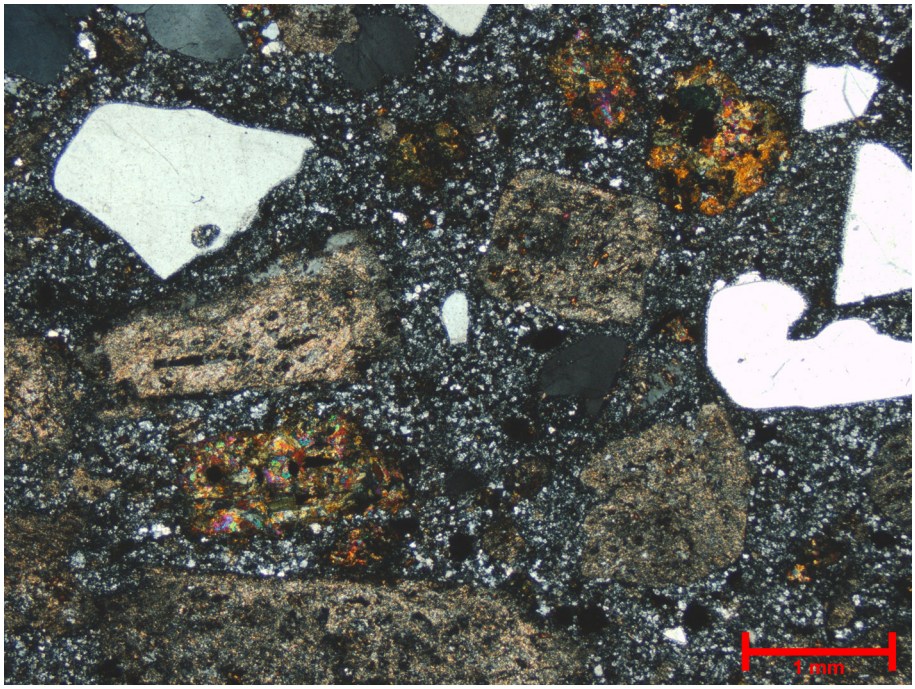

Figure 27: *Representative photomicrograph (in cross-polarised light) of the Kain Porphyry (GSNSW 8827JAF0193, GA 1949548).Porphyritic dacite contains phenocrysts of sericitised plagioclase (base and centre), quartz (right and left) and ferromagnesian minerals replaced by epidote and/or chlorite. The groundmass is massive, microcrystalline and finely micropoikilitic in texture (not obvious at this scale).*

Zircon Description

Zircons from this sample are mostly subhedral, and notably blocky to prismatic, with very few elongate crystals. Aspect ratios (length/width) are 1–3 (but mostly less than 2), and long axes are 50–250 µm. In transmitted light, the grains are predominantly transparent, and colourless to pale pink to pale yellow, and no inheritance is apparent (Figure 28). Few crystals host inclusions of any kind.

Cathodoluminescence (CL) images reveal a variety of emission patterns that contrasts with the apparent uniformity of the population in transmitted light. The intensity of the CL emission ranges from low to high, and zoning ranges from low-contrast concentric oscillatory zoning parallel to the crystal faces, through sector zoning in some grains with high CL emission, to coarser banding parallel to the long axes of the crystals. Some grains feature cores with low CL emission, which appear to have sharp, disconformable contacts with high-CL, mostly structureless overgrowths (Figure 28). Most of the zoning patterns are typical of magmatic zircon.

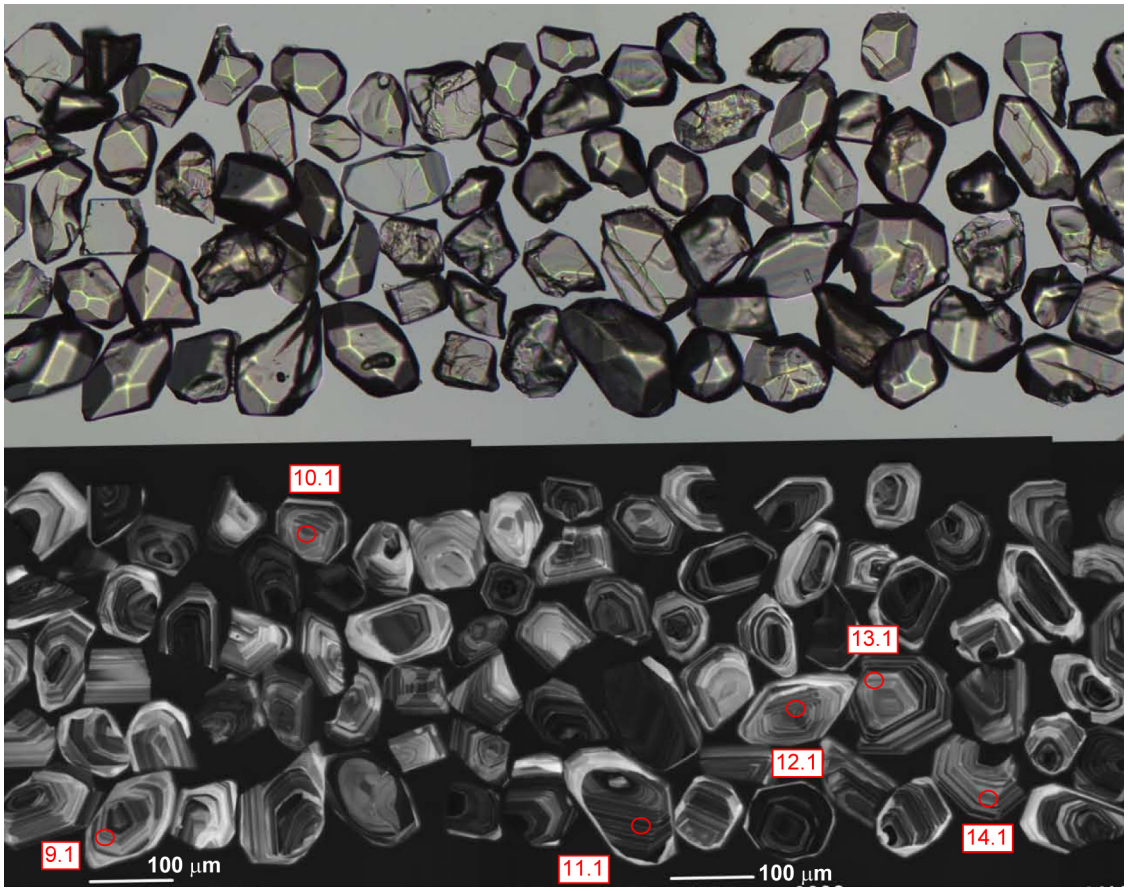

Figure 28: *Representative zircons from the Kain Porphyry (GSNSW 8827JAF0193, GA 1949548). Transmitted-light image is shown in the upper half; cathodoluminescence image in the lower half. SHRIMP analysis sites are indicated, and labelled with grain and spot number.*

U-Pb Isotopic Results

Twenty-nine analyses were obtained from 29 individual zircons, and the results are presented in Figure 29 and Table 6. The analysed zircons feature a relatively wide range of low to moderate U contents (42–595 ppm, median 124 ppm), but Th/U is uniformly moderate (0.44–0.78, median 0.58).

Two analyses (2.1.1 and 14.1.1; red fill in Figure 29) yielded high common Pb contents ($^{206}Pb_c$ > 2%), and are interpreted to have been affected by loss of radiogenic Pb during one or more events of unknown age. Their $^{238}U/^{206}Pb$ dates are unreliable, and these analyses are not considered further.

The remaining 27 analyses have uniformly low $^{206}Pb_c$ (maximum 0.84%, median 0.05%), yielded individual $^{238}U/^{206}Pb$ dates between c. 423 Ma and c. 401 Ma, and define a single group (Group 1; yellow fill in Figure 29) with a weighted mean date of 414.1 ± 2.8 Ma (MSWD = 1.00).

Geochronological Interpretation

The weighted mean date of 414.1 ± 2.8 Ma for the 27 analyses in Group 1 is indistinguishable from the median $^{238}U/^{206}Pb$ date for the same 27 analyses (414.0 +3.4/-2.6 Ma), and the absence of significant asymmetry in the uncertainties associated with the latter suggests that the group represents a single population of analyses with an approximately normal distribution. Consequently, the weighted mean $^{238}U/^{206}Pb$ date of 414.1 ± 2.8 Ma is interpreted as the best estimate of the age of magmatic crystallisation of the Kain Porphyry.

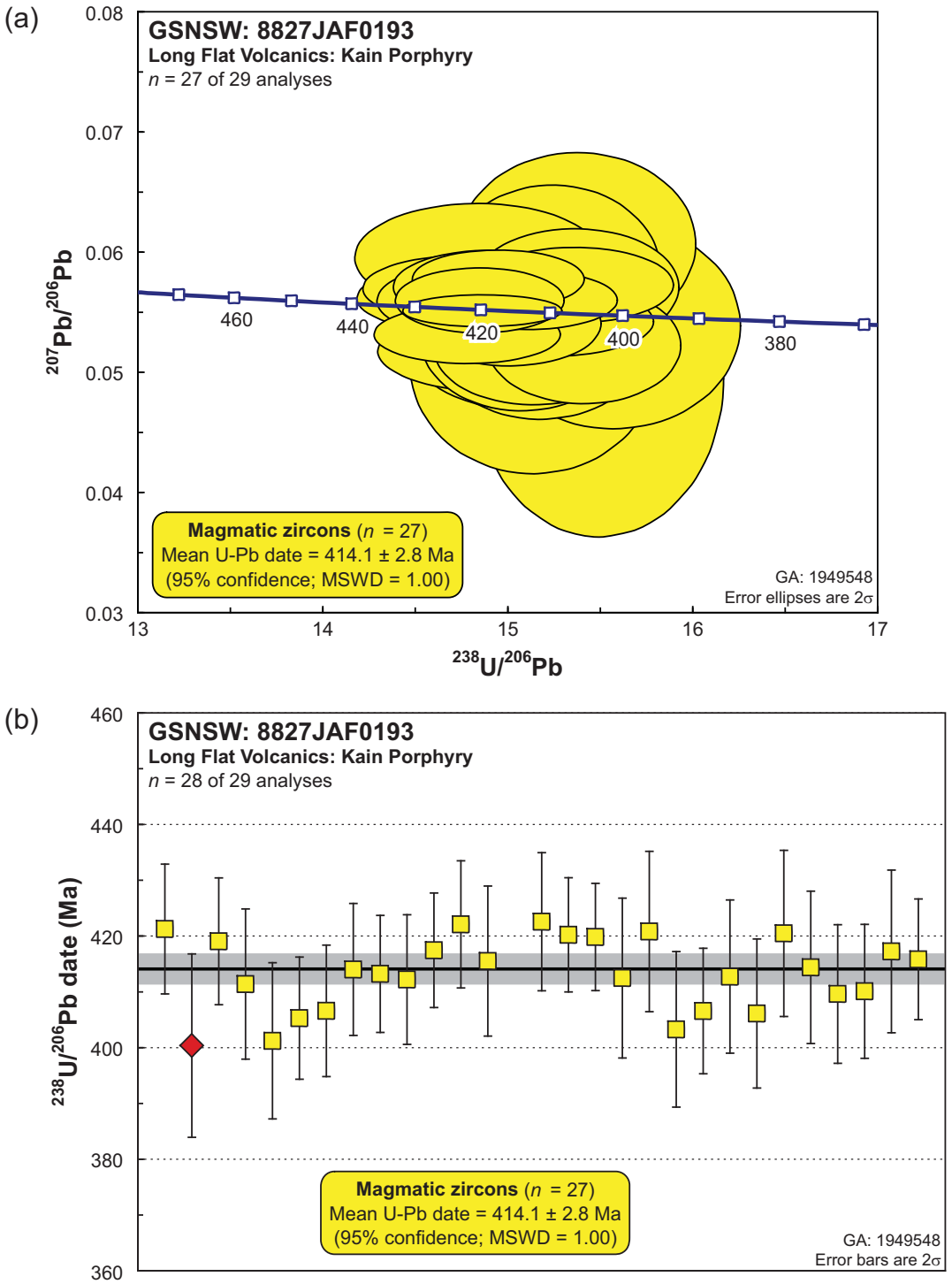

Figure 29: *SHRIMP U-Pb data for zircons from the Kain Porphyry (GSNSW 8827JAF0193, GA 1949548). One analysis with very large uncertainties (14.1.1) is not shown in either panel. (a) Tera-Wasserburg concordia diagram (analysis 2.1.1, with a very large uncertainty on $^{207}Pb/^{206}Pb$, is not shown); (b) $^{238}U/^{206}Pb$ dates in order of acquisition. Yellow fill: magmatic zircons; red fill: not considered due to high $^{206}Pb_c$. Heavy black line and grey band: weighted mean $^{238}U/^{206}Pb$ date and its 95% confidence interval, respectively.*

This age is indistinguishable from that of the 414.0 ± 2.5 Ma Croppies Gunyah Rhyolite Member (GSNSW 8827CJS0070, GA 1989476; this volume), and all three previously-dated members of the Long Flat Volcanics (i.e. the 413.4 ± 2.6 Ma Kadoona Dacite, the 412.3 ± 2.3 Ma Toggannoggra Rhyolite, and the 413.0 ± 2.3 Ma Manar Ignimbrite; Bodorkos and Simpson, 2008). The mapped intrusive relationship between the Kain Porphyry and the eruptive units of the Long Flat Volcanics (Wyborn and Owen, 1986; Fitzherbert *et al.*, in press) is not invalidated by the SHRIMP zircon data, because the apparent age reversals are not significant with respect to the uncertainties associated with each of the dates.

The magmatic crystallisation age of 414.1 ± 2.8 Ma for the Kain Porphyry is also indistinguishable from the 411.3 ± 2.6 Ma 'northern phase' of the Braidwood Granodiorite (GSNSW8827JAF0300, GA 1974961; this volume), the previously dated 'western' and 'eastern' phases of that pluton (410.8 ± 3.2 Ma and 410.2 ± 3.1 Ma; Bodorkos and Simpson, 2008), and the 411.5 ± 3.1 Ma Boro Granite of the Glenbog Suite (Bodorkos and Simpson, 2008, Fitzherbert *et al.*, in press).

Table 6: SHRIMP U-Pb zircon data from the Kain Porphyry (GSNSW 8827JAF0193, GA 1949548). All dates are $^{238}U/^{206}Pb$ unless otherwise indicated.

Sess. no.	Grain.area .replicate	$^{206}Pb_c$ (%)	U (ppm)	Th (ppm)	$^{232}Th/^{238}U$	$^{238}U/^{206}Pb$	±1σ (%)	$^{207}Pb/^{206}Pb$	±1σ (%)	Date (Ma)	±1σ (Ma)	Disc. (%)
Group 1: Magmatic zircons (n = 27)												
90021	15.1.1	-0.05	124	89	0.74	14.761	1.51	0.05697	1.98	422.6	6.2	16
90021	12.1.1	-0.05	152	80	0.54	14.778	1.39	0.05312	1.85	422.1	5.7	-21
90021	1.1.1	-0.11	130	61	0.49	14.808	1.43	0.05596	2.24	421.3	5.8	7
90021	19.1.1	-0.15	187	82	0.45	14.824	1.77	0.05617	2.14	420.8	7.2	9
90021	24.1.1	-0.34	154	115	0.77	14.837	1.83	0.05957	3.08	420.5	7.4	40
90021	16.1.1	0.16	307	162	0.55	14.846	1.26	0.05598	1.98	420.2	5.1	8
90021	17.1.1	0.05	595	256	0.44	14.860	1.18	0.05511	0.98	419.8	4.8	-1
90021	3.1.1	-0.18	139	95	0.71	14.888	1.40	0.05712	2.18	419.1	5.7	18
90021	11.1.1	-0.24	284	191	0.69	14.948	1.27	0.05775	1.73	417.5	5.1	25
90021	28.1.1	0.25	181	136	0.78	14.956	1.80	0.05176	2.74	417.2	7.3	-34
90021	29.1.1	0.20	183	115	0.65	15.008	1.34	0.05403	2.66	415.8	5.4	-10
90021	13.1.1	-0.04	74	37	0.51	15.019	1.67	0.05450	2.65	415.5	6.7	-6
90021	25.1.1	0.34	69	29	0.44	15.062	1.70	0.05323	4.89	414.4	6.8	-18
90021	8.1.1	0.42	120	80	0.69	15.076	1.47	0.05268	4.58	414.0	5.9	-24
90021	9.1.1	0.07	214	138	0.67	15.106	1.31	0.05600	1.78	413.2	5.2	9
90021	22.1.1	-0.09	63	36	0.58	15.124	1.72	0.05639	2.76	412.7	6.9	13
90021	18.1.1	0.68	61	26	0.45	15.134	1.79	0.05058	7.31	412.5	7.2	-46
90021	10.1.1	0.42	128	87	0.70	15.144	1.45	0.05182	3.62	412.2	5.8	-33
90021	4.1.1	0.52	69	39	0.58	15.175	1.69	0.05390	5.95	411.4	6.7	-11
90021	27.1.1	0.01	104	66	0.65	15.225	1.51	0.05423	2.18	410.1	6.0	-7
90021	26.1.1	-0.40	98	45	0.48	15.243	1.57	0.05822	5.18	409.6	6.2	31
90021	7.1.1	0.20	107	70	0.68	15.360	1.49	0.05708	3.50	406.6	5.9	22
90021	21.1.1	-0.15	131	55	0.44	15.361	1.43	0.05726	2.25	406.6	5.6	23
90021	23.1.1	-0.73	72	33	0.48	15.378	1.70	0.06073	5.11	406.1	6.7	55
90021	6.1.1	0.33	147	102	0.72	15.411	1.39	0.05223	3.80	405.3	5.5	-27
90021	20.1.1	0.84	68	30	0.46	15.491	1.78	0.04943	10.91	403.3	7.0	-58
90021	5.1.1	0.35	55	33	0.62	15.572	1.80	0.05384	6.52	401.2	7.0	-9
Not considered, due to high $^{206}Pb_c$ (> 2%; n = 2)												
90021	2.1.1	2.39	42	21	0.51	15.607	2.12	0.03933	19.47	400.4	8.2	-199
90021	14.1.1	30.17	115	67	0.60	16.899	5.44	0.04681	72.16	370.6	19.6	-89

BINDOOK GROUP: LONG FLAT VOLCANICS: CROPPIES GUNYAH RHYOLITE MEMBER

GA SAMPLENO:	**1989476**
GSNSW SITEID:	**8827CJS0070**
PARENT UNIT(S)	Bindook Group: Long Flat Volcanics
FORMAL NAME:	Croppies Gunyah Rhyolite Member
INFORMAL NAME:	–
LITHOLOGY:	Densely-welded rhyolitic ignimbrite
PROVINCE:	Eastern Lachlan Orogen
1:250 000 SHEET:	CANBERRA (SI/55-16)
1:100 000 SHEET:	BRAIDWOOD (8827)
LOCATION (GDA94):	35.202012 °S, 149.726991 °E
LOCATION (MGA94):	Zone 55, 748261 mE, 6101147 mN
ANALYTICAL SESSION NO(S):	90093 (see Table 1 for parameters derived from concurrent measurements of $^{238}U/^{206}Pb$ and $^{207}Pb/^{206}Pb$ reference zircons)
INTERPRETED AGE:	**414.0 ± 2.5 Ma** (95% confidence; 26 analyses of 26 zircons)
GEOLOGICAL ATTRIBUTION:	Magmatic crystallisation
ISOTOPIC RATIO(S) USED:	$^{238}U/^{206}Pb$ (^{204}Pb-corrected)

Sampling Details

This sample was taken from some low, weathered outcrops about 50 m east of a north-south trending farm track, about 2 km south of its intersection with Lower Boro Road, and about 1 km south of Bunnerong homestead.

Relationships and Rationale for Dating

The unit sampled is a weakly-foliated, densely-welded rhyolitic ignimbrite of the Croppies Gunyah Rhyolite Member (Fitzherbert *et al.*, in press), which is part of the Long Flat Volcanics, within the Early Devonian Bindook Group in the eastern Lachlan Orogen (Felton and Huleatt, 1976; Wyborn and Owen, 1986; Fitzherbert *et al.*, in press).

The Croppies Gunyah Rhyolite Member is interpreted as one of the lowermost units of the eruptive components of the Long Flat Volcanics: it locally underlies the 413.0 ± 2.3 Ma Manar Ignimbrite Member, and is possibly a lateral equivalent of the 413.4 ± 2.6 Ma Kadoona Dacite Member or the conformably overlying 412.3 ± 2.3 Ma Toggannoggra Rhyolite Member in southwestern BRAIDWOOD (Bodorkos and Simpson, 2008). The Long Flat Volcanics are intruded by the Braidwood Granodiorite of the Braidwood Suite, which has previously yielded SHRIMP zircon $^{238}U/^{206}Pb$ dates of 410.8 ± 3.2 Ma and 410.2 ± 3.1 Ma, as well as the 411.5 ± 3.1 Ma Boro Granite of the Glenbog Suite (Bodorkos and Simpson, 2008; Fitzherbert *et al.*, in press).

The aim was to obtain a magmatic crystallisation age for the lower part of the Long Flat Volcanics, for comparison with the existing data described above. The age will also be compared with new data from the Kain Porphyry (GSNSW 8827JAF0193, GA 1949548; this volume), which intrudes the Croppies Gunyah Rhyolite Member, and the northern phase of the Braidwood Granodiorite (GSNSW 8827JAF0300, GA 1974961; this volume).

Petrography

This sample is a medium-grained, densely welded rhyolitic ignimbrite with a weak overprinting tectonic fabric that has enhanced the pyroclastic features. Phenocrysts (whole and fragmented) up to 5 mm in length comprise about 35% of the rock, and are composed of 18% plagioclase, 10% quartz, 5% K-feldspar, and 2% biotite (Figure 30). Plagioclase forms equant to tabular phenocrysts that are strongly sericitised, however, tabular crystals of perthitic K-feldspar are only lightly clay-dusted. Quartz crystals are embayed and strained, and some have undergone in situ fracturing. Biotite laths have been entirely replaced by chlorite and fine-grained opaque oxide minerals (probably magnetite). Accessory minerals include apatite, zircon and allanite. The matrix is a very finely microcrystalline quartzofeldspathic mosaic that contains highly attenuated relict shards and lenses (up to 9 mm long) of slightly more coarsely microcrystalline material with fine-grained spherulitic texture. Some of the larger lenses contain 'microphenocrysts' of quartz or feldspar, and are interpreted as flattened pumice clasts.

Figure 30: *Representative photomicrograph (in cross-polarised light) of the Croppies Gunyah Rhyolite (GSNSW 8827CJS0070, GA 1989476). Densely welded rhyolitic ignimbrite contains crystals of quartz (right), altered plagioclase (lower left), K-feldspar (top right), and rare chloritised biotite (top centre). The finely microcrystalline, welded matrix contains lenses of more coarsely microcrystalline material (upper half), which are interpreted as strongly flattened pumice clasts.*

Zircon Description

Zircons from this sample are predominantly euhedral and range from equant to prismatic, with very few elongate crystals. Aspect ratios (length/width) are 1–3 (but mostly less than 2), and long axes are 40–220 µm. In transmitted light, the grains are transparent to translucent and pale- to medium-brown. Few crystals host inclusions of any kind, but many grains have undergone fine-scale cracking, and some display brown staining in their central areas (Figure 31).

Cathodoluminescence (CL) images reveal a variety of emission intensities, but also highlight a relatively consistent pattern of concentric oscillatory zoning with moderate to high contrast, which

suggests that the population is predominantly of magmatic origin. Some grains feature cores with high CL emission, which appear to have sharp, disconformable contacts with dark, concentrically-zoned overgrowths (Figure 31), and it is likely that such cores represent zircon inheritance.

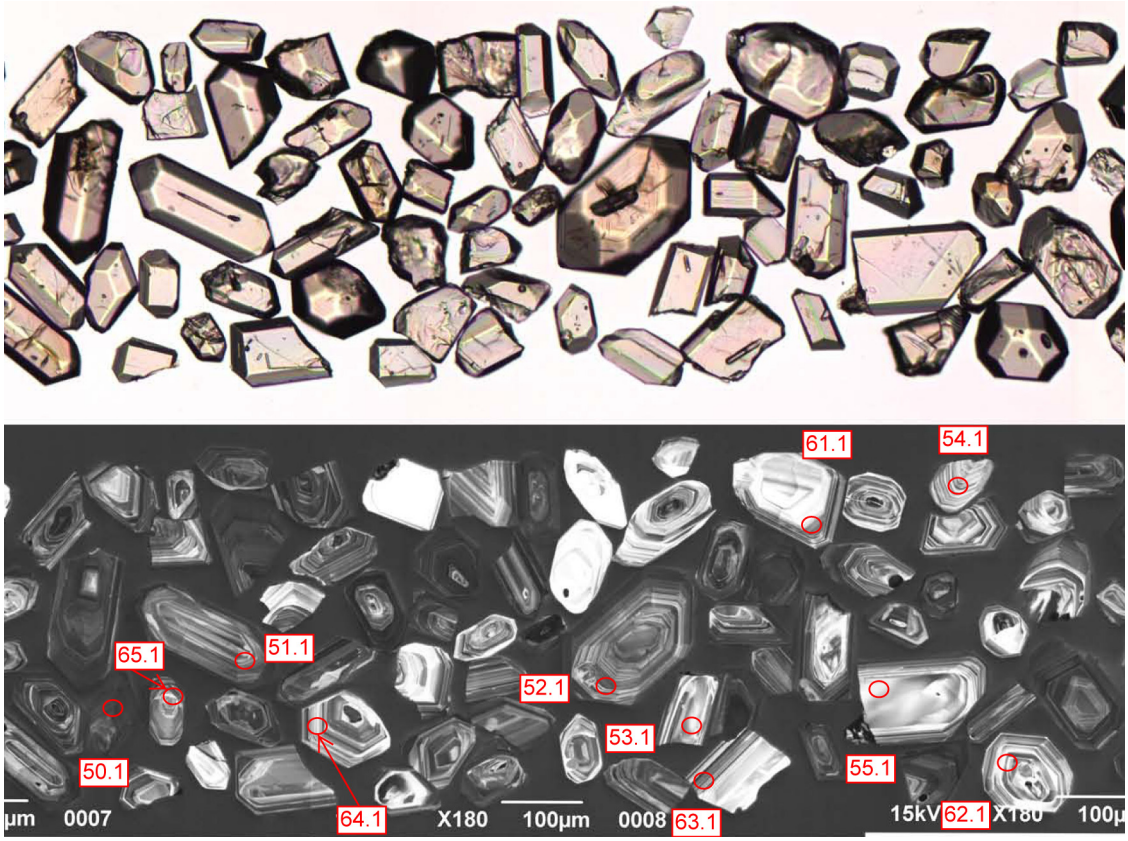

Figure 31: *Representative zircons from the Croppies Gunyah Rhyolite (GSNSW 8827CJS0070, GA 1989476). Transmitted-light image is shown in the upper half; cathodoluminescence image in the lower half. SHRIMP analysis sites are indicated, and labelled with grain and spot number.*

U-Pb Isotopic Results

Thirty-nine analyses were obtained from 39 individual zircons, and the results are presented in Figure 32 and Table 7. The analysed zircons feature a relatively wide range of U contents (55–887 ppm, median 254 ppm), but consistently moderate Th/U (0.42–1.14, median 0.56).

Five analyses (48.1.1, 49.1.1, 53.1.1, 58.1.1, and 67.1.1; not shown in Figure 32) were adversely affected by instrumental instability during data acquisition, and are not considered further. An additional five analyses (42.1.1, 44.1.1, 56.1.1, 57.1.1, and 60.1.1; red fill in Figure 32) yielded high common Pb contents ($^{206}Pb_c$ > 1.3%), and are interpreted to have been affected by loss of radiogenic Pb during one or more events of unknown age. Consequently, their $^{238}U/^{206}Pb$ dates are unreliable, and these analyses are not considered further.

The remaining 29 analyses are mostly characterised by low $^{206}Pb_c$ (maximum 1.09%, median 0.12%), and can be divided into three groups (Table 7):

- 26 analyses of 26 zircons (Group 1; yellow fill in Figure 32) with individual $^{238}U/^{206}Pb$ dates between c. 423 Ma and c. 403 Ma, which yielded a weighted mean date of 414.0 ± 2.5 Ma (MSWD =1.38),
- a single analysis (Group 2; blue fill in Figure 32) with a $^{207}Pb/^{206}Pb$ date of 1179 ± 32 Ma (2σ), and
- two analyses of two zircons (Group 3; white fill in Figure 32) with individual $^{238}U/^{206}Pb$ dates between c. 402 Ma and c. 399 Ma.

Geochronological Interpretation

The weighted mean date of 414.0 ± 2.5 Ma for the 26 analyses in Group 1 is indistinguishable from the median $^{238}U/^{206}Pb$ date for the same 26 analyses (415.2 +1.7/-2.5 Ma), and the absence of significant asymmetry in the uncertainties associated with the latter suggests that the group represents a single population of analyses with an approximately normal distribution.

Consequently, the weighted mean $^{238}U/^{206}Pb$ date of 414.0 ± 2.5 Ma is interpreted as the best estimate of the age of magmatic crystallisation of the Croppies Gunyah Rhyolite. The single 1179 ± 32 Ma (2σ) analysis in Group 2 is interpreted as an inherited individual of Proterozoic age.

The magmatic crystallisation age of 414.0 ± 2.5 Ma for the Croppies Gunyah Rhyolite is indistinguishable from that of the cross-cutting 414.1 ± 2.8 Ma Kain Porphyry (GSNSW 8827JAF0193, GA 1949548; this volume), and the mapped intrusive relationship between the Kain Porphyry and the eruptive units of the Long Flat Volcanics (Wyborn and Owen, 1986; Fitzherbert *et al.*, in press) is not invalidated by the SHRIMP zircon data, because the apparent age reversal is not significant with respect to the uncertainties associated with each of the dates.

In broader comparison with existing SHRIMP zircon $^{238}U/^{206}Pb$ dates, the magmatic crystallisation age of 414.0 ± 2.5 Ma for the Croppies Gunyah Rhyolite is indistinguishable from those of the 413.0 ± 2.3 Ma Manar Ignimbrite, the 413.4 ± 2.6 Ma Kadoona Dacite, and the 412.3 ± 2.3 Ma Toggannoggra Rhyolite (Bodorkos and Simpson, 2008). It is also indistinguishable from the 411.3 ± 2.6 Ma 'northern phase' of the Braidwood Granodiorite (GSNSW 8827JAF0300, GA 1974961; this volume), as well as the 410.8 ± 3.2 Ma 'western phase' and the 410.2 ± 3.1 Ma 'eastern phase' of that pluton, and the nearby 411.5 ± 3.1 Ma Boro Granite of the Glenbog Suite (Bodorkos and Simpson, 2008).

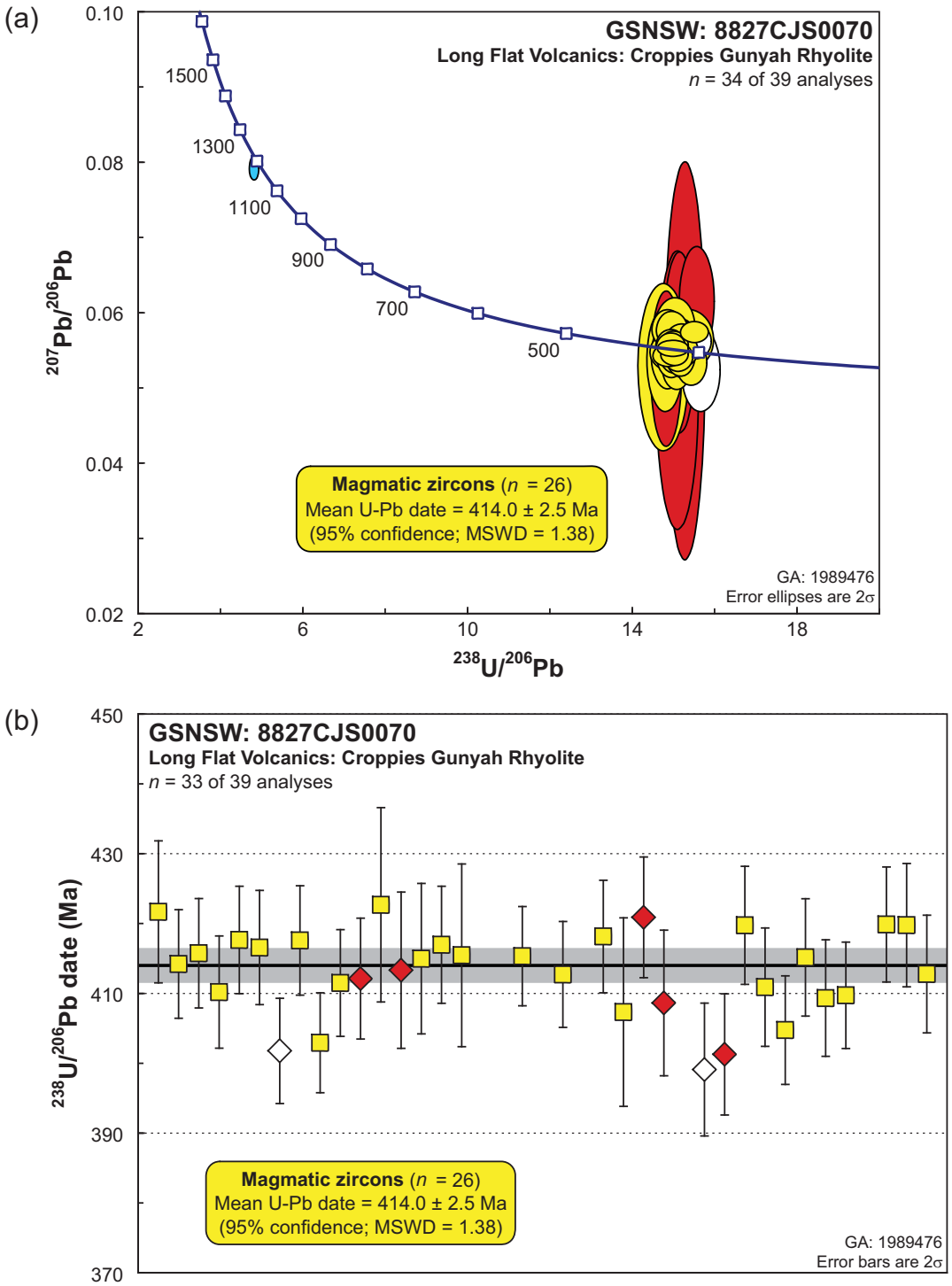

Figure 32: *SHRIMP U-Pb data for zircons from the Croppies Gunyah Rhyolite (GSNSW 8827CJS0070, GA 1989476). Five analyses affected by instrumental instability (48.1.1, 49.1.1, 53.1.1, 58.1.1 and 67.1.1) are not shown in either panel. (a) Tera-Wasserburg concordia diagram; (b) $^{238}U/^{206}Pb$ dates in order of acquisition (one analysis with a pre-450 Ma date is not shown). Yellow fill: magmatic zircons; blue fill: Mesoproterozoic inheritance; white fill: affected by loss of radiogenic Pb; red fill: not considered due to high $^{206}Pb_c$. Heavy black line and grey band: weighted mean $^{238}U/^{206}Pb$ date and its 95% confidence interval, respectively. Five analyses (48.1.1, 49.1.1, 53.1.1, 58.1.1 and 67.1.1) are not shown.*

Table 7: SHRIMP U-Pb zircon data from the Croppies Gunyah Rhyolite (GSNSW 8827CJS0070, GA 1989476). All dates are $^{238}U/^{206}Pb$ unless otherwise indicated.

Sess. no.	Grain.area .replicate	$^{206}Pb_c$ (%)	U (ppm)	Th (ppm)	$^{232}Th/^{238}U$	$^{238}U/^{206}Pb$	±1σ (%)	$^{207}Pb/^{206}Pb$	±1σ (%)	Date (Ma)	±1σ (Ma)	Disc. (%)
Group 2: Mesoproterozoic inherited individual (n = 1; $^{207}Pb/^{206}Pb$ date tabulated)												
90093	51.1.1	0.08	238	119	0.52	4.802	0.96	0.07927	0.81	1179	16	-3
Group 1: Magmatic zircons (n = 26)												
90093	43.1.1	1.09	55	31	0.58	14.757	1.70	0.05272	8.66	422.7	7.0	-25
90093	32.1.1	0.57	102	48	0.48	14.793	1.25	0.05374	5.27	421.7	5.1	-15
90093	68.1.1	0.08	582	302	0.54	14.859	1.01	0.05433	1.15	419.9	4.1	-8
90093	69.1.1	0.39	202	87	0.45	14.862	1.09	0.05424	3.30	419.8	4.4	-9
90093	61.1.1	-0.17	224	98	0.45	14.863	1.04	0.05786	1.80	419.8	4.2	25
90093	54.1.1	0.07	252	113	0.46	14.922	0.99	0.05551	1.67	418.1	4.0	4
90093	36.1.1	-0.02	347	382	1.14	14.941	0.95	0.05546	1.32	417.6	3.8	3
90093	39.1.1	0.20	336	159	0.49	14.943	0.97	0.05445	2.32	417.6	3.9	-7
90093	46.1.1	0.02	217	121	0.58	14.966	1.04	0.05768	1.72	417.0	4.2	24
90093	37.1.1	0.03	887	486	0.57	14.981	1.01	0.05524	0.82	416.6	4.1	1
90093	34.1.1	0.05	289	211	0.75	15.011	0.97	0.05564	1.36	415.7	3.9	5
90093	47.1.1	-0.03	172	95	0.57	15.022	1.63	0.05478	2.01	415.5	6.5	-3
90093	50.1.1	0.13	717	293	0.42	15.027	0.88	0.05447	1.16	415.3	3.6	-6
90093	64.1.1	0.20	216	121	0.58	15.033	1.04	0.05488	2.19	415.2	4.2	-2
90093	45.1.1	-0.17	80	59	0.76	15.040	1.34	0.05808	2.76	415.0	5.4	28
90093	33.1.1	0.32	314	154	0.50	15.068	0.97	0.05294	2.46	414.2	3.9	-21
90093	70.1.1	0.16	228	144	0.65	15.123	1.05	0.05618	2.17	412.8	4.2	11
90093	52.1.1	0.12	359	197	0.57	15.125	0.95	0.05406	1.44	412.7	3.8	-10
90093	41.1.1	0.14	342	173	0.52	15.171	0.96	0.05413	1.96	411.5	3.8	-9
90093	62.1.1	-0.06	234	127	0.56	15.194	1.06	0.05622	1.66	410.9	4.2	12
90093	35.1.1	0.34	253	158	0.65	15.221	1.01	0.05547	2.67	410.2	4.0	5
90093	66.1.1	0.07	371	176	0.49	15.239	0.96	0.05497	1.60	409.7	3.8	0
90093	65.1.1	0.24	225	108	0.50	15.254	1.05	0.05431	2.29	409.3	4.2	-6
90093	55.1.1	0.11	99	65	0.68	15.332	1.71	0.05640	2.96	407.3	6.7	15
90093	63.1.1	0.45	306	221	0.75	15.433	0.99	0.05330	2.29	404.7	3.9	-16
90093	40.1.1	-0.01	495	243	0.51	15.504	0.92	0.05740	0.98	402.9	3.6	26
Group 3: Affected by loss of radiogenic Pb (n = 2)												
90093	38.1.1	0.18	305	247	0.84	15.550	0.97	0.05614	1.68	401.8	3.8	14
90093	59.1.1	0.77	115	52	0.47	15.658	1.23	0.05238	4.38	399.1	4.8	-24
Not considered, due to high $^{206}Pb_c$ (> 1.3%; n = 5)												
90093	56.1.1	3.54	400	160	0.41	14.822	1.06	0.05253	8.06	420.9	4.3	-27
90093	44.1.1	15.69	420	295	0.73	15.102	1.40	0.04965	15.30	413.3	5.6	-57
90093	42.1.1	11.40	397	331	0.86	15.148	1.08	0.05603	8.80	412.1	4.3	10
90093	57.1.1	5.62	246	150	0.63	15.281	1.32	0.05356	20.24	408.6	5.2	-14
90093	60.1.1	1.31	188	82	0.45	15.570	1.11	0.06151	4.85	401.3	4.3	64
Not considered, due to instrumental instability (n = 5)												
90093	58.1.1	0.46	258	177	0.71	14.767	1.02	0.05372	2.59	422.4	4.2	-15
90093	67.1.1	0.49	326	178	0.56	14.806	1.14	0.05201	2.26	421.3	4.7	-32
90093	48.1.1	0.03	234	193	0.85	15.290	1.48	0.06214	9.15	408.4	5.8	66
90093	49.1.1	0.07	491	173	0.36	15.536	0.91	0.05494	1.09	402.1	3.6	2
90093	53.1.1	0.14	174	130	0.77	15.799	1.29	0.05615	2.59	395.6	4.9	16

Moss Vale and Burragorang 1:100 000 sheet areas

TOUGA GRANITE

GA SAMPLENO:	**1985433**
GSNSW SITEID:	**8928LMC0363**
PARENT UNIT(S):	—
FORMAL NAME:	Touga Granite
INFORMAL NAME:	—
LITHOLOGY:	Melanocratic hornblende granodiorite
PROVINCE:	Eastern Lachlan Orogen
1:250 000 SHEET:	WOLLONGONG (SI/56-9)
1:100 000 SHEET:	MOSS VALE (8928)
LOCATION (GDA94):	34.960106 °S, 150.068406 °E
LOCATION (MGA94):	Zone 56, 232317 mE, 6127455 mN
ANALYTICAL SESSION NO(S):	90064 (see Table 1 for parameters derived from concurrent measurements of $^{238}U/^{206}Pb$ and $^{207}Pb/^{206}Pb$ reference zircons)
INTERPRETED AGE:	**325.5 ± 2.6 Ma** (95% confidence; 29 analyses of 29 zircons)
GEOLOGICAL ATTRIBUTION:	Magmatic crystallisation
ISOTOPIC RATIO(S) USED:	$^{238}U/^{206}Pb$ (^{204}Pb-corrected)

Sampling Details

This sample was taken from some fresh outcrops in the bed of a steep-sided creek, about 1 km east of the Shoalhaven River, and about 1.5 km west of Touga homestead.

Relationships and Rationale for Dating

The unit sampled is a melanocratic hornblende-bearing granodiorite of the Touga Granite, which intrudes Ordovician turbiditic sedimentary rocks of the Adaminaby Group in the eastern Lachlan Orogen, and was assumed to be of Carboniferous age (Rose, 1966).

This sample was selected for SHRIMP analysis in order to test the hypothesis that the Touga Granite is contemporaneous with other plutonic rocks of assumed Carboniferous age in southern MOSS VALE, including the undated Tullyangela Granite and Bundundah Granite. The latter intrudes the Late Devonian Yalwal Volcanics (which include the Grassy Gully Rhyolite Member: GSNSW 8928LMC0073, GA 1985436; this volume), and is unconformably overlain by the Permian Snapper Point Formation, within the Shoalhaven Group of the Sydney Basin (Rose, 1966; Trigg and Campbell, in prep.). Carboniferous felsic rocks on BATHURST (Pogson and Watkins, 1998) and DUBBO (Meakin and Morgan, 1999), some 200–300 km to the north-northwest, yielded SHRIMP zircon $^{238}U/^{206}Pb$ dates ranging from 340.7 ± 3.2 Ma to 314 ± 8 Ma (Fanning, 1997; Black, 1998).

The aim was to obtain a magmatic crystallisation age for the Touga Granite, for comparison with that of the nearby Tullyangela Granite (GSNSW 8928LMC0364, GA 1985434; this volume), the Bundundah Granite (GSNSW 8928LMC0365, GA 1985435; this volume), and the Grassy Gully Rhyolite Member (GSNSW 8928LMC0073, GA 1985436; this volume).

Petrography

This sample is an even- and medium-grained (2–3 mm) melanocratic and quartz-poor hornblende granodiorite, which in hand specimen contains abundant very pale green vitreous plagioclase, biotite, amphibole and very clear quartz. In thin section, the rock comprises 45% plagioclase, 16% quartz, 13% K-feldspar, 12% hornblende, 8% biotite, 3% clinopyroxene, 2% opaque oxide minerals, 1% titanite, and accessory zircon and conspicuous bladed apatite. Plagioclase of andesine composition ($An_{34–42}$) occurs as subhedral tabular crystals that are often clustered (Figure 33). Hornblende is pale- to olive-green in colour, and is unevenly distributed. In one half of the thin section, it forms large and irregular but optically continuous crystals that include small, elongate chadacrysts of plagioclase: in the other half, hornblende occurs as isolated subhedral grains, and in small aggregates with biotite and minor relic clinopyroxene. Biotite is pale to mid tan in colour, and occurs as subhedral laths and more irregular anhedral grains. Clinopyroxene is colourless and forms anhedral laths, most of which have been partly replaced by hornblende, biotite, or both (Figure 33). Quartz is mainly interstitial, and occurs predominantly as small, irregular grains associated with plagioclase. K-feldspar is also interstitial, but forms larger micropoikilitic grains that host inclusions of earlier-crystallised minerals. Some of the opaque oxide minerals display square and rhombic crystal shapes, and are probably magnetite. Titanite forms skeletal crystals up to 4 mm in length, within aggregates of plagioclase grains.

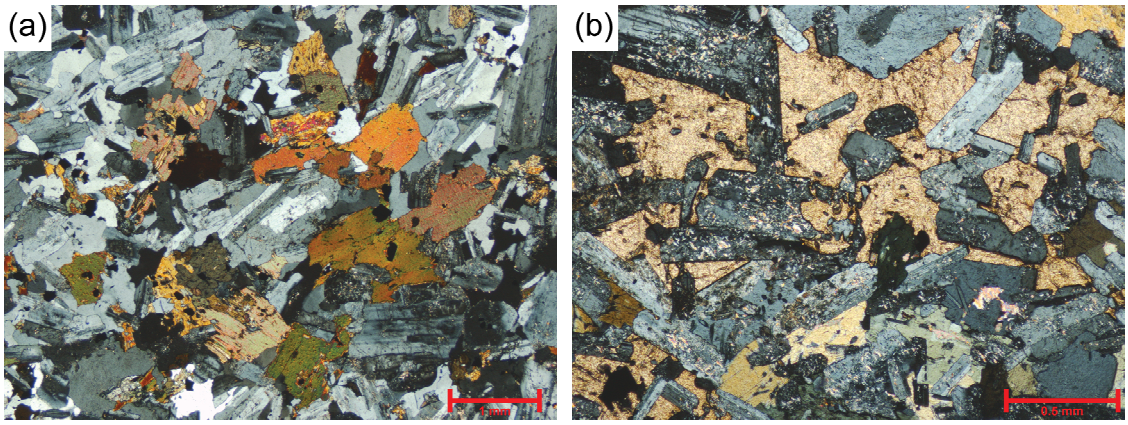

Figure 33: *Representative photomicrographs (in cross-polarised light) of the Touga Granite (GSNSW 8928LMC0363, GA 1985433). (a) Granodiorite with abundant bladed plagioclase crystals, hornblende (centre left, and near top), biotite (centre right), interstitial quartz and K-feldspar, and a small anhedral grain of relic clinopyroxene enclosed by hornblende (red and yellow grain, upper centre). (b) Optically continuous titanite crystal (upper half and lower left) enclosing smaller crystals of lightly sericitised plagioclase. Greenish hornblende grains (lower half) display a similar subophitic texture.*

Zircon Description

Zircons from this sample are mostly subhedral to anhedral, with external morphologies ranging from rounded grains to equant prismatic crystals. Aspect ratios (length/width) are 1–4 (but rarely exceed 3), and long axes are 90–350 µm (Figure 34). In transmitted light, the zircons are mostly translucent (with subordinate transparent grains), and predominantly pale- to medium-brown. Small inclusions of pale- and dark-coloured minerals are common in some crystals, but many grains display longitudinal cracking and/or fracturing in their central areas.

Cathodoluminescence (CL) images reveal a range of emission patterns. Although CL intensity varies strongly from grain to grain, many of the larger anhedral crystals are characterised by broad, low-contrast concentric oscillatory or sector zoning. Smaller, subhedral grains feature high-contrast

broad banding parallel to the long axes (Figure 34), and these zoning patterns are typical of magmatic zircon. Rare crystals host small, rounded central regions disconformably overgrown by mantles of sharply contrasting CL intensity, and these cores are interpreted as inheritance.

Figure 34: *Representative zircons from the Touga Granite (GSNSW 8928LMC0363, GA 1985433). Transmitted-light image is shown in the upper half; cathodoluminescence image in the lower half. SHRIMP analysis sites are indicated, and labelled with grain and spot number.*

U-Pb Isotopic Results

Thirty-one analyses were obtained from 30 individual zircons (with grain 1 analysed twice), and the results are presented in Figure 35, and Table 8. The analysed zircons are characterised by widely varied U contents (84–1618 ppm, median 318 ppm), and similarly scattered, although generally high, Th/U (0.06–1.35, median 0.95).

The 31 analyses are mostly characterised by low $^{206}Pb_c$ (maximum 1.42%, median 0.22%), and can be divided into two groups (Table 8):

- 29 analyses of 29 zircons (Group 1; yellow fill in Figure 35) with individual $^{238}U/^{206}Pb$ dates between c. 339 Ma and c. 316 Ma, which yielded a weighted mean date of 325.5 ± 2.6 Ma (MSWD = 1.40), and
- two analyses of two zircons (Group 2; pink fill in Figure 35) with individual $^{238}U/^{206}Pb$ dates between c. 346 Ma and c. 345 Ma, which yielded a weighted mean date of 345.5 ± 6.3 Ma (MSWD = 0.01).

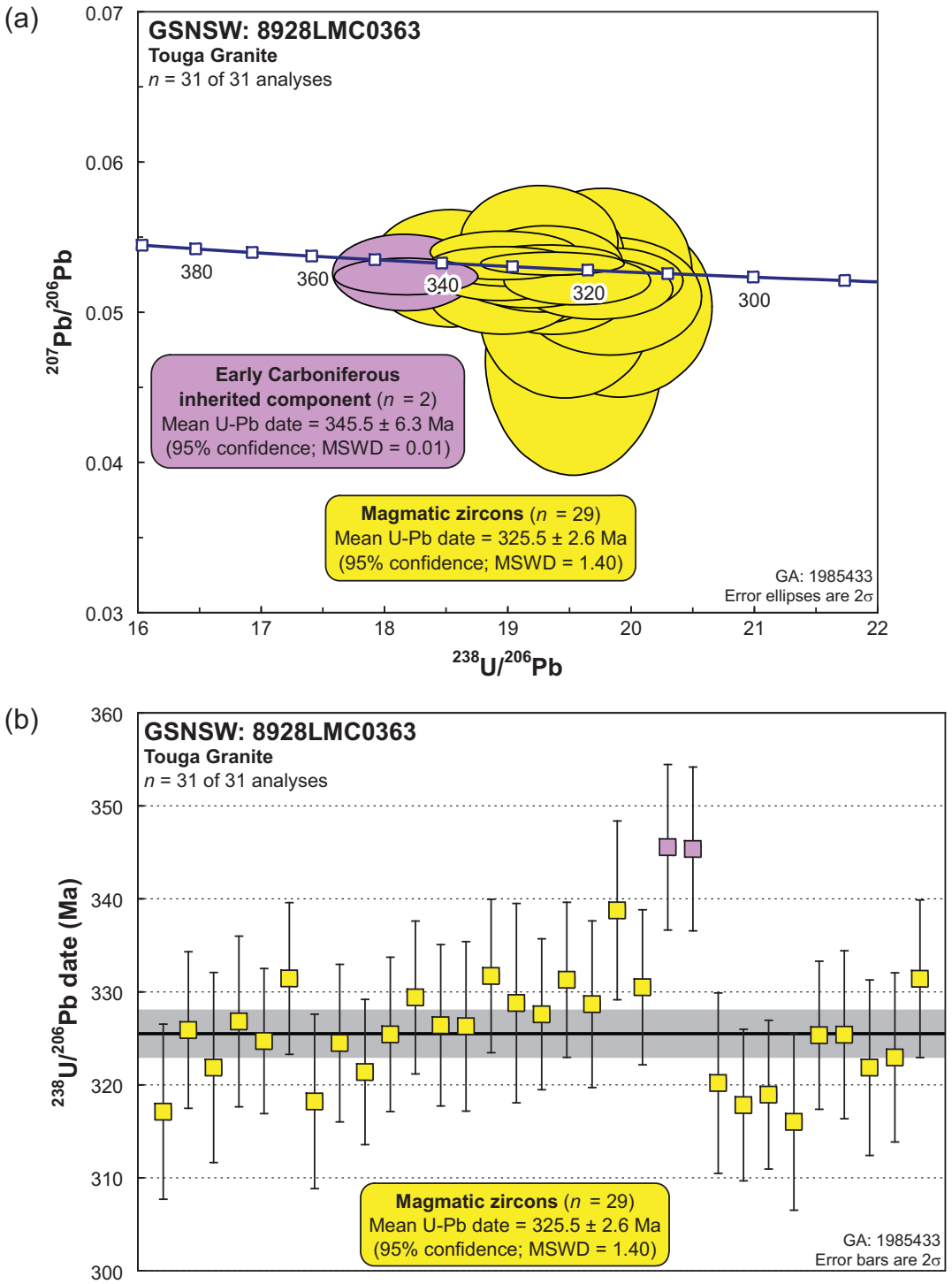

Figure 35: *SHRIMP U-Pb data for zircons from the Touga Granite (GSNSW 8928LMC0363, GA 1985433). (a) Tera-Wasserburg concordia diagram; (b) $^{238}U/^{206}Pb$ dates in order of acquisition. Yellow fill: magmatic zircons; pink fill: Early Carboniferous inheritance. Heavy black line and grey band: weighted mean $^{238}U/^{206}Pb$ date and its 95% confidence interval, respectively.*

Geochronological Interpretation

The weighted mean date of 325.5 ± 2.6 Ma obtained from the 29 analyses in Group 1 is indistinguishable from the median $^{238}U/^{206}Pb$ date for the same 29 analyses (325.4 +2.2/-2.5 Ma), and the absence of significant asymmetry in the uncertainties associated with the latter suggests that Group 1 represents a single population of analyses with an approximately normal distribution.

Consequently, the weighted mean $^{238}U/^{206}Pb$ date of 325.5 ± 2.6 Ma is interpreted as the best estimate of the age of magmatic crystallisation of the Touga Granite. The weighted mean $^{238}U/^{206}Pb$ date of 345.5 ± 6.3 Ma obtained from the two analyses in Group 2 is interpreted to reflect inheritance from one or more sources containing Early Carboniferous zircons.

The magmatic crystallisation age of 325.5 ± 2.6 Ma for the Touga Granite is indistinguishable from that of the 324.4 ± 3.2 Ma Bundundah Granite to the east (GSNSW 8928LMC0365, GA 1985435; this volume) and establishes Middle Carboniferous plutonism in southern MOSS VALE. However, both intrusions are substantially younger than the 382.4 ± 3.0 Ma Tullyangela Granite (GSNSW 8928LMC0364, GA 1985434; this volume), with which they were previously grouped (Rose, 1966). The Tullyangela Granite appears instead to be temporally associated with Late Devonian eruption of the nearby Yalwal Volcanics, which include the 384.5 ± 4.4 Ma Grassy Gully Rhyolite Member (GSNSW 8928LMC0073, GA 1985436; this volume).

Table 8: SHRIMP U-Pb zircon data from the Touga Granite (GSNSW 8928LMC0363, GA 1985433). All dates are $^{238}U/^{206}Pb$ unless otherwise indicated.

Sess. no.	Grain.area .replicate	$^{206}Pb_c$ (%)	U (ppm)	Th (ppm)	$^{232}Th/^{238}U$	$^{238}U/^{206}Pb$	±1σ (%)	$^{207}Pb/^{206}Pb$	±1σ (%)	Date (Ma)	±1σ (Ma)	Disc. (%)
Group 2: Early Carboniferous inherited component (n = 2)												
90064	20.1.1	0.26	341	394	1.19	18.160	1.32	0.05264	1.99	345.6	4.4	-9
90064	21.1.1	0.05	1195	672	0.58	18.170	1.31	0.05238	0.95	345.4	4.4	-13
Group 1: Magmatic zircons (n = 29)												
90064	1.2.1	0.29	160	162	1.04	18.534	1.46	0.05294	3.03	338.8	4.8	-4
90064	14.1.1	0.12	551	606	1.14	18.939	1.28	0.05261	1.43	331.7	4.1	-6
90064	6.1.1	0.00	636	56	0.09	18.954	1.26	0.05326	0.84	331.4	4.1	3
90064	30.1.1	0.25	374	302	0.83	18.956	1.31	0.05126	2.20	331.4	4.2	-24
90064	17.1.1	0.01	456	472	1.07	18.963	1.29	0.05402	1.04	331.3	4.2	12
90064	19.1.1	0.03	424	271	0.66	19.009	1.29	0.05324	1.16	330.5	4.2	3
90064	11.1.1	0.13	504	658	1.35	19.075	1.28	0.05253	1.38	329.4	4.1	-6
90064	15.1.1	0.68	84	60	0.73	19.111	1.67	0.04977	8.37	328.8	5.4	-44
90064	18.1.1	0.22	417	402	1.00	19.117	1.40	0.05147	1.86	328.7	4.5	-20
90064	16.1.1	0.18	619	508	0.85	19.183	1.27	0.05211	1.43	327.6	4.1	-11
90064	4.1.1	0.27	151	132	0.90	19.229	1.44	0.05334	2.95	326.8	4.6	5
90064	12.1.1	0.44	291	319	1.13	19.254	1.36	0.05472	2.79	326.4	4.3	23
90064	13.1.1	0.13	161	139	0.89	19.261	1.43	0.05414	2.53	326.3	4.6	16
90064	2.1.1	0.13	313	324	1.07	19.285	1.32	0.05231	1.81	325.9	4.2	-8
90064	10.1.1	0.17	371	405	1.13	19.313	1.31	0.05330	1.88	325.4	4.1	5
90064	27.1.1	0.10	160	148	0.95	19.316	1.42	0.05186	2.30	325.4	4.5	-14
90064	26.1.1	-0.02	708	494	0.72	19.319	1.26	0.05346	0.79	325.3	4.0	7
90064	5.1.1	0.04	1618	101	0.06	19.357	1.23	0.05323	0.59	324.7	3.9	4
90064	8.1.1	0.31	287	213	0.76	19.371	1.34	0.05147	2.35	324.5	4.2	-19
90064	29.1.1	0.57	163	161	1.02	19.465	1.44	0.04958	4.39	322.9	4.6	-46
90064	3.1.1	1.42	100	91	0.94	19.533	1.63	0.04593	9.74	321.9	5.1	-102
90064	28.1.1	0.83	135	141	1.08	19.534	1.50	0.04690	6.81	321.8	4.7	-86
90064	9.1.1	0.21	926	734	0.82	19.563	1.25	0.05211	1.26	321.4	3.9	-10
90064	22.1.1	1.02	118	85	0.74	19.638	1.55	0.04728	8.63	320.2	4.9	-80
90064	24.1.1	0.25	590	615	1.08	19.716	1.28	0.05155	1.61	318.9	4.0	-17
90064	7.1.1	0.49	120	115	0.99	19.762	1.51	0.05286	4.18	318.2	4.7	1
90064	23.1.1	0.21	318	329	1.07	19.787	1.31	0.05211	1.75	317.8	4.1	-9
90064	1.1.1	0.43	286	345	1.25	19.833	1.52	0.05108	3.15	317.1	4.7	-23
90064	25.1.1	0.40	105	69	0.68	19.903	1.54	0.05037	4.89	316.0	4.8	-33

BUNDUNDAH GRANITE

GA SAMPLENO:	**1985435**
GSNSW SITEID:	**8928LMC0365**
PARENT UNIT(S):	—
FORMAL NAME:	Bundundah Granite
INFORMAL NAME:	—
LITHOLOGY:	Porphyritic leucocratic microgranite
PROVINCE:	Eastern Lachlan Orogen
1:250 000 SHEET:	WOLLONGONG (SI/56-9)
1:100 000 SHEET:	MOSS VALE (8928)
LOCATION (GDA94):	34.908109 °S, 150.391329 °E
LOCATION (MGA94):	Zone 56, 261660 mE, 6134041 mN
ANALYTICAL SESSION NO(S):	90064 (see Table 1 for parameters derived from concurrent measurements of $^{238}U/^{206}Pb$ and $^{207}Pb/^{206}Pb$ reference zircons)
INTERPRETED AGE:	**324.4 ± 3.2 Ma** (95% confidence; 22 analyses of 22 zircons)
GEOLOGICAL ATTRIBUTION:	Magmatic crystallisation
ISOTOPIC RATIO(S) USED:	$^{238}U/^{206}Pb$ (^{204}Pb-corrected)

Sampling Details

This sample was taken from a rubbly outcrop in a wooded area on the eastern bank of Yalwal Creek, about 1.2 km north of the point where Yalwah Road crosses the creek.

Relationships and Rationale for Dating

The unit sampled is a porphyritic pink leucocratic microgranite occurring as a syn-plutonic dyke within the volumetrically dominant coarser-grained phase of the Bundundah Granite in the eastern Lachlan Orogen. This pluton was assumed to be of Carboniferous age (Rose, 1966): it intrudes the Late Devonian Yalwal Volcanics (including the Grassy Gully Rhyolite Member: GSNSW 8928LMC0073, GA 1985436; this volume), and it is unconformably overlain by the Permian Snapper Point Formation, within the Shoalhaven Group of the Sydney Basin (Rose, 1966; Trigg and Campbell, in prep.).

This sample was selected for SHRIMP analysis in order to test the hypothesis that the Bundundah Granite is contemporaneous with other plutonic rocks of assumed Carboniferous age in southern MOSS VALE, including the undated Touga Granite and Tullyangela Granite. Carboniferous felsic rocks on BATHURST (Pogson and Watkins, 1998) and DUBBO (Meakin and Morgan, 1999), some 200–300 km to the north-northwest, yielded SHRIMP zircon $^{238}U/^{206}Pb$ dates ranging from 340.7 ± 3.2 Ma to 314 ± 8 Ma (Fanning, 1997; Black, 1998).

The aim was to obtain a magmatic crystallisation age for the Bundundah Granite, for comparison with that of the Touga Granite (GSNSW 8928LMC0363, GA 1985433; this volume), the Tullyangela Granite (GSNSW 8928LMC0364, GA 1985434; this volume), and the Grassy Gully Rhyolite Member (GSNSW 8928LMC0073, GA 1985436; this volume).

Petrography

This sample is a sparsely porphyritic and fine-grained pink leucocratic microgranite. Phenocrysts are 1–8 mm in diameter, and comprise rounded and embayed quartz (some of which contain small

irregular-shaped inclusions of K-feldspar), pink alkali feldspar and altered biotite (Figure 36). The granular groundmass is fine- to medium-grained (less than 1 mm), and comprises 50% perthitic K-feldspar, 35% clear quartz, and 15% plagioclase (Figure 36). Irregularly-shaped, infilling fluorite is an accessory mineral, and the rock also contains small veinlets and disseminations of fine-grained pyrite. Micrographic intergrowth of quartz and K-feldspar is common, especially at the margins of the more euhedral phenocrysts, and is probably indicative of rapid cooling.

Biotite has been replaced by clay minerals and fine-grained opaque oxide minerals, K-feldspar is clay-dusted, and pyrite is partly replaced by opaque oxide minerals with cubic crystal shapes.

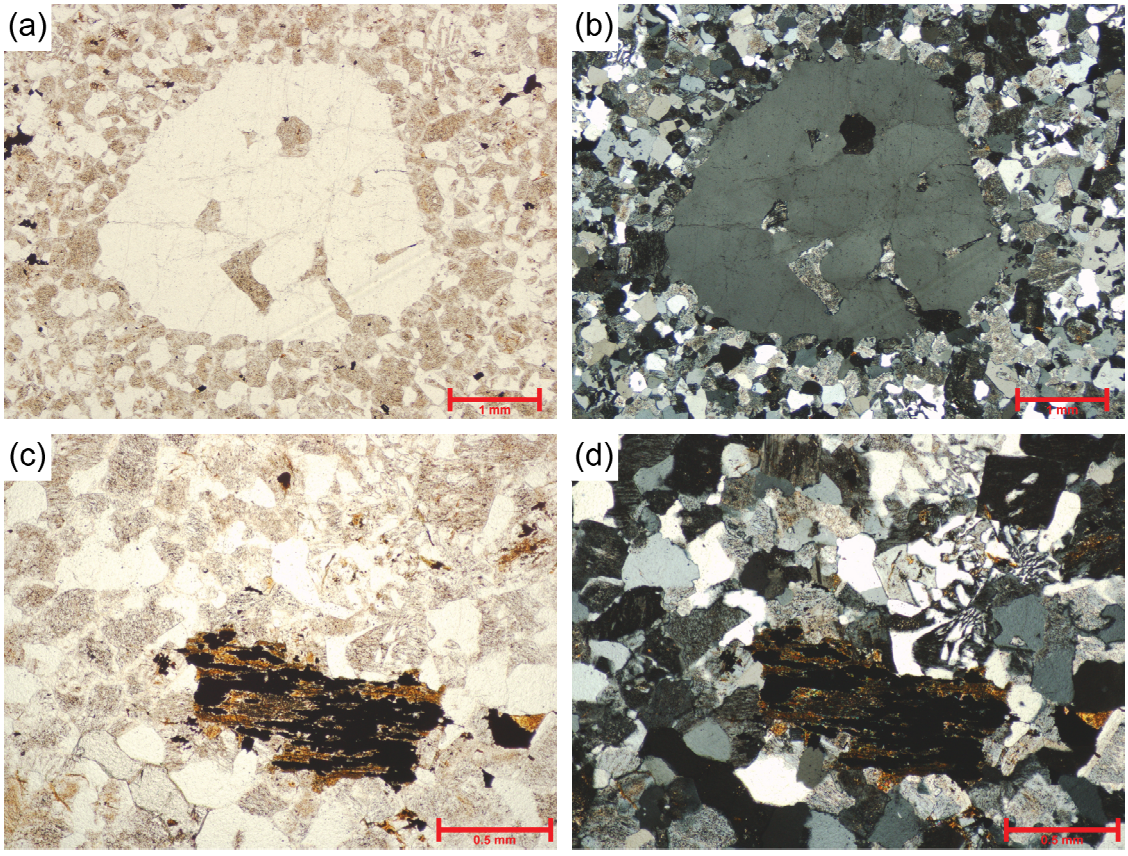

Figure 36: *Representative photomicrographs of the Bundundah Granite (GSNSW 8928LMC0365, GA 1985435). (a) Plane-polarised light view of a large, embayed quartz 'phenocryst' within massive, leucocratic microgranite dominated by quartz, K-feldspar and plagioclase. (b) Cross-polarised light view of (a), showing fine-grained quartz, K-feldspar and plagioclase, and small areas of micrographic intergrowth. (c) Plane-polarised light view of the microgranite mosaic in detail, showing an anhedral fluorite grain (lower left), and a probable biotite crystal replaced by fine-grained opaque oxide and clay minerals. (d) Cross-polarised light view of (c), highlighting micrographic intergrowths around a euhedral K-feldspar grain (top right).*

Zircon Description

Zircons from this sample are predominantly euhedral, with external morphologies ranging from prismatic to elongate. Aspect ratios (length/width) are 2–8, and long axes are 90–300 µm (Figure 37). In transmitted light, the zircons are predominantly transparent, colourless to pale brown, and many contain characteristic elongate cavities parallel to the long axis.

Cathodoluminescence (CL) images reveal relatively uniformly high emission intensity but low contrast (Figure 37). Fine-scale concentric oscillatory and sector zoning is best developed in equant grains, with elongate crystals generally characterised by broader banding parallel to the long axes. These zoning patterns are typical of magmatic zircon. Rare grains contain central regions with relatively high-contrast oscillatory zoning, typically disconformably overgrown by the high-intensity, low-contrast zircon characteristic of the rest of the population (Figure 37). These central regions are interpreted as inherited cores with magmatic overgrowths.

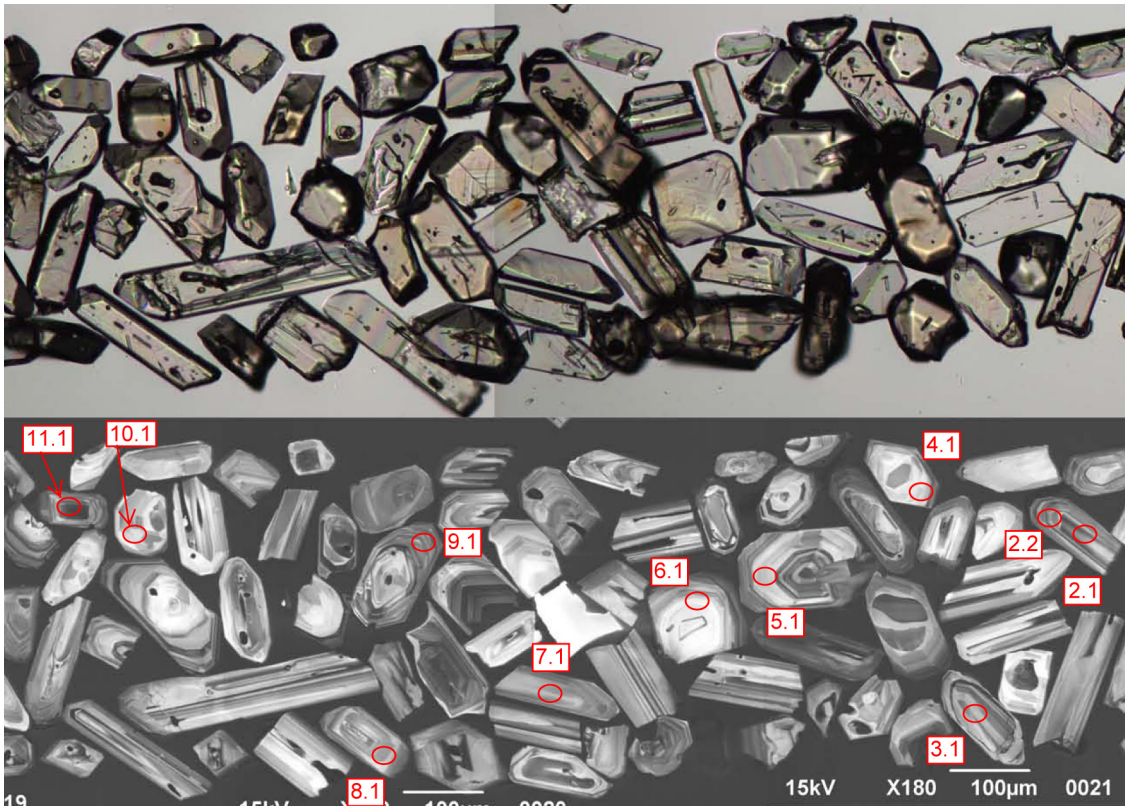

Figure 37: *Representative zircons from the Bundundah Granite (GSNSW 8928LMC0365, GA 1985435). Transmitted-light image is shown in the upper half; cathodoluminescence image in the lower half. SHRIMP analysis sites are indicated, and labelled with grain and spot number.*

U-Pb Isotopic Results

Thirty-one analyses were obtained from 30 individual zircons (with grain 2 analysed twice), and the results are presented in Figure 38, and Table 9. The analysed zircons are characterised by predominantly low U contents (38–354 ppm, median 112 ppm), but widely varied Th/U (0.06–1.22, median 0.56).

Two analyses (8.1.1 and 23.1.1; red fill in Figure 38) yielded high common Pb contents ($^{206}Pb_c$ > 2%), and are interpreted to have been affected by loss of radiogenic Pb during one or more events of unknown age. Consequently, their $^{238}U/^{206}Pb$ dates are unreliable, and these analyses are not considered further.

The remaining 29 analyses are mostly characterised by low $^{206}Pb_c$ (maximum 1.16%, median 0.32%), and can be divided into four groups (Table 9):

- 22 analyses of 22 zircons (Group 1; yellow fill in Figure 38) with individual $^{238}U/^{206}Pb$ dates between c. 335 Ma and c. 316 Ma, which yielded a weighted mean $^{238}U/^{206}Pb$ date of 324.4 ± 3.2 Ma (MSWD = 1.53),
- a single analysis (Group 2; blue fill in Figure 38) with a $^{238}U/^{206}Pb$ date of 552 ± 14 Ma (2σ),
- two analyses of two zircons (Group 3; pink fill in Figure 38) with individual $^{207}Pb/^{206}Pb$ dates between c. 2449 Ma and c. 2314 Ma, and
- four analyses of four zircons (Group 4; white fill in Figure 38) with individual $^{238}U/^{206}Pb$ dates between c. 311 Ma and c. 296 Ma.

Geochronological Interpretation

The weighted mean date of 324.4 ± 3.2 Ma obtained from the 22 analyses in Group 1 is indistinguishable from the median $^{238}U/^{206}Pb$ date for the same 22 analyses (324.7 +2.3/-5.1 Ma), and the absence of significant asymmetry in the uncertainties associated with the latter suggests that Group 1 represents a single population of analyses with an approximately normal distribution. Consequently, the weighted mean $^{238}U/^{206}Pb$ date of 324.4 ± 3.2 Ma is interpreted as the best estimate of the age of magmatic crystallisation of the Bundundah Granite.

The single 552 ± 14 Ma (2σ) analysis in Group 2 is interpreted as an inherited individual of Late Neoproterozoic age, and the two pre-2000Ma analyses in Group 3 are similarly interpreted as Paleoproterozoic inheritance. The four analyses in Group 4 are slightly younger than the main magmatic population defined by Group 1, and are interpreted to have been affected by minor post-crystallisation loss of radiogenic Pb.

The magmatic crystallisation age of 324.4 ± 3.2 Ma for the Bundundah Granite is indistinguishable from that of the 325.5 ± 2.6 Ma Touga Granite to the west (GSNSW 8928LMC0363, GA 1985433; this volume), and establishes Middle Carboniferous plutonism in southern MOSS VALE. However, both intrusions are substantially younger than the 382.4 ± 3.0 Ma Tullyangela Granite (GSNSW 8928LMC0364, GA 1985434; this volume), with which they were previously grouped (Rose, 1966). The Tullyangela Granite appears instead to be temporally associated with Late Devonian eruption of the nearby Yalwal Volcanics, which include the 384.5 ± 4.4 Ma Grassy Gully Rhyolite Member (GSNSW 8928LMC0073, GA 1985436; this volume).

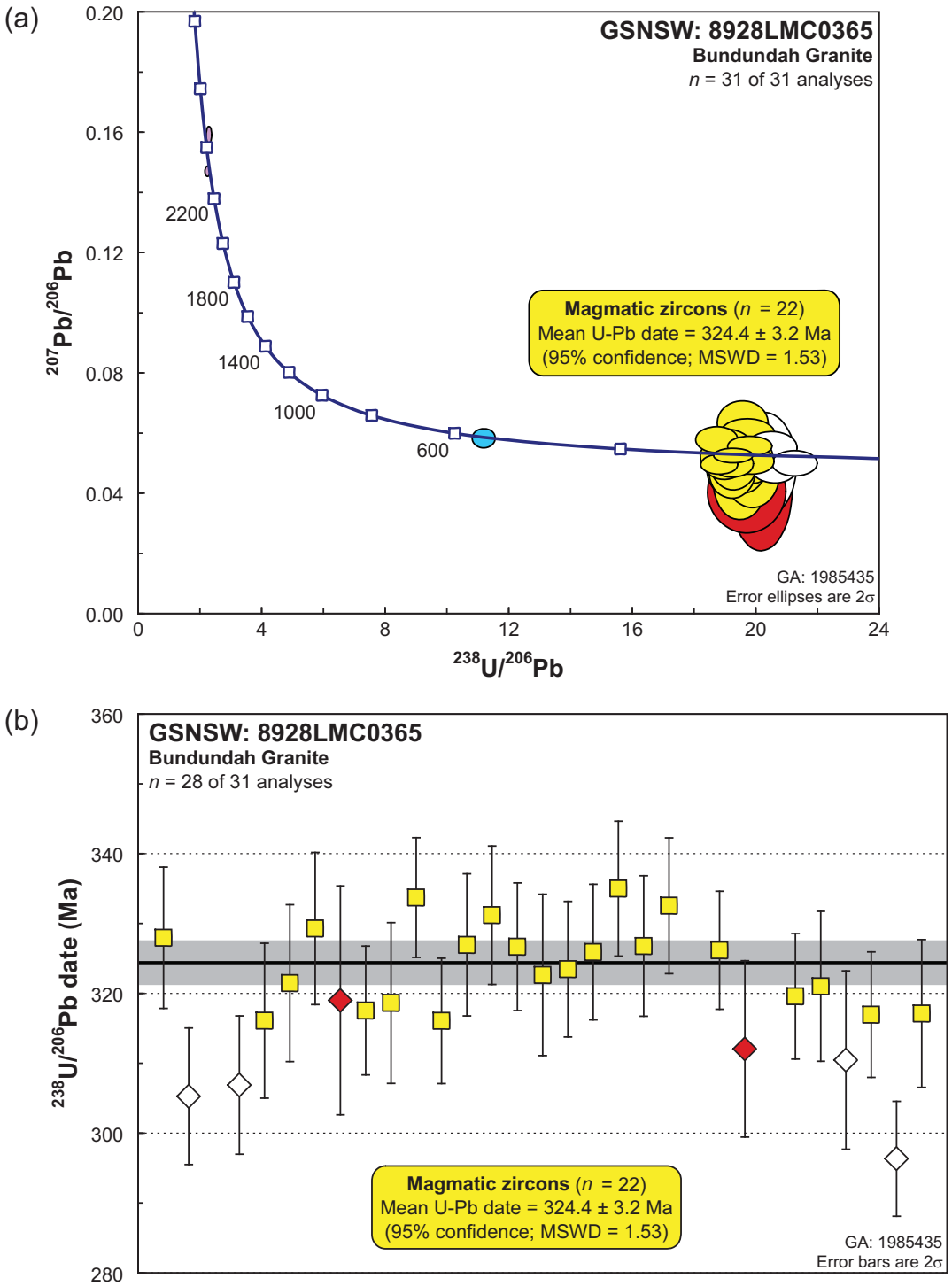

Figure 38: *SHRIMP U-Pb data for zircons from the Bundundah Granite (GSNSW 8928LMC0365, GA 1985435). (a) Tera-Wasserburg concordia diagram; (b) $^{238}U/^{206}Pb$ dates in order of acquisition (three analyses with pre-360 Ma dates are not shown). Yellow fill: magmatic zircons; blue fill: Neoproterozoic inheritance; pink fill: Paleoproterozoic inheritance; white fill: affected by loss of radiogenic Pb; red fill: not considered due to high $^{206}Pb_c$. Heavy black line and grey band: weighted mean $^{238}U/^{206}Pb$ date and its 95% confidence interval, respectively.*

Table 9: SHRIMP U-Pb zircon data from the Bundundah Granite (GSNSW 8928LMC0365, GA 1985435). All dates are $^{238}U/^{206}Pb$ unless otherwise indicated.

Sess. no.	Grain.area .replicate	$^{206}Pb_c$ (%)	U (ppm)	Th (ppm)	$^{232}Th/^{238}U$	$^{238}U/^{206}Pb$	±1σ (%)	$^{207}Pb/^{206}Pb$	±1σ (%)	Date (Ma)	±1σ (Ma)	Disc. (%)
Group 3: Paleoproterozoic inherited individuals (n = 2; $^{207}Pb/^{206}Pb$ dates tabulated)												
90064	3.1.1	0.21	62	60	1.00	2.269	1.50	0.15941	0.72	2449	12	4
90064	21.1.1	0.02	114	129	1.17	2.220	1.42	0.14721	0.47	2314	8	-3
Group 2: Neoproterozoic inherited individual (n = 1)												
90064	24.1.1	0.19	237	13	0.06	11.177	1.32	0.05811	2.30	552.4	7.0	-3
Group 1: Magmatic zircons (n = 22)												
90064	2.2.1	-0.33	140	75	0.55	18.747	1.48	0.05769	3.03	335.0	4.8	55
90064	11.1.1	0.67	354	364	1.06	18.821	1.32	0.04943	2.71	333.7	4.3	-50
90064	20.1.1	0.23	120	113	0.97	18.889	1.50	0.05195	4.65	332.5	4.9	-15
90064	14.1.1	0.56	110	60	0.56	18.969	1.54	0.05038	4.87	331.2	5.0	-36
90064	7.1.1	0.24	68	32	0.49	19.081	1.70	0.05531	4.32	329.3	5.4	29
90064	1.1.1	1.08	112	87	0.80	19.160	1.58	0.04770	7.85	328.0	5.1	-74
90064	13.1.1	0.09	85	56	0.68	19.221	1.60	0.05507	2.65	326.9	5.1	27
90064	19.1.1	0.89	111	57	0.53	19.231	1.58	0.04669	7.44	326.8	5.0	-90
90064	15.1.1	0.45	163	84	0.53	19.237	1.44	0.04967	3.70	326.7	4.6	-45
90064	22.1.1	0.24	282	171	0.63	19.268	1.33	0.05235	1.87	326.2	4.2	-8
90064	18.1.1	0.91	128	69	0.56	19.284	1.53	0.04840	6.29	325.9	4.9	-64
90064	17.1.1	0.31	112	43	0.39	19.433	1.54	0.05262	4.17	323.5	4.9	-3
90064	16.1.1	1.09	62	47	0.79	19.484	1.84	0.04364	11.82	322.6	5.8	-141
90064	6.1.1	0.75	60	30	0.52	19.557	1.79	0.05001	8.39	321.5	5.6	-39
90064	26.1.1	-0.59	65	31	0.49	19.586	1.72	0.06322	4.79	321.0	5.4	123
90064	25.1.1	0.36	157	83	0.55	19.676	1.44	0.05170	4.39	319.6	4.5	-15
90064	10.1.1	-0.13	46	24	0.53	19.736	1.85	0.05965	3.31	318.6	5.8	85
90064	9.1.1	-0.23	128	76	0.62	19.805	1.49	0.05539	2.46	317.5	4.6	35
90064	30.1.1	0.55	72	34	0.49	19.832	1.71	0.05122	6.55	317.1	5.3	-21
90064	28.1.1	0.24	147	84	0.59	19.843	1.45	0.05252	3.59	317.0	4.5	-3
90064	5.1.1	1.16	60	37	0.64	19.899	1.80	0.04591	9.74	316.1	5.5	-102
90064	12.1.1	0.32	142	169	1.22	19.900	1.45	0.05042	3.53	316.1	4.5	-32
Group 4: Affected by loss of radiogenic Pb (n = 4)												
90064	27.1.1	0.83	38	19	0.52	20.269	2.11	0.04929	14.48	310.5	6.4	-48
90064	4.1.1	0.30	73	42	0.60	20.511	1.65	0.05492	4.06	306.9	5.0	33
90064	2.1.1	0.72	164	150	0.95	20.622	1.64	0.04968	5.33	305.3	4.9	-41
90064	29.1.1	0.51	235	143	0.63	21.259	1.42	0.04981	3.45	296.3	4.1	-37
Not considered, due to high $^{206}Pb_c$ (> 2%; n = 2)												
90064	8.1.1	2.04	69	61	0.92	19.712	2.63	0.04052	14.12	319.0	8.2	-200
90064	23.1.1	2.07	49	29	0.60	20.163	2.07	0.04230	21.02	312.0	6.3	-167

TULLYANGELA GRANITE

GA SAMPLENO:	**1985434**
GSNSW SITEID:	**8928LMC0364**
PARENT UNIT(S):	—
FORMAL NAME:	Tullyangela Granite
INFORMAL NAME:	—
LITHOLOGY:	Melanocratic quartz diorite
PROVINCE:	Eastern Lachlan Orogen
1:250 000 SHEET:	WOLLONGONG (SI/56-9)
1:100 000 SHEET:	MOSS VALE (8928)
LOCATION (GDA94):	34.928929 °S, 150.155977 °E
LOCATION (MGA94):	Zone 56, 240217 mE, 6131145 mN
ANALYTICAL SESSION NO(S):	90064 (see Table 1 for parameters derived from concurrent measurements of $^{238}U/^{206}Pb$ and $^{207}Pb/^{206}Pb$ reference zircons)
INTERPRETED AGE:	**382.4 ± 3.0 Ma** (95% confidence; 28 analyses of 27 zircons)
GEOLOGICAL ATTRIBUTION:	Magmatic crystallisation
ISOTOPIC RATIO(S) USED:	$^{238}U/^{206}Pb$ (^{204}Pb-corrected)

Sampling Details

This sample was taken from some low outcrop in Tullyangela Clearing, about 400 m southeast of the most southerly intersection of Tolwong Road and the secondary track that traverses the Clearing, and about 7 km east-northeast of Touga homestead.

Relationships and Rationale for Dating

The unit sampled is a fine- to medium-grained, melanocratic quartz diorite within the Tullyangela Granite, which was of assumed Carboniferous age (Rose, 1966). It intrudes Ordovician turbiditic sedimentary rocks of the Adaminaby Group in the eastern Lachlan Orogen, and it is unconformably overlain by the Permian Nowra Sandstone and Berry Siltstone, within the Shoalhaven Group of the Sydney Basin (Rose, 1966; Trigg and Campbell, in prep.).

This sample was selected for SHRIMP analysis in order to test the hypothesis that the Tullyangela Granite is contemporaneous with other plutonic rocks of assumed Carboniferous age in southern MOSS VALE, including the undated Touga Granite and Bundundah Granite. The latter intrudes the Late Devonian Yalwal Volcanics (which include the Grassy Gully Rhyolite Member: GSNSW 8928LMC0073, GA 1985436; this volume), and is unconformably overlain by the Permian Snapper Point Formation, within the Shoalhaven Group of the Sydney Basin (Rose, 1966; Trigg and Campbell, in prep.). Carboniferous felsic rocks on BATHURST (Pogson and Watkins, 1998) and DUBBO (Meakin and Morgan, 1999), some 200–300 km to the north-northwest, yielded SHRIMP zircon $^{238}U/^{206}Pb$ dates ranging from 340.7 ± 3.2 Ma to 314 ± 8 Ma (Fanning, 1997; Black, 1998).

The aim was to obtain a magmatic crystallisation age for the Tullyangela Granite, for comparison with that of the Touga Granite (GSNSW 8928LMC0363, GA 1985433; this volume), the Bundundah Granite (GSNSW 8928LMC0365, GA 1985435; this volume), and the Grassy Gully Rhyolite Member (GSNSW 8928LMC0073, GA 1985436; this volume).

Petrography

This sample is a fine- to medium-grained, equigranular (1.0–1.5 mm) and melanocratic quartz diorite, cross-cut by millimetre-scale veins of fine-grained leucogranite. In hand specimen, it contains abundant white to milky plagioclase, but is otherwise a dark greenish-grey colour, and comprises 30–40% ferromagnesian minerals. In thin section, the rock has a crudely intergranular texture (Figure 39), and consists of 45% plagioclase, 15% hornblende, 12% clinopyroxene (probably augite), 20% ferromagnesian minerals (clinopyroxene and/or hornblende) that are completely replaced by fibrous actinolite and lesser fibrous to vermicular chlorite, 6% quartz, 2% opaque oxide minerals, and accessory zircon, titanite and apatite. Plagioclase occurs as lath-shaped crystals of andesine to labradorite composition ($An_{44–54}$) that are twinned but unzoned. Ferromagnesian minerals are mostly equant and anhedral, and fill the spaces between plagioclase crystals. Clinopyroxene of probable augite composition is colourless to very pale pink, and many grains are rimmed by amphibole (Figure 39). Hornblende is pale- to medium yellowish-green in colour. Small, irregular patches of quartz fill the spaces between plagioclase grains and ferromagnesian minerals. Opaque oxide minerals are blotchy to very skeletal in form, zircon and apatite crystals are bladed, and titanite is interstitial.

In addition to the widespread replacement of ferromagnesian minerals by secondary actinolite and chlorite, plagioclase displays sericite-clay alteration, and the rock also contains minor granular epidote as a secondary phase.

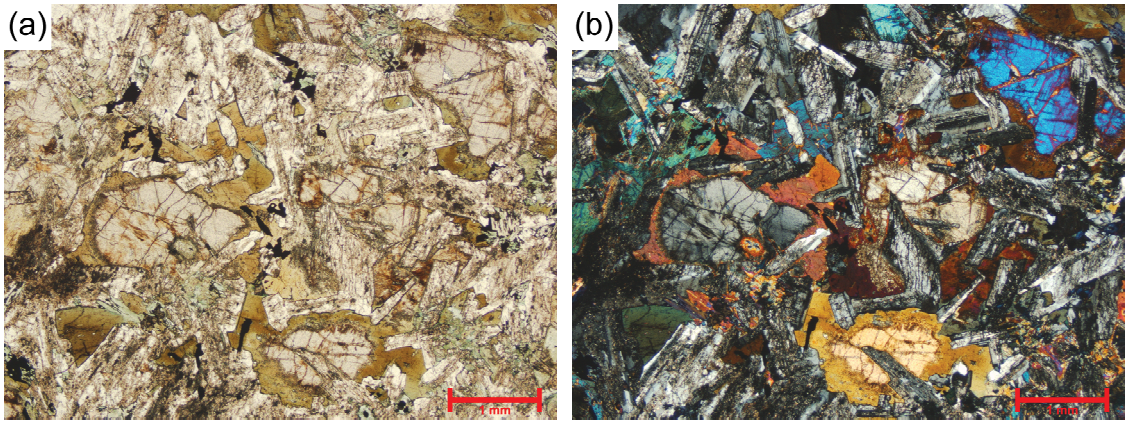

Figure 39: *Representative photomicrographs of the Tullyangela Granite (GSNSW 8928LMC0364, GA 1985434). (a) Plane-polarised light view of medium-grained diorite with poorly developed subophitic texture, defined by high-relief clinopyroxene (left and right of centre, and top right) and green hornblende enclosing smaller, more euhedral laths of plagioclase. Blebby opaque oxide minerals and a very small, triangular titanite crystal (upper left) are also evident. (b) Cross-polarised light view of (a), highlighting subophitic enclosure of plagioclase by clinopyroxene and hornblende.*

Zircon Description

Zircons from this sample are mostly euhedral, with subordinate subhedral and anhedral grain fragments, and the crystals are notably elongate. Aspect ratios (length/width) are 2–8 (but rarely less than 3), and long axes are 80–330 µm (Figure 40). In transmitted light, most grains are transparent and colourless to pale-brown, commonly with elongate cavities parallel to the long axes of the crystals. Inclusions are rare, and predominantly comprise apatite.

Cathodoluminescence (CL) images reveal a range of CL emissions, but a remarkably uniform and distinctive zoning pattern dominated by broad and poorly-defined banding parallel to the long axes

of the grains (Figure 40). Concentric zoning is rare, characteristically diffuse in character where present, and does not resemble well-defined oscillatory zoning. These patterns are typical of magmatic zircon, and the presence of cavities may indicate rapid crystallisation. No crystal displays any heterogeneity in CL patterns, and no inheritance was identified.

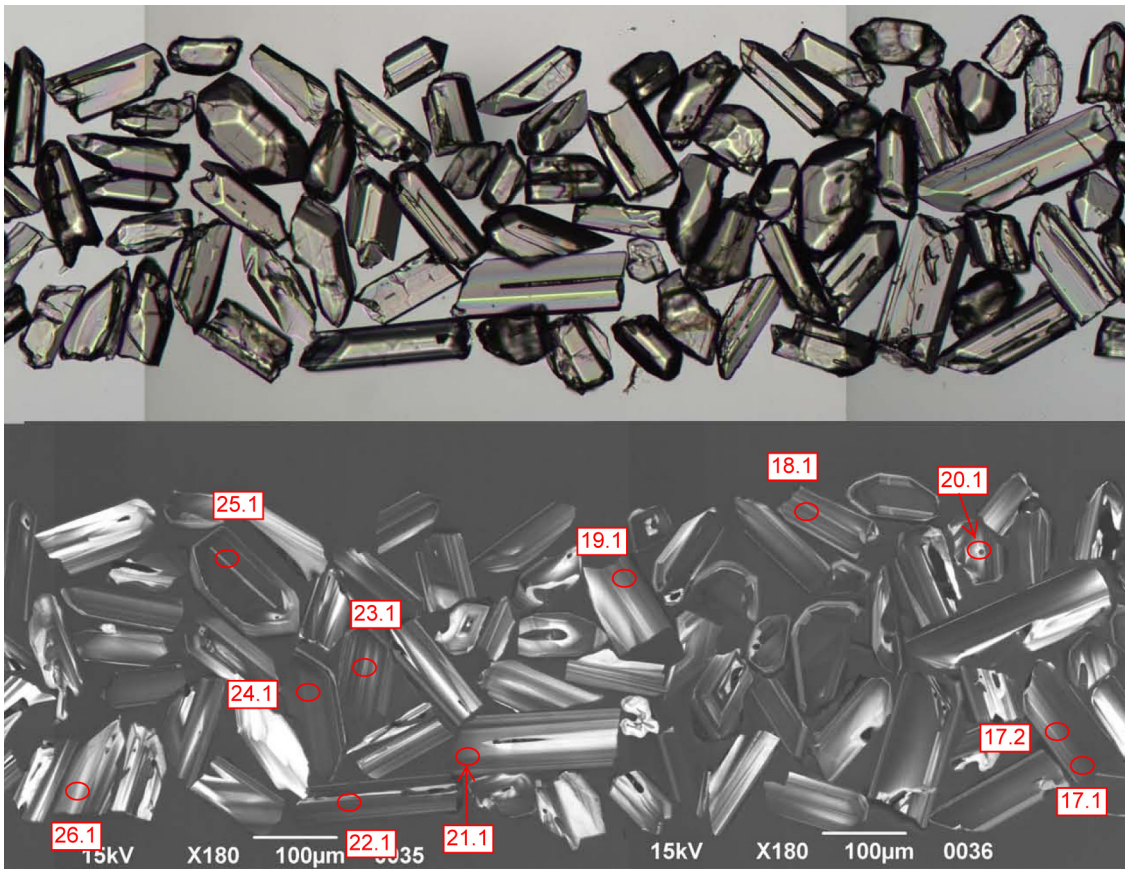

Figure 40: *Representative zircons from the Tullyangela Granite (GSNSW 8928LMC0364, GA 1985434). Transmitted-light image is shown in the upper half; cathodoluminescence image in the lower half. SHRIMP analysis sites are indicated, and labelled with grain and spot number.*

U-Pb Isotopic Results

Thirty-one analyses were obtained from 30 individual zircons (with grain 17 analysed twice), and the results are presented in Figure 41, and Table 10. The analysed zircons are characterised by predominantly moderate U contents (124–699 ppm, median 394 ppm), and moderate Th/U (0.44–1.08, median 0.79).

The 31 analyses have uniformly low $^{206}Pb_c$ (maximum 0.41%, median 0.14%), and can be divided into three groups (Table 10):

- 28 analyses of 27 zircons (Group 1; yellow fill in Figure 41) with individual $^{238}U/^{206}Pb$ dates between c. 392 Ma and c. 374 Ma, which yielded a weighted mean date of 382.4 ± 3.0 Ma (MSWD = 1.40),
- a single analysis (Group 2; pink fill in Figure 41) with a $^{238}U/^{206}Pb$ date of 397.5 ± 9.8 Ma (2σ), and
- two analyses of two zircons (Group 3; white fill in Figure 41) with individual $^{238}U/^{206}Pb$ dates between c. 372 Ma and c. 367 Ma.

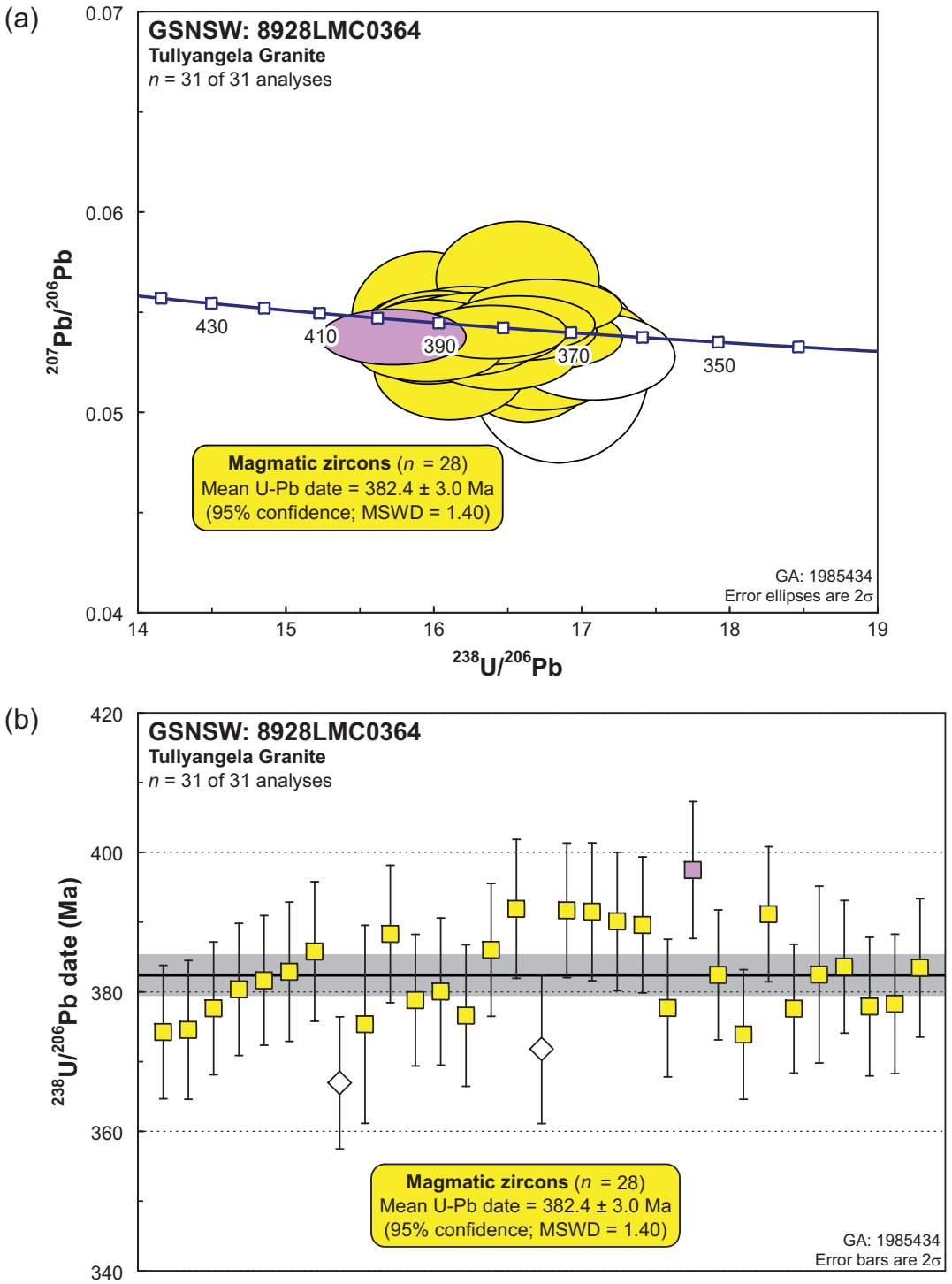

Figure 41: *SHRIMP U-Pb data for zircons from the Tullyangela Granite (GSNSW 8928LMC0364, GA 1985434). (a) Tera-Wasserburg concordia diagram; (b) $^{238}U/^{206}Pb$ dates in order of acquisition. Yellow fill: magmatic zircons; pink fill: Early Devonian inheritance; white fill: affected by loss of radiogenic Pb. Heavy black line and grey band: weighted mean $^{238}U/^{206}Pb$ date and its 95% confidence interval, respectively.*

Geochronological Interpretation

The weighted mean date of 382.4 ± 3.0 Ma obtained from the 28 analyses in Group 1 is indistinguishable from the median $^{238}U/^{206}Pb$ date for the same 28 analyses (382.0 +3.8/-4.1 Ma), and the absence of significant asymmetry in the uncertainties associated with the latter suggests that Group 1 represents a single population of analyses with an approximately normal distribution.

Consequently, the weighted mean $^{238}U/^{206}Pb$ date of 382.4 ± 3.0 Ma is interpreted as the best estimate of the age of magmatic crystallisation of the Tullyangela Granite. The single 397.5 ± 9.8 Ma (2σ) analysis in Group 2 is interpreted as Middle Devonian inheritance. The two analyses in Group 3 are very slightly younger than the main magmatic population defined by Group 1, and are interpreted to have been affected by minor post-crystallisation loss of radiogenic Pb.

The magmatic crystallisation age of 382.4 ± 3.0 Ma for the Tullyangela Granite is substantially older than those of the 325.5 ± 2.6 Ma Touga Granite (GSNSW 8928LMC0363, GA 1985433; this volume) and the 324.4 ± 3.2 Ma Bundundah Granite (GSNSW 8928LMC0365, GA 1985435; this volume), with which it was previously grouped (Rose, 1966). Instead, emplacement of the Tullyangela Granite predated, and was unrelated to, the surrounding Middle Carboniferous plutonism in southern MOSS VALE.

However, the magmatic crystallisation age of 382.4 ± 3.0 Ma for the Tullyangela Granite is indistinguishable from that of the nearby 384.5 ± 4.4 Ma Grassy Gully Rhyolite Member (GSNSW 8928LMC0073, GA 1985436; this volume), within the Yalwal Volcanics, and establishes that plutonic rocks temporally equivalent to the Late Devonian volcanic succession are exposed at least locally.

Table 10: SHRIMP U-Pb zircon data from the Tullyangela Granite (GSNSW 8928LMC0364, GA 1985434). All dates are $^{238}U/^{206}Pb$ unless otherwise indicated.

Sess. no.	Grain.area .replicate	$^{206}Pb_c$ (%)	U (ppm)	Th (ppm)	$^{232}Th/^{238}U$	$^{238}U/^{206}Pb$	±1σ (%)	$^{207}Pb/^{206}Pb$	±1σ (%)	Date (Ma)	±1σ (Ma)	Disc. (%)
Group 2: Middle Devonian inherited individual (n = 1)												
90064	21.1.1	0.04	529	440	0.86	15.724	1.27	0.05376	1.06	397.5	4.9	-9
Group 1: Magmatic zircons (n = 28)												
90064	15.1.1	0.19	359	299	0.86	15.954	1.31	0.05466	2.53	391.9	5.0	2
90064	17.1.1	0.11	572	481	0.87	15.963	1.27	0.05302	1.15	391.7	4.8	-16
90064	18.1.1	0.17	394	301	0.79	15.972	1.30	0.05367	1.71	391.5	4.9	-9
90064	24.1.1	0.20	571	486	0.88	15.987	1.28	0.05382	1.36	391.1	4.8	-7
90064	17.2.1	0.14	367	276	0.78	16.030	1.31	0.05392	1.63	390.1	5.0	-6
90064	19.1.1	0.14	416	271	0.67	16.052	1.29	0.05398	1.40	389.6	4.9	-5
90064	10.1.1	0.32	333	249	0.77	16.107	1.31	0.05217	2.02	388.3	4.9	-25
90064	14.1.1	0.09	534	453	0.88	16.205	1.27	0.05345	1.24	386.0	4.8	-10
90064	7.1.1	0.12	310	197	0.66	16.215	1.34	0.05418	1.59	385.8	5.0	-2
90064	27.1.1	0.14	489	388	0.82	16.310	1.28	0.05370	1.74	383.6	4.8	-7
90064	30.1.1	0.22	265	198	0.77	16.317	1.33	0.05347	2.02	383.4	5.0	-9
90064	6.1.1	0.02	552	504	0.94	16.342	1.34	0.05486	0.84	382.9	5.0	6
90064	26.1.1	0.00	209	99	0.49	16.359	1.71	0.05617	1.35	382.5	6.3	20
90064	22.1.1	0.15	669	696	1.08	16.362	1.25	0.05380	1.10	382.4	4.7	-5
90064	5.1.1	0.06	699	662	0.98	16.396	1.25	0.05400	1.02	381.6	4.6	-3
90064	4.1.1	0.22	543	427	0.81	16.454	1.28	0.05287	1.37	380.3	4.7	-15
90064	12.1.1	0.18	381	336	0.91	16.467	1.43	0.05349	1.85	380.0	5.3	-8
90064	11.1.1	0.09	435	349	0.83	16.522	1.28	0.05405	1.44	378.8	4.7	-2
90064	29.1.1	0.06	680	615	0.94	16.546	1.36	0.05408	0.96	378.3	5.0	-1
90064	28.1.1	-0.13	230	151	0.68	16.564	1.35	0.05667	2.07	377.9	5.0	27
90064	20.1.1	0.19	237	101	0.44	16.574	1.35	0.05354	2.45	377.7	4.9	-7
90064	3.1.1	0.03	368	265	0.74	16.576	1.30	0.05407	1.14	377.6	4.8	-1
90064	25.1.1	0.10	630	574	0.94	16.578	1.26	0.05441	1.06	377.6	4.6	3
90064	13.1.1	0.35	188	115	0.63	16.623	1.39	0.05365	3.17	376.6	5.1	-5
90064	9.1.1	0.16	346	264	0.79	16.680	1.95	0.05357	1.90	375.3	7.1	-6
90064	2.1.1	0.15	468	355	0.78	16.717	1.37	0.05370	1.23	374.5	5.0	-4
90064	1.1.1	0.27	342	252	0.76	16.731	1.32	0.05258	1.94	374.2	4.8	-17
90064	23.1.1	0.04	426	327	0.79	16.747	1.28	0.05524	1.04	373.9	4.6	13
Group 3: Affected by loss of radiogenic Pb (n = 2)												
90064	16.1.1	0.41	124	73	0.60	16.843	1.48	0.05215	3.68	371.8	5.3	-21
90064	8.1.1	0.12	345	246	0.74	17.073	1.33	0.05277	1.69	366.9	4.7	-13

YALWAL VOLCANICS: GRASSY GULLY RHYOLITE MEMBER

GA SAMPLENO:	**1985436**
GSNSW SITEID:	**8928LMC0073**
PARENT UNIT(S)	Yalwal Volcanics
FORMAL NAME:	Grassy Gully Rhyolite Member
INFORMAL NAME:	—
LITHOLOGY:	Aphyric spherulitic rhyolite
PROVINCE:	Eastern Lachlan Orogen
1:250 000 SHEET:	WOLLONGONG (SI/56-9)
1:100 000 SHEET:	MOSS VALE (8928)
LOCATION (GDA94):	34.845629 °S, 150.426369 °E
LOCATION (MGA94):	Zone 56, 264684 mE, 6141055 mN
ANALYTICAL SESSION NO(S):	90068 (see Table 1 for parameters derived from concurrent measurements of $^{238}U/^{206}Pb$ and $^{207}Pb/^{206}Pb$ reference zircons)
INTERPRETED AGE:	**384.5 ± 4.4 Ma** (95% confidence; 24 analyses of 24 zircons)
GEOLOGICAL ATTRIBUTION:	Magmatic crystallisation
ISOTOPIC RATIO(S) USED:	$^{238}U/^{206}Pb$ (^{204}Pb-corrected)

Sampling Details

This sample was taken from a large outcrop 'bar' extending into the bed of the Shoalhaven River from its northern bank, within the Coolendel bush reserve and recreational area.

Relationships and Rationale for Dating

The unit sampled is a cream-coloured, almost aphyric, and extensively seriticised rhyolite within the Grassy Gully Rhyolite Member, which is part of the Late Devonian Yalwal Volcanics in the eastern Lachlan Orogen (Rose, 1966; Trigg and Campbell, in prep.). It is intruded by the undated (but presumed Carboniferous) Bundundah Granite (GSNSW 8928LMC0365, GA 1985435; this volume), so it was considered likely that the Grassy Gully Rhyolite was older than all the plutonic rocks of assumed Carboniferous age in southern MOSS VALE, including the undated Touga Granite and Tullyangela Granite. Late Devonian volcanic rocks on BATHURST, some 200–250 km to the north-northwest, yielded a SHRIMP zircon $^{238}U/^{206}Pb$ date of 376 ± 4 Ma (Pogson and Watkins, 1998).

The aim was to obtain a magmatic crystallisation age for the Grassy Gully Rhyolite, for comparison with that of the Bundundah Granite (GSNSW 8928LMC0365, GA 1985435; this volume), the Touga Granite (GSNSW 8928LMC0363, GA 1985433; this volume), and the Tullyangela Granite (GSNSW 8928LMC0364, GA 1985434; this volume).

Petrography

This sample is an almost-aphyric, extensively seriticised rhyolite that was originally glassy. Rare (1–2%), tabular sericitised crystals up to 1.5 mm in length were probably feldspar phenocrysts, and elongate aggregates of fine-grained white mica and opaque oxide minerals were probably laths of biotite (Figure 42). Accessory zircon occurs as very small, rounded grains. The groundmass contains a regular, planar flow-banding defined by alternating 0.5–2.5 mm-thick layers of spherulite-rich and spherulite-poor material (Figure 42). The former layers consist almost entirely of overlapping spherulites (each 0.2–0.3 mm in diameter), which produce a 'snowflake' texture. The latter comprise fine- to very fine-grained microcrystalline felsic material incorporating rare, scattered spherulites.

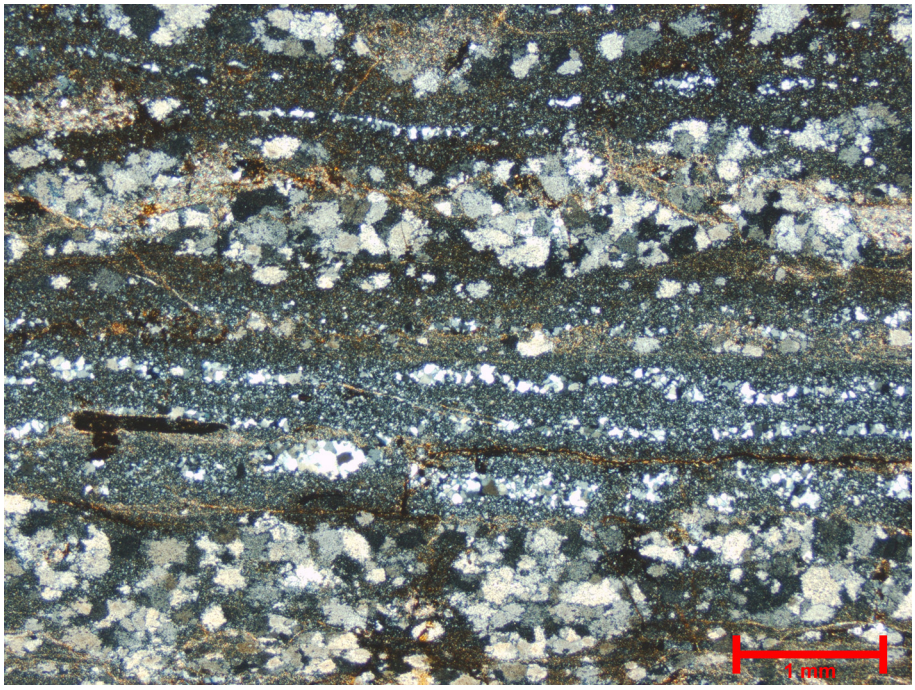

Figure 42: *Representative photomicrograph (in cross-polarised light) of the Grassy Gully Rhyolite (GSNSW 8928LMC0073, GA 1985436). Well-developed flow banding, defined by alternating spherulite-rich and spherulite-poor bands, in sericite-altered, almost aphyric rhyolite lava. A large, dark biotite lath (left) is replaced by opaque oxide minerals and sericite.*

Zircon Description

Zircons from this sample range from euhedral shapes to rounded grains and anhedral fragments, and are predominantly equant to prismatic. Elongate crystals are rare, aspect ratios (length/width) are 1–4 (but mostly less than 3), and long axes are 80–320 µm (Figure 43). In transmitted light, most grains are transparent to translucent (although some are mottled and opaque), and colourless to pale pink or pale brown. The population is strongly heterogeneous, with many cracked grains, some rounded crystals that display evidence for external pitting and abrasion, and some inclusion-rich crystals among a majority that are inclusion-free.

Cathodoluminescence (CL) images reveal a range of moderate to high emission intensities, and mostly high-contrast zoning patterns (Figure 43). A significant population is defined by uniform, relatively finely-developed banding parallel to the long axes, and appears to be magmatic in origin, as do subordinate elongate euhedral crystals with well-developed oscillatory zoning. Many grains contain central areas with high CL emission but low-contrast zoning (Figure 43). These grain areas are often cracked and fractured, and sometimes disconformably overgrown by oscillatory-zoned zircon, consistent with an inherited origin.

U-Pb Isotopic Results

Thirty-two analyses were obtained from 32 individual zircons, and the results are presented in Figure 44, and Table 11. The analysed zircons yielded mostly moderate U contents (152–564 ppm, median 368 ppm) and predominantly low to moderate Th/U (0.13–0.53, median 0.21).

The 32 analyses are mostly characterised by low $^{206}Pb_c$ (maximum 1.14%, median 0.18%), and can be divided into three groups (Table 11):

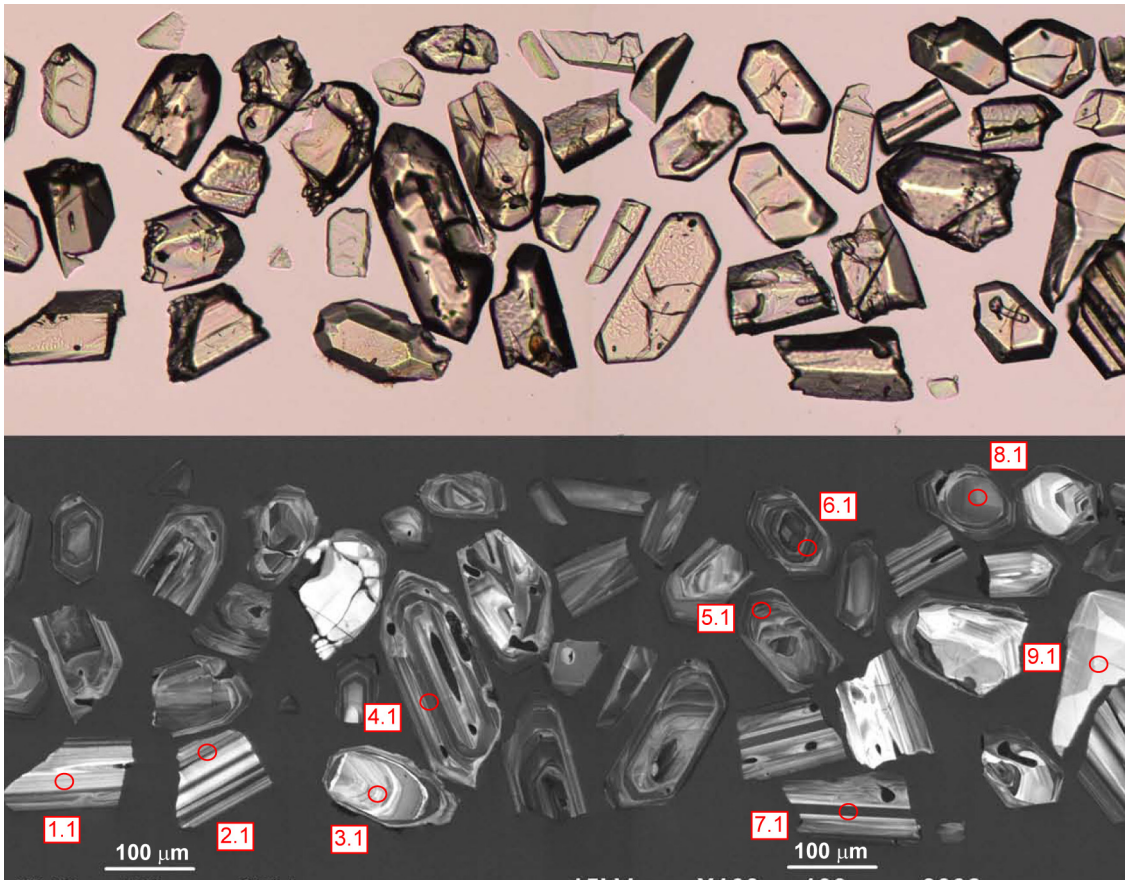

Figure 43: *Representative zircons from the Grassy Gully Rhyolite (GSNSW 8928LMC0073, GA 1985436). Transmitted-light image is shown in the upper half; cathodoluminescence image in the lower half. SHRIMP analysis sites are indicated, and labelled with grain and spot number.*

- 24 analyses of 24 zircons (Group 1; yellow fill in Figure 44) with individual $^{238}U/^{206}Pb$ dates between c. 399 Ma and c. 371 Ma, which yielded a weighted mean date of 384.5 ± 4.4 Ma (MSWD = 1.06),
- five analyses of five zircons (Group 2; yellow fill in Figure 44) with individual $^{238}U/^{206}Pb$ dates between c. 532 Ma and c. 471 Ma, and
- three analyses of three zircons (Group 3; yellow fill in Figure 44) with individual $^{207}Pb/^{206}Pb$ dates between c. 2294 Ma and c. 1030 Ma.

Geochronological Interpretation

The weighted mean date of 384.5 ± 4.4 Ma obtained from the 24 analyses in Group 1 is indistinguishable from the median $^{238}U/^{206}Pb$ date for the same 24 analyses (383.6 +7.2/-1.6 Ma). However, the uncertainties associated with the latter display significant asymmetry, which suggests that the analyses in the Group 1 population do not approximate a normal distribution. The Group 1 data are broadly characterised by increasing U content and decreasing uncertainty magnitude with decreasing $^{238}U/^{206}Pb$ date (Table 11), which raises the possibility that some of the younger analyses have been affected by post-crystallisation loss of radiogenic Pb, thereby lowering the mean $^{238}U/^{206}Pb$ date of the group. However, the extent of any such skewing is unlikely to be significant, as the measured uncertainties within the Group 1 population fully account for the overall scatter (MSWD = 1.06).

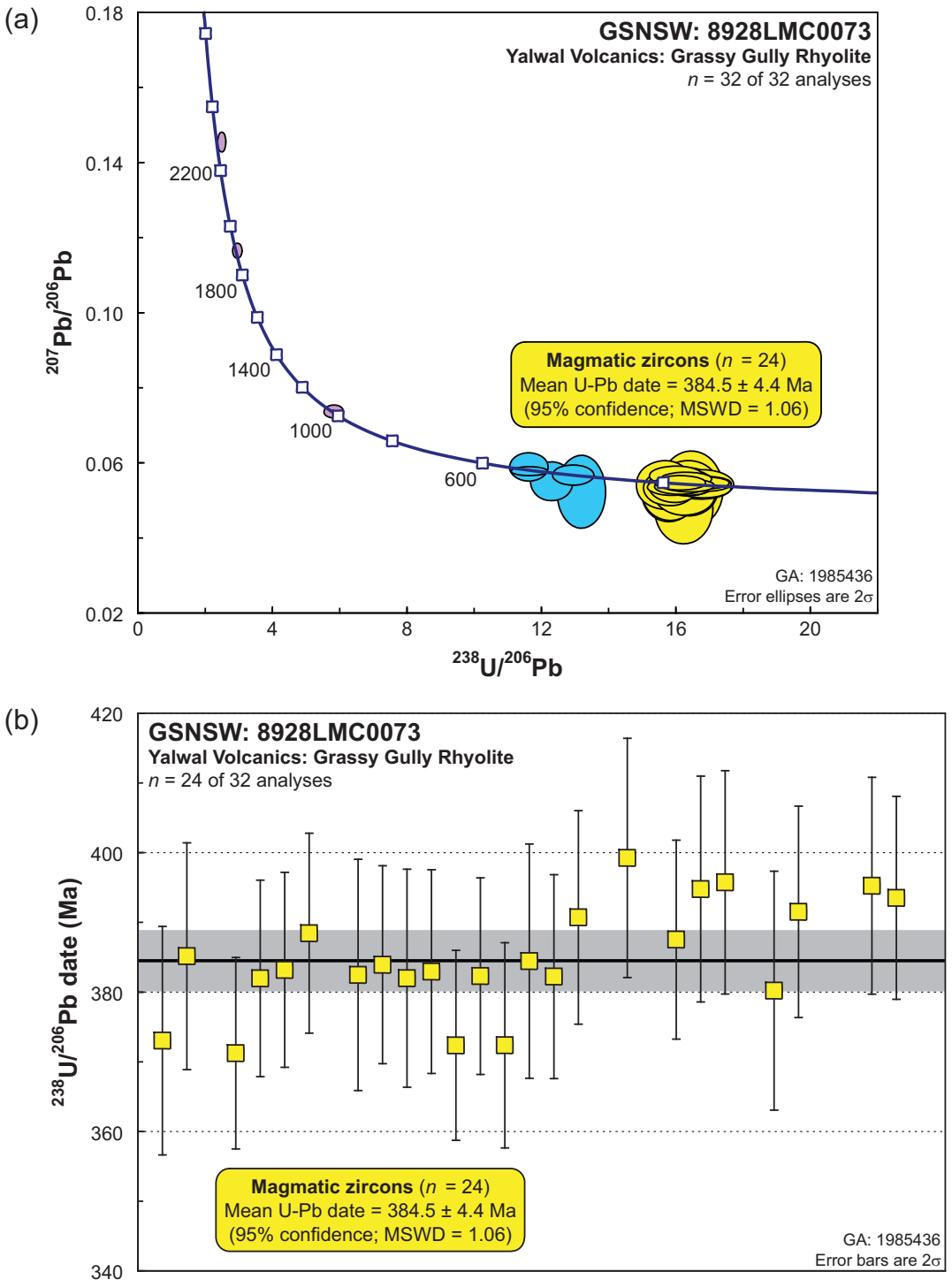

Figure 44: *SHRIMP U-Pb data for zircons from the Grassy Gully Rhyolite (GSNSW 8928LMC0073, GA 1985436). (a) Tera-Wasserburg concordia diagram; (b) $^{238}U/^{206}Pb$ dates in order of acquisition (eight analyses with pre-420 Ma dates are not shown). Yellow fill: magmatic zircons; blue fill: Paleozoic inheritance; pink fill: Proterozoic inheritance. Heavy black line and grey band: weighted mean $^{238}U/^{206}Pb$ date and its 95% confidence interval, respectively.*

Consequently, the weighted mean $^{238}U/^{206}Pb$ date of 384.5 ± 4.4 Ma is interpreted as a minimum estimate of the age of magmatic crystallisation of the Grassy Gully Rhyolite, but a good approximation overall. The five analyses in Group 2 are interpreted to reflect Early Paleozoic (Cambrian and Ordovician inheritance), and the three analyses in Group 3 are similarly interpreted as Proterozoic inheritance.

The magmatic crystallisation age of 384.5 ± 4.4 Ma for the Grassy Gully Rhyolite is substantially older than those of the 325.5 ± 2.6 Ma Touga Granite (GSNSW 8928LMC0363, GA 1985433; this volume) and the 324.4 ± 3.2 Ma Bundundah Granite (GSNSW 8928LMC0365, GA 1985435; this volume), but is indistinguishable from that of the 382.4 ± 3.0 Ma Tullyangela Granite (GSNSW 8928LMC0364, GA 1985434; this volume). This result establishes that plutonic rocks temporally equivalent to the Late Devonian Yalwal Volcanics are exposed at least locally, and that emplacement of the Tullyangela Granite substantially predated the surrounding Middle Carboniferous plutonism in southern MOSS VALE.

Table 11: SHRIMP U-Pb zircon data from the Grassy Gully Rhyolite (GSNSW 8928LMC0073, GA 1985436). All dates are $^{238}U/^{206}Pb$ unless otherwise indicated.

Sess. no.	Grain.area .replicate	$^{206}Pb_c$ (%)	U (ppm)	Th (ppm)	$^{232}Th/^{238}U$	$^{238}U/^{206}Pb$	±1σ (%)	$^{207}Pb/^{206}Pb$	±1σ (%)	Date (Ma)	±1σ (Ma)	Disc. (%)
Group 3: Proterozoic inherited individuals (n = 3; $^{207}Pb/^{206}Pb$ dates tabulated)												
90068	21.1.1	-0.01	106	82	0.81	2.488	2.01	0.14556	0.74	2294	13	5
90068	3.1.1	0.04	112	68	0.63	2.936	2.00	0.11657	0.72	1904	13	1
90068	25.1.1	0.04	253	118	0.48	5.812	1.94	0.07357	0.94	1030	19	1
Group 2: Paleozoic inherited individuals (n = 5)												
90068	28.1.1	0.23	185	90	0.50	11.621	2.02	0.05878	2.63	532.1	10.3	5
90068	32.1.1	0.00	616	614	1.03	11.632	1.90	0.05756	0.86	531.6	9.7	-3
90068	29.1.1	0.37	142	81	0.59	12.304	2.09	0.05491	3.87	503.7	10.1	-19
90068	8.1.1	0.16	227	186	0.84	12.940	1.96	0.05662	1.96	479.9	9.0	-1
90068	19.1.1	0.86	78	44	0.59	13.183	2.26	0.05209	7.69	471.3	10.3	-39
Group 1: Magmatic zircons (n = 24)												
90068	20.1.1	0.62	83	35	0.43	15.652	2.22	0.05397	4.94	399.2	8.6	-7
90068	24.1.1	0.81	170	144	0.88	15.795	2.09	0.05139	5.77	395.7	8.0	-35
90068	30.1.1	0.34	209	89	0.44	15.815	2.03	0.05310	3.58	395.3	7.8	-16
90068	23.1.1	0.55	117	193	1.70	15.834	2.11	0.05126	5.46	394.8	8.1	-36
90068	31.1.1	0.16	525	90	0.18	15.887	1.91	0.05343	1.69	393.5	7.3	-12
90068	27.1.1	0.41	252	162	0.66	15.970	2.00	0.05374	3.48	391.5	7.6	-8
90068	18.1.1	-0.09	178	111	0.65	16.004	2.02	0.05635	1.85	390.7	7.7	19
90068	7.1.1	0.15	431	470	1.13	16.100	1.90	0.05352	1.61	388.4	7.2	-10
90068	22.1.1	0.14	565	110	0.20	16.140	1.90	0.05448	1.39	387.5	7.1	1
90068	1.1.1	1.14	97	69	0.74	16.242	2.18	0.04750	8.02	385.1	8.1	-81
90068	16.1.1	0.71	231	92	0.41	16.274	2.25	0.05124	4.27	384.4	8.4	-35
90068	10.1.1	-0.06	408	362	0.92	16.296	1.91	0.05552	1.38	383.9	7.1	13
90068	6.1.1	0.12	633	237	0.39	16.328	1.88	0.05420	1.51	383.2	7.0	-1
90068	12.1.1	0.37	247	40	0.17	16.339	1.97	0.05435	2.58	382.9	7.3	1
90068	9.1.1	0.18	75	71	0.98	16.360	2.23	0.05394	4.85	382.5	8.3	-4
90068	14.1.1	0.18	467	212	0.47	16.368	1.90	0.05378	1.97	382.3	7.1	-5
90068	17.1.1	0.19	241	303	1.30	16.371	1.97	0.05433	2.36	382.2	7.3	1
90068	11.1.1	0.65	143	169	1.23	16.381	2.11	0.05204	5.01	382.0	7.8	-25
90068	5.1.1	0.07	535	162	0.31	16.382	1.90	0.05378	1.26	382.0	7.0	-5
90068	26.1.1	0.87	88	92	1.08	16.461	2.32	0.05277	7.86	380.2	8.6	-16
90068	2.1.1	0.53	304	50	0.17	16.786	2.26	0.05411	3.00	373.0	8.2	1
90068	15.1.1	0.07	203	170	0.86	16.817	2.03	0.05313	2.01	372.4	7.4	-10
90068	13.1.1	0.04	632	153	0.25	16.817	1.88	0.05450	1.19	372.4	6.8	5
90068	4.1.1	0.10	419	253	0.63	16.870	1.90	0.05427	1.53	371.2	6.9	3

ARTHURSLEIGH SUITE: PLEASANT HILL GRANITE

GA SAMPLENO:	**1985440**
GSNSW SITEID:	**8928LMC0002**
PARENT UNIT(S)	Arthursleigh Suite
FORMAL NAME:	Pleasant Hill Granite
INFORMAL NAME:	—
LITHOLOGY:	Coarse-grained equigranular granodiorite
PROVINCE:	Eastern Lachlan Orogen
1:250 000 SHEET:	WOLLONGONG (SI/56-9)
1:100 000 SHEET:	MOSS VALE (8928)
LOCATION (GDA94):	34.618536 °S, 150.051618 °E
LOCATION (MGA94):	Zone 56, 229670 mE, 6165305 mN
ANALYTICAL SESSION NO(S):	90093 (see Table 1 for parameters derived from concurrent measurements of $^{238}U/^{206}Pb$ and $^{207}Pb/^{206}Pb$ reference zircons)
INTERPRETED AGE:	**412.6 ± 2.2 Ma** (95% confidence; 39 analyses of 39 zircons)
GEOLOGICAL ATTRIBUTION:	Magmatic crystallisation
ISOTOPIC RATIO(S) USED:	$^{238}U/^{206}Pb$ (^{204}Pb-corrected)

Sampling Details

This sample was taken from some large, fresh boulders on the northern verge of the Canyonleigh Road, near the power substation located about 8 km west-southwest of the locality of Canyonleigh.

Relationships and Rationale for Dating

The unit sampled is a coarse-grained leucocratic granodiorite of the Pleasant Hill Granite, which is part of the Arthursleigh Suite in the eastern Lachlan Orogen (Thomas *et al.*, 2002; Trigg and Campbell, in prep.). Plutons of this Suite (which include the 416.7 ± 3.1 Ma Marulan Granite; Black, 2005) intrude, but are broadly contemporaneous with, felsic volcanic rocks of the Early Devonian Bindook Group. Locally and on neighbouring GOULBURN (Thomas *et al.*, 2002), the Bindook Group includes the 414.4 ± 2.9 Ma Barrallier Ignimbrite (Black, 2006), the Newacres Ignimbrite Member of the Quialigo Volcanics, which has yielded SHRIMP zircon $^{238}U/^{206}Pb$ dates of 414.4 ± 2.9 Ma (Black, 2006), 411 ± 3 Ma and 409 ± 4 Ma (Wilde, 2002), and the Tangerang Formation, which includes the Kerillon Tuff Member (GSNSW 8928LMC0368, GA 1985439; this volume).

The aim was to obtain a magmatic crystallisation age, for comparison with that of the Kerillon Tuff (GSNSW 8928LMC0368, GA 1985439; this volume). The age will also be compared with the existing data described above.

Petrography

This sample is a massive, medium- to coarse-grained (3.5–5.5 mm) equigranular granodiorite. It comprises 40% plagioclase, 30% quartz, 20% K-feldspar, 5% hornblende, 5% biotite, and accessory opaque oxide minerals (probably magnetite), titanite, zircon, apatite and allanite. Plagioclase is euhedral to subhedral, with blocky to tabular shapes, polysynthetic twinning, and compositional zoning (Figure 45). Typically, cores are sericitised and rims are clear, but the compositional range is relatively narrow (andesine throughout: $An_{34–43}$ on a cleavage section). Quartz occurs as large, weakly strained grains up to 5 mm in diameter with irregular margins (some of which host small inclusions of crystallised melt), and as finer-grained interstitial material between plagioclase

crystals. Perthitic K-feldspar forms irregular interstitial grains up to 5 mm diameter, and the larger crystals host small inclusions of plagioclase and ferromagnesian minerals. Hornblende is pleochroic from pale green to lime-green to olive-green, and occurs both as individual subhedral crystals 1–2 mm in length, and as smaller grains in clusters with biotite (Figure 45). Biotite is mostly unaltered, straw-yellow to chocolate-brown in colour, and commonly hosts tiny zircon and apatite crystals. Allanite occurs as a single zoned crystal 1.5 mm in length.

Little alteration is evident, with K-feldspar only lightly dusted with clay minerals, and relatively uncommon partial replacement of biotite by chlorite and white mica. Overall, the mineralogy indicates the granodiorite has a metaluminous, oxidised affinity, consistent with the rest of the Arthursleigh Suite in this area.

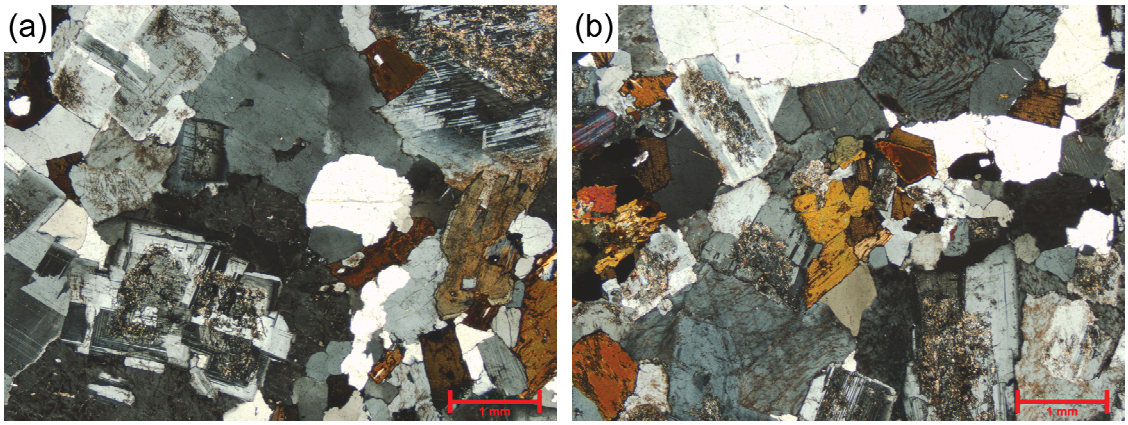

Figure 45: *Representative photomicrographs (in cross-polarised light) of the Pleasant Hill Granite (GSNSW 8928LMC0002, GA 1985440). (a) Zoned plagioclase (lower and upper left), strained quartz (centre and top), perthitic K-feldspar (lower left) and biotite (lower right corner). The large, weakly zoned crystal (right, near biotite) is allanite. (b) Plagioclase with sericitised cores (lower right), perthitic K-feldspar (top and lower left), clear quartz, hornblende (yellowish grain in centre, and in cluster with opaque oxide minerals at left), and biotite (small dark brown grains in centre and lower left).*

Zircon Description

Zircons from this sample are mostly euhedral and equant to prismatic, rather than elongate. Aspect ratios (length/width) are 1–4 (but mostly less than 3), and long axes are 40–210 µm (Figure 46). In transmitted light, the crystals are predominantly transparent and colourless to pale pink, and no inheritance (in the form of cores or discrete grains) is apparent. Some crystals host inclusions of pale- and dark-coloured minerals, but most grains are inclusion-free.

Cathodoluminescence (CL) images reveal a uniformly moderate intensity of emission, and are dominated by low-contrast concentric oscillatory zoning parallel to the crystal faces (Figure 46). These zoning patterns are typical of magmatic zircon. Rare grains feature cores with low CL emission, which appear to have sharp, disconformable contacts with their concentrically zoned overgrowths, and probably represent inheritance.

U-Pb Isotopic Results

Thirty-nine analyses were obtained from 39 individual zircons, and the results are presented in Table 12 and Figure 47. The analysed zircons are characterised by moderate U contents (110–545 ppm, median 213 ppm), and mostly moderate Th/U (0.37–1.09, median 0.51).

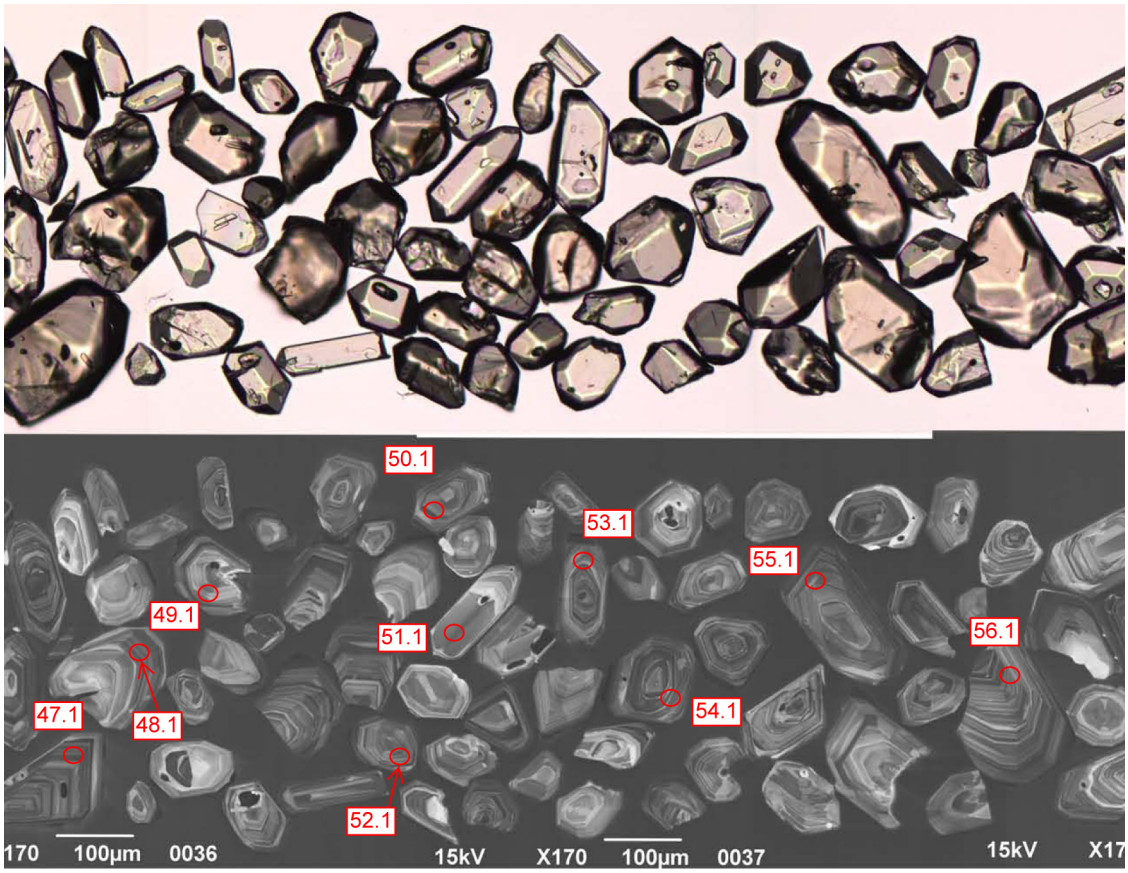

Figure 46: *Representative zircons from the Pleasant Hill Granite (GSNSW 8928LMC0002, GA 1985440). Transmitted-light image is shown in the upper half; cathodoluminescence image in the lower half. SHRIMP analysis sites are indicated, and labelled with grain and spot number.*

All 39 analyses have low $^{206}Pb_c$ (maximum 0.94%, median 0.09%), yielded individual $^{238}U/^{206}Pb$ dates between c. 424 Ma and c. 403 Ma, and define a single group (Group 1; yellow fill in Figure 47) with a weighted mean date of 412.6 ± 2.2 Ma (MSWD = 1.29).

Geochronological Interpretation

The weighted mean date of 412.6 ± 2.2 Ma for the 39 analyses in Group 1 is indistinguishable from the median $^{238}U/^{206}Pb$ date for the same 39 analyses (412.9 +1.5/-2.6 Ma), and the absence of significant asymmetry in the uncertainties associated with the latter suggests that the group represents a single population of analyses with an approximately normal distribution. Consequently, the weighted mean $^{238}U/^{206}Pb$ date of 412.6 ± 2.2 Ma is interpreted as the best estimate of the age of magmatic crystallisation of the Pleasant Hill Granite.

The magmatic crystallisation age of 412.6 ± 2.2 Ma for the Pleasant Hill Granite is marginally younger than the 416.7 ± 3.1 Ma Marulan Granite (Black, 2005); however, the age determined here appears to better fit the interpreted intrusive relationship with the felsic volcanic rocks of the host Bindook Group. Specifically, the magmatic crystallisation age of 412.6 ± 2.2 Ma for the Pleasant Hill Granite is indistinguishable from that of the 412.7 ± 2.2 Ma Kerillon Tuff Member of the Tangerang Formation (GSNSW 8928LMC0368, GA 1985439; this volume), the 414.4 ± 2.9 Ma Barrallier Ignimbrite (Black, 2006), and the Newacres Ignimbrite Member of the Quialigo

Volcanics, which has yielded SHRIMP zircon $^{238}U/^{206}Pb$ dates of 414.4 ± 2.9 Ma (Black, 2006), 411 ± 3 Ma and 409 ± 4 Ma (Wilde, 2002).

Table 12: SHRIMP U-Pb zircon data from the Pleasant Hill Granite (GSNSW 8928LMC0002, GA 1985440). All dates are $^{238}U/^{206}Pb$ unless otherwise indicated.

Sess. no.	Grain.area .replicate	$^{206}Pb_c$ (%)	U (ppm)	Th (ppm)	$^{232}Th/^{238}U$	$^{238}U/^{206}Pb$	±1σ (%)	$^{207}Pb/^{206}Pb$	±1σ (%)	Date (Ma)	±1σ (Ma)	Disc. (%)
Group 1: Magmatic zircons (n = 39)												
90093	60.1.1	0.22	201	87	0.45	14.709	1.07	0.05440	2.83	424.0	4.4	-9
90093	41.1.1	0.11	201	119	0.61	14.760	1.05	0.05384	2.81	422.6	4.3	-14
90093	35.1.1	-0.27	279	178	0.66	14.858	0.98	0.05862	1.89	419.9	4.0	32
90093	64.1.1	0.23	327	152	0.48	14.927	0.98	0.05463	2.23	418.0	4.0	-5
90093	47.1.1	0.07	545	207	0.39	14.944	0.91	0.05495	1.30	417.6	3.7	-2
90093	63.1.1	0.47	133	65	0.51	14.967	1.21	0.05161	5.45	416.9	4.9	-36
90093	32.1.1	0.15	174	88	0.52	14.976	1.07	0.05430	2.67	416.7	4.3	-8
90093	46.1.1	0.27	205	85	0.43	14.978	1.06	0.05357	2.50	416.6	4.3	-15
90093	33.1.1	0.33	295	151	0.53	14.990	0.98	0.05249	2.77	416.3	3.9	-26
90093	38.1.1	-0.03	113	57	0.52	14.991	1.18	0.05540	2.01	416.3	4.8	3
90093	58.1.1	0.17	214	118	0.57	15.027	1.04	0.05374	2.52	415.3	4.2	-13
90093	36.1.1	0.52	143	65	0.47	15.031	1.13	0.05237	3.35	415.2	4.5	-27
90093	34.1.1	0.05	169	87	0.54	15.044	1.06	0.05470	1.77	414.9	4.3	-4
90093	49.1.1	0.35	192	125	0.67	15.060	1.10	0.05469	2.73	414.4	4.4	-4
90093	50.1.1	0.02	349	202	0.60	15.070	1.07	0.05520	1.60	414.2	4.3	2
90093	51.1.1	-0.08	288	303	1.09	15.071	0.98	0.05485	1.41	414.2	3.9	-2
90093	40.1.1	0.06	143	69	0.50	15.076	1.12	0.05580	2.02	414.0	4.5	7
90093	59.1.1	-0.16	110	39	0.37	15.094	1.21	0.05779	2.31	413.5	4.9	26
90093	69.1.1	-0.19	218	91	0.43	15.113	1.11	0.05518	2.11	413.0	4.4	2
90093	65.1.1	0.17	213	177	0.86	15.117	1.06	0.05436	3.15	412.9	4.2	-7
90093	56.1.1	0.09	220	88	0.42	15.156	1.07	0.05405	1.97	411.9	4.3	-9
90093	61.1.1	0.06	332	163	0.51	15.158	1.11	0.05534	1.63	411.8	4.4	3
90093	55.1.1	-0.02	325	149	0.47	15.180	0.96	0.05495	1.18	411.3	3.8	0
90093	48.1.1	-0.06	312	152	0.50	15.199	0.98	0.05579	1.33	410.8	3.9	8
90093	62.1.1	-0.23	181	93	0.53	15.205	1.09	0.05771	2.22	410.6	4.3	26
90093	68.1.1	0.01	239	111	0.48	15.217	1.03	0.05619	1.53	410.3	4.1	12
90093	52.1.1	0.14	251	126	0.52	15.233	1.01	0.05391	2.12	409.9	4.0	-10
90093	57.1.1	0.18	187	100	0.55	15.246	1.09	0.05490	2.44	409.5	4.3	0
90093	39.1.1	0.09	160	75	0.49	15.248	1.15	0.05401	2.18	409.5	4.6	-9
90093	42.1.1	0.09	269	207	0.80	15.275	1.45	0.05600	1.85	408.8	5.7	11
90093	43.1.1	0.01	215	163	0.78	15.279	1.08	0.05675	1.47	408.7	4.3	18
90093	54.1.1	0.10	334	141	0.44	15.298	0.96	0.05397	1.69	408.2	3.8	-9
90093	44.1.1	0.42	121	60	0.51	15.303	1.20	0.04948	3.94	408.1	4.7	-58
90093	37.1.1	0.25	288	148	0.53	15.305	0.98	0.05291	2.65	408.0	3.9	-20
90093	66.1.1	-0.02	425	228	0.55	15.331	0.95	0.05650	1.16	407.3	3.7	16
90093	45.1.1	0.94	79	36	0.47	15.355	1.44	0.04892	9.56	406.7	5.7	-65
90093	70.1.1	0.14	307	195	0.66	15.402	1.20	0.05469	1.97	405.5	4.7	-2
90093	67.1.1	0.12	210	93	0.46	15.478	1.06	0.05593	2.26	403.6	4.2	11
90093	53.1.1	-0.01	289	162	0.58	15.521	0.98	0.05564	1.27	402.5	3.8	9

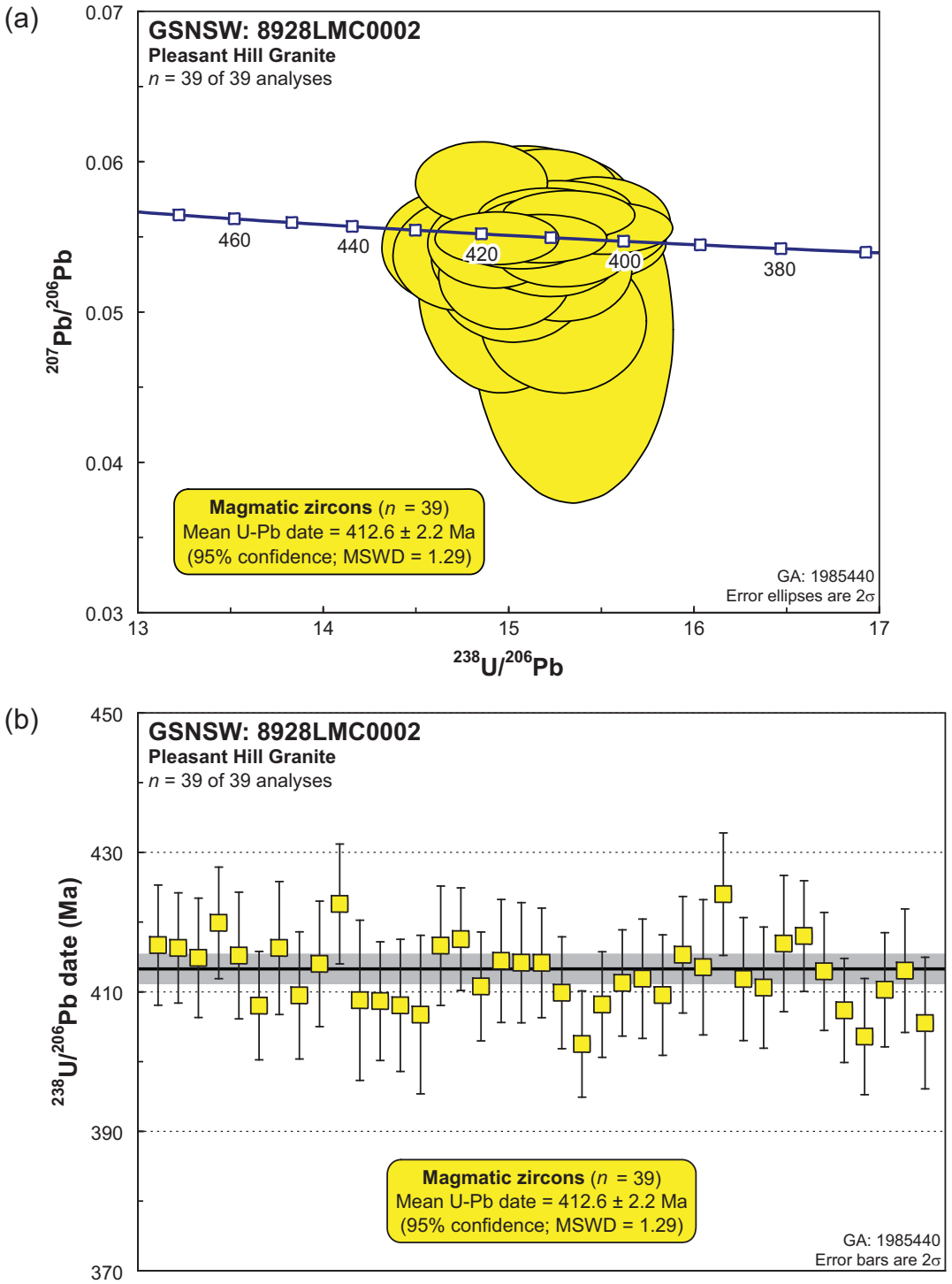

Figure 47: *SHRIMP U-Pb data for zircons from the Pleasant Hill Granite (GSNSW 8928LMC0002, GA 1985440). (a) Tera-Wasserburg concordia diagram; (b) $^{238}U/^{206}Pb$ dates in order of acquisition. Yellow fill: magmatic zircons. Heavy black line and grey band: weighted mean $^{238}U/^{206}Pb$ date and its 95% confidence interval, respectively.*

BINDOOK GROUP: TANGERANG FORMATION: KERILLON TUFF MEMBER

GA SAMPLENO:	**1985439**
GSNSW SITEID:	**8928LMC0368**
PARENT UNIT(S)	Bindook Group: Tangerang Formation
FORMAL NAME:	Kerillon Tuff Member
INFORMAL NAME:	—
LITHOLOGY:	Crystal-rich welded dacitic ignimbrite
PROVINCE:	Eastern Lachlan Orogen
1:250 000 SHEET:	WOLLONGONG (SI/56-9)
1:100 000 SHEET:	MOSS VALE (8928)
LOCATION (GDA94):	34.761303 °S, 150.010232 °E
LOCATION (MGA94):	Zone 56, 226345 mE, 6149354 mN
ANALYTICAL SESSION NO(S):	90093 (see Table 1 for parameters derived from concurrent measurements of $^{238}U/^{206}Pb$ and $^{207}Pb/^{206}Pb$ reference zircons)
INTERPRETED AGE:	**412.7 ± 2.2 Ma** (95% confidence; 33 analyses of 33 zircons)
GEOLOGICAL ATTRIBUTION:	Magmatic crystallisation
ISOTOPIC RATIO(S) USED:	$^{238}U/^{206}Pb$ (^{204}Pb-corrected)

Sampling Details

This sample was taken from some low outcrops in a lightly wooded area near the northwestern bank of Tangarang Creek, about 250 m northeast of where Marulan South Road crosses the creek.

Relationships and Rationale for Dating

The unit sampled is a crystal-rich welded dacitic ignimbrite of the Kerillon Tuff Member, which is part of the Tangerang Formation, within the Early Devonian Bindook Group in the eastern Lachlan Orogen (Thomas *et al.*, 2002; Trigg and Campbell, in prep.). These volcanic rocks, which also include the 414.4 ± 2.9 Ma Barrallier Ignimbrite (Black, 2006), and the Newacres Ignimbrite Member of the Quialigo Volcanics, which has yielded SHRIMP zircon $^{238}U/^{206}Pb$ dates of 414.4 ± 2.9 Ma (Black, 2006), 411 ± 3 Ma and 409 ± 4 Ma (Wilde, 2002), are intruded by granitic plutons of the Arthursleigh Suite, which includes the 416.7 ± 3.1 Ma Marulan Granite (Black, 2005) and the Pleasant Hill Granite (GSNSW 8928LMC0002, GA 1985440; this volume).

The aim was to obtain a magmatic crystallisation age, for comparison with that of the Pleasant Hill Granite (GSNSW 8928LMC0002, GA 1985440; this volume). The age will also be compared with the existing data described above.

Petrography

This sample is a dark-grey, medium-grained and moderately crystal-rich welded dacitic ignimbrite that contains abundant volcanic lithic clasts, and flattened pumice clasts defining a eutaxitic texture. It contains 15–20% plagioclase crystals, 15% angular lithic fragments, 12% quartz, and 2–3% ex-ferromagnesian minerals, and accessory zircon and opaque oxide minerals (probably magnetite), in a dark and finely microcrystalline matrix (Figure 48). The crystals have been strongly fragmented during eruption and emplacement. Quartz sometimes occurs as embayed phenocrysts up to 2 mm in diameter, but more commonly forms angular crystal slivers up to 0.5 mm in size, and heavily sericite-epidote altered plagioclase is similarly fragmented. Euhedral to subhedral ex-ferromagnesian minerals are completely replaced by chlorite, smectite and epidote (Figure 48).

Lithic fragments are up to 5 mm in size. Most of these are porphyritic, probably coherent dacite clasts (derived from either lava or shallow intrusions), comprising feldspar and quartz phenocrysts in a microcrystalline or micropoikilitic groundmass. Flattened pumice clasts form lenses up to 15 mm in length, and are sparsely porphyritic, with microphenocrysts of quartz and feldspar (Figure 48). Abundant tiny vesicles are also evident, despite strong chloritisation.

The matrix is dark, very finely microcrystalline and pervasively clay-altered, which largely obscures the dense welding except around the margins of the larger crystals. This sample is overprinted by a pervasive alteration assemblage of chlorite, smectite, granular epidote, sericite and minor titanite.

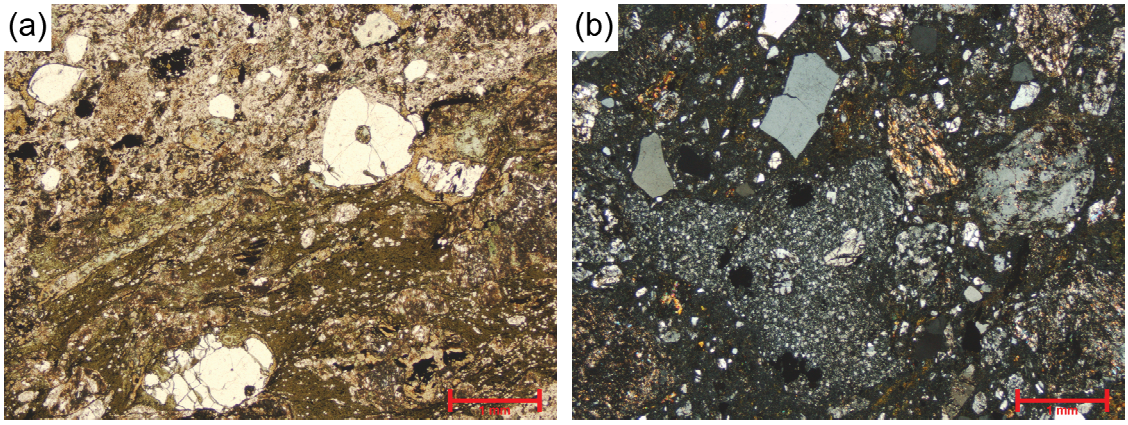

Figure 48: *Representative photomicrographs of the Kerillon Tuff (GSNSW 8928LMC0368, GA 1985439). (a) Plane-polarised light view of a large, flattened pumice clast (lower half) preserving a vesicular texture, despite strong chloritisation. Crystals of quartz and heavily altered plagioclase (upper half) are also evident. (b) Cross-polarised light view of the texture typical of this altered ignimbrite. A clast of porphyritic dacite (centre and left) features a coarsely microcrystalline groundmass. Elsewhere, phenocrysts and angular crystal fragments comprise abundant clear quartz, subordinate variably-altered plagioclase (top right and bottom right), and rare small ex-ferromagnesian grains replaced by chlorite and smectite (top centre and top left). The matrix is very finely microcrystalline and clay-altered.*

Zircon Description

Zircons from this sample display a wide range of external morphologies, ranging from euhedral elongate and prismatic crystals to anhedral fragments and rounded grains with abraded surfaces. The grains are quite small: aspect ratios (length/width) are 1–4 (but mostly less than 3), and long axes are 50–170 µm (Figure 49). In transmitted light, crystals of probable magmatic origin are predominantly transparent, mostly colourless to pale pink, and largely inclusion-free. Most grains of probable detrital or inherited origin (such as the grain lower right of 45.1; Figure 49) are characteristically rounded and feature the pitted surfaces typical of mechanical abrasion, but others (such as grain 48.1; Figure 49) are not easily distinguished from the magmatic population.

Cathodoluminescence (CL) images reveal a range of emission intensities and patterns, broadly corresponding to the two zircon populations identified in transmitted light. Zircons of magmatic origin display moderate to high emission and characteristic low-contrast zoning, in concentric oscillatory patterns and as broad banding parallel to the long axis (Figure 49). These patterns are typical of magmatic zircon, although rare grains host small cores with lower CL emission, which appear to have sharp, disconformable contacts with their brighter, zoned overgrowths. Rounded grains are characterised by CL emission of low intensity and low contrast, and zoning patterns truncated at high angles by the grain margins, consistent with abrasion during sedimentary transport.

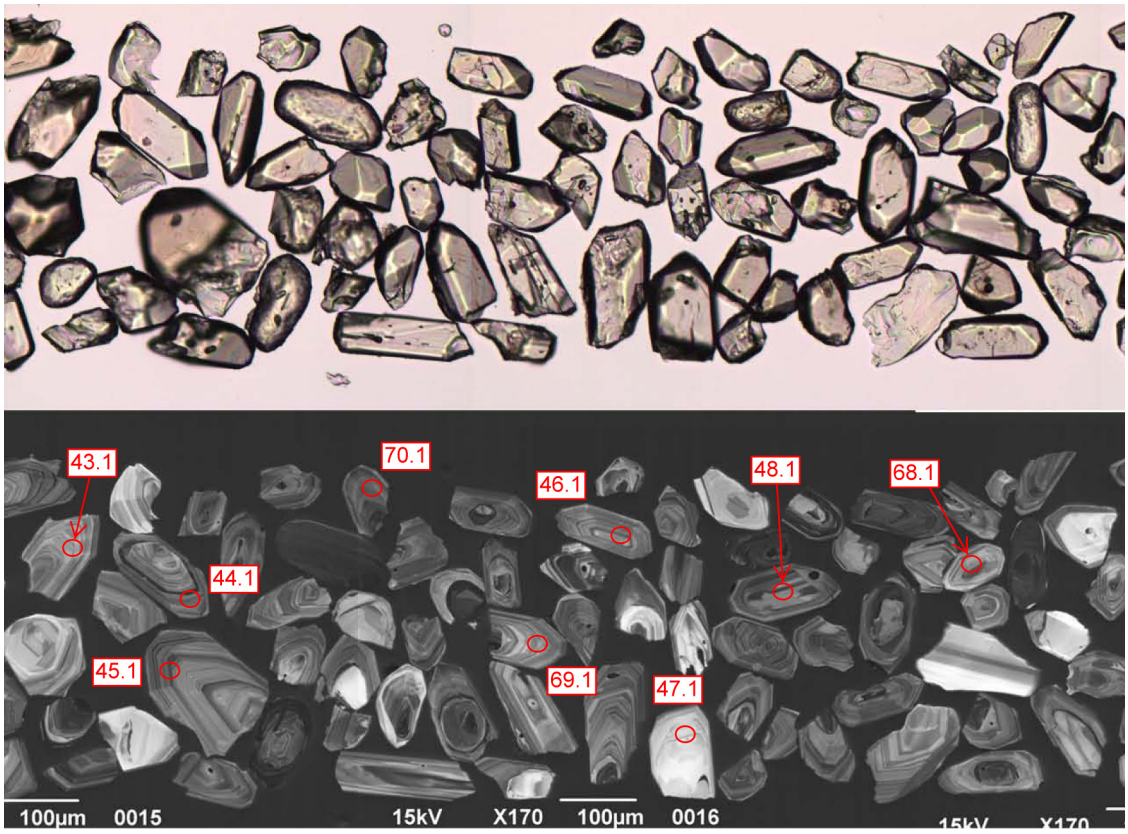

Figure 49: *Representative zircons from the Kerillon Tuff (GSNSW 8928LMC0368, GA 1985439). Transmitted-light image is shown in the upper half; cathodoluminescence image in the lower half. SHRIMP analysis sites are indicated, and labelled with grain and spot number.*

U-Pb Isotopic Results

Thirty-nine analyses were obtained from 39 individual zircons, and the results are presented in Figure 50, and Table 13. Most zircons feature low to moderate U contents (37–288 ppm, median 157 ppm), and uniformly moderate Th/U (0.37–0.82, median 0.48). One inherited grain was analysed, and yielded a similar U content (161 ppm), but much higher Th/U (1.59).

One analysis (40.1.1; not shown in Figure 50) was adversely affected by instrumental instability during data acquisition, and is not considered further. A further three analyses (43.1.1, 47.1.1, and 56.1.1; red fill in Figure 50) yielded high common Pb contents ($^{206}Pb_c$ > 1.5%), and are interpreted to have been affected by loss of radiogenic Pb during one or more events of unknown age. Consequently, their $^{238}U/^{206}Pb$ dates are unreliable, and these analyses are not considered further.

The remaining 35 analyses have uniformly low $^{206}Pb_c$ (maximum 0.83%, median 0.09%), and can be divided into two groups (Table 13):

- 33 analyses of 33 zircons (Group 1; yellow fill in Figure 50) with individual $^{238}U/^{206}Pb$ dates between c. 420 Ma and c. 404 Ma, which yielded a weighted mean date of 412.7 ± 2.2 Ma (MSWD = 0.95), and
- two analyses of two zircons (Group 2; blue fill in Figure 50) with individual $^{238}U/^{206}Pb$ dates between c. 499 Ma and c. 427 Ma.

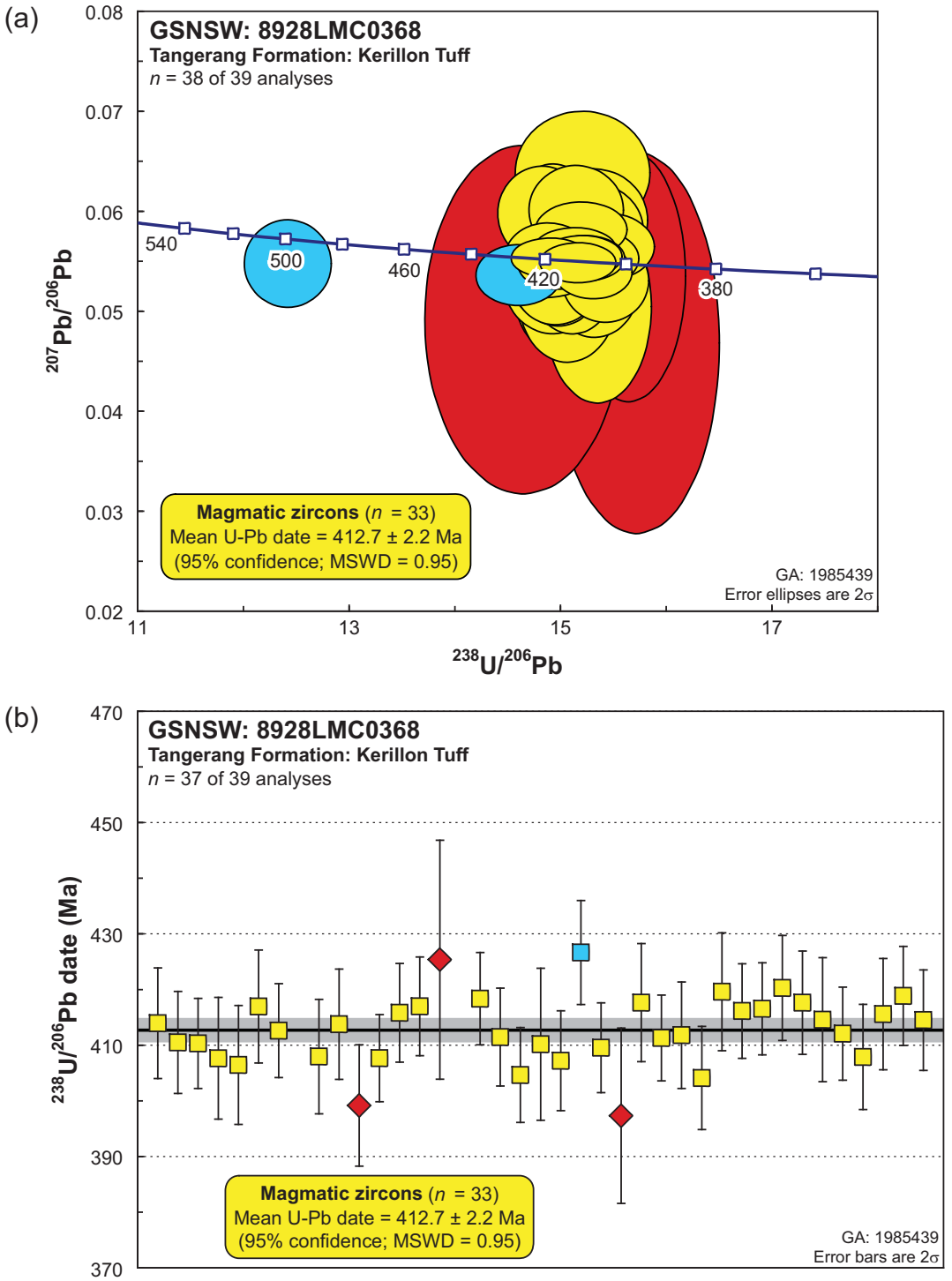

Figure 50: *SHRIMP U-Pb data for zircons from the Kerillon Tuff (GSNSW 8928LMC0368, GA 1985439). One analysis affected by instrumental instability (40.1.1) is not shown in either panel. (a) Tera-Wasserburg concordia diagram; (b) $^{238}U/^{206}Pb$ dates in order of acquisition (one analysis with a pre-470 Ma date is not shown). Yellow fill: magmatic zircons; blue fill: Ordovician–Silurian inheritance; red fill: not considered due to high $^{206}Pb_c$. Heavy black line and grey band: weighted mean $^{238}U/^{206}Pb$ date and its 95% confidence interval, respectively.*

Geochronological Interpretation

The weighted mean date of 412.7 ± 2.2 for the 33 analyses in Group 1 is indistinguishable from the median $^{238}U/^{206}Pb$ date for the same 33 analyses (412.6 +3.2/-3.3 Ma), and the absence of significant asymmetry in the uncertainties associated with the latter suggests that the group represents a single population of analyses with an approximately normal distribution.

Consequently, the weighted mean $^{238}U/^{206}Pb$ date of 412.7 ± 2.2 Ma is interpreted as the best estimate of the age of magmatic crystallisation of the Kerillon Tuff. The two analyses in Group 2 are interpreted as Ordovician and Silurian inheritance.

The magmatic crystallisation age of 412.7 ± 2.2 Ma for the Kerillon Tuff is indistinguishable from all existing SHRIMP zircon $^{238}U/^{206}Pb$ dates for the Bindook Group, including the 414.4 ± 2.9 Ma Barrallier Ignimbrite (Black, 2006), and the Newacres Ignimbrite Member of the Quialigo Volcanics, which has yielded ages of 414.4 ± 2.9 Ma (Black, 2006), 411 ± 3 Ma and 409 ± 4 Ma (Wilde, 2002). The magmatic crystallisation age of 412.7 ± 2.2 Ma for the Kerillon Tuff is also indistinguishable from that of the 412.6 ± 2.2 Ma Pleasant Hill Granite (GSNSW 8928LMC0002, GA 1985440; this volume), but is marginally younger than the 416.7 ± 3.1 Ma Marulan Granite (Black, 2005). The latter result is at odds with the inference that plutonic rocks of the Arthursleigh Suite intrude and postdate the Bindook Group (Thomas *et al.*, 2002; Johnston *et al.*, in press); however, the Marulan Granite age is indistinguishable from the 414.4 ± 2.9 Ma Barrallier Ignimbrite and the 414.4 ± 2.9 Ma Newacres Ignimbrite Member of the Quialigo Volcanics (Black, 2006).

Table 13: SHRIMP U-Pb zircon data from the Kerillon Tuff (GSNSW 8928LMC0368, GA 1985439). All dates are $^{238}U/^{206}Pb$ unless otherwise indicated.

Sess. no.	Grain.area .replicate	$^{206}Pb_c$ (%)	U (ppm)	Th (ppm)	$^{232}Th/^{238}U$	$^{238}U/^{206}Pb$	±1σ (%)	$^{207}Pb/^{206}Pb$	±1σ (%)	Date (Ma)	±1σ (Ma)	Disc. (%)
Group 2: Ordovician–Silurian inherited individuals (n = 2)												
90093	48.1.1	0.19	161	248	1.59	12.428	1.34	0.05486	3.25	498.9	6.5	-19
90093	54.1.1	0.09	134	47	0.37	14.615	1.13	0.05374	2.29	426.7	4.7	-16
Group 1: Magmatic zircons (n = 33)												
90093	64.1.1	-0.33	143	65	0.47	14.844	1.16	0.05987	3.20	420.3	4.7	42
90093	61.1.1	0.12	190	87	0.47	14.868	1.30	0.05421	2.07	419.6	5.3	-9
90093	70.1.1	0.13	181	72	0.41	14.896	1.10	0.05578	2.30	418.9	4.5	6
90093	49.1.1	-0.04	233	95	0.42	14.914	1.02	0.05542	1.46	418.4	4.1	3
90093	57.1.1	0.27	84	38	0.46	14.941	1.31	0.05361	4.36	417.6	5.3	-15
90093	65.1.1	-0.39	162	75	0.48	14.941	1.15	0.05883	4.12	417.6	4.6	34
90093	46.1.1	0.53	174	139	0.82	14.965	1.10	0.05299	3.24	417.0	4.4	-21
90093	38.1.1	0.39	94	56	0.61	14.966	1.26	0.05427	3.95	417.0	5.1	-8
90093	63.1.1	0.08	244	112	0.47	14.982	1.03	0.05486	1.87	416.5	4.1	-2
90093	62.1.1	0.30	217	113	0.54	14.996	1.05	0.05301	3.37	416.1	4.2	-21
90093	45.1.1	0.37	174	79	0.47	15.008	1.10	0.05384	3.28	415.8	4.4	-12
90093	69.1.1	0.71	120	50	0.43	15.017	1.24	0.05262	5.29	415.6	5.0	-25
90093	66.1.1	0.03	185	70	0.39	15.055	1.39	0.05633	1.71	414.6	5.6	12
90093	71.1.1	0.03	208	82	0.41	15.058	1.13	0.05515	1.70	414.5	4.5	1
90093	33.1.1	0.74	102	51	0.51	15.079	1.24	0.05111	4.83	413.9	5.0	-41
90093	42.1.1	0.56	108	65	0.62	15.085	1.24	0.05342	4.99	413.8	5.0	-16
90093	39.1.1	0.22	202	95	0.49	15.129	1.06	0.05260	3.68	412.6	4.2	-24
90093	67.1.1	0.01	215	94	0.45	15.149	1.05	0.05632	1.53	412.1	4.2	13
90093	59.1.1	-0.34	147	71	0.50	15.160	1.20	0.06018	2.99	411.8	4.8	48
90093	50.1.1	0.22	151	75	0.51	15.172	1.10	0.05482	3.41	411.5	4.4	-2
90093	58.1.1	0.06	287	206	0.74	15.179	0.97	0.05493	1.47	411.3	3.9	0
90093	34.1.1	-0.06	124	80	0.67	15.209	1.15	0.05827	1.93	410.5	4.6	32
90093	35.1.1	0.05	267	176	0.68	15.216	1.02	0.05559	1.52	410.3	4.0	6
90093	52.1.1	-0.36	37	16	0.45	15.222	1.72	0.06390	3.90	410.2	6.8	80
90093	55.1.1	0.06	239	161	0.70	15.245	1.02	0.05541	1.66	409.6	4.0	5
90093	41.1.1	-0.31	99	66	0.69	15.307	1.30	0.05818	3.28	408.0	5.1	31
90093	68.1.1	0.05	124	85	0.71	15.310	1.19	0.05537	2.15	407.9	4.7	5
90093	44.1.1	0.19	288	103	0.37	15.318	0.99	0.05403	2.01	407.7	3.9	-9
90093	36.1.1	-0.39	66	30	0.47	15.319	1.38	0.05921	3.53	407.7	5.5	41
90093	53.1.1	0.34	147	71	0.50	15.336	1.14	0.05290	4.16	407.2	4.5	-20
90093	37.1.1	0.83	88	54	0.63	15.366	1.36	0.05060	7.73	406.4	5.3	-45
90093	51.1.1	0.39	172	71	0.43	15.436	1.09	0.05316	3.17	404.6	4.3	-17
90093	60.1.1	-0.16	131	64	0.51	15.457	1.18	0.05655	2.39	404.1	4.6	17
Not considered, due to high $^{206}Pb_c$ (> 1.5%; n = 3)												
90093	47.1.1	1.51	40	13	0.33	14.661	2.61	0.04930	14.35	425.4	10.7	-62
90093	43.1.1	3.69	78	37	0.49	15.655	1.41	0.05363	9.52	399.2	5.5	-11
90093	56.1.1	1.70	31	13	0.42	15.730	2.04	0.04697	16.48	397.3	7.9	-88
Not considered, due to instrumental instability (n = 1)												
90093	40.1.1	0.54	76	44	0.60	15.772	1.48	0.05021	6.87	396.3	5.7	-48

'MOUNT GIBRALTAR MICROSYENITE'

GA SAMPLENO:	**1985437**
GSNSW SITEID:	**8928LMC0366**
PARENT UNIT(S):	—
FORMAL NAME:	—
INFORMAL NAME:	'Mount Gibraltar microsyenite'
LITHOLOGY:	Aegirine-bearing microsyenite
PROVINCE:	Sydney Basin
1:250 000 SHEET:	WOLLONGONG (SI/56-9)
1:100 000 SHEET:	BURRAGORANG (8929)
LOCATION (GDA94):	34.472177 °S, 150.430233 °E
LOCATION (MGA94):	Zone 56, 263980 mE, 6182491 mN
ANALYTICAL SESSION NO(S):	90064 (see Table 1 for parameters derived from concurrent measurements of $^{238}U/^{206}Pb$ and $^{207}Pb/^{206}Pb$ reference zircons)
INTERPRETED AGE:	**325.4 ± 4.1 Ma** (95% confidence; 7 analyses of 7 zircons)
GEOLOGICAL ATTRIBUTION:	Youngest inherited zircon component
ISOTOPIC RATIO(S) USED:	$^{238}U/^{206}Pb$ (^{204}Pb-corrected)

Sampling Details

This sample was taken from some large, fresh boulders on the floor of the quarry on the southern flank of Mount Gibraltar, within the township of Bowral. Access was via a driveway near the water storage tanks on the northern side of Oxley Drive.

Relationships and Rationale for Dating

The unit sampled is a massive, fine- to medium-grained aegirine-bearing syenite within the informally-named 'Mount Gibraltar microsyenite' (Rose, 1966), which is one of several plutonic to subvolcanic alkaline bodies intruding the southern part of the Sydney Basin. The Mount Gibraltar microsyenite was emplaced into Triassic sedimentary rocks of the Wianamatta Group (Moffitt, 1999), and Evernden and Richards (1962) reported a K-Ar hornblende date of ~178 Ma, which was interpreted as a magmatic crystallisation age.

The aim was to obtain a magmatic crystallisation age for the Mount Gibraltar microsyenite, for comparison with the existing data described above.

Petrography

This sample is a massive, equigranular microsyenite. In hand specimen, the rock is blotchy green and pink in colour, reflecting irregular fine masses of chloritised ferromagnesian minerals juxtaposed against abundant euhedral laths of feldspar and small amounts of calcite infilling cavities. In thin section, the rock comprises 70% alkali feldspar, 20–25% sodic pyroxene (aegirine to aegirine-augite), 5–10% cavity-fill material (described below), and accessory granular opaque oxide minerals and bladed apatite (Figure 51). Alkali feldspar occurs in two forms, subhedral to euhedral, columnar crystals and less well-formed more interstitial grains. Both forms are simply twinned in places, and the interstitial grains in particular show evidence of some exsolution in the form of relatively coarse microperthite of oligoclase composition, which is highlighted by sericite alteration. Moderate axial angles (~40º) were observed on some of the clearest columnar crystals that showed no evidence of perthitic intergrowth, and are consistent with anorthoclase compositions, although the

characteristic polysynthetic twinning was not observed. Sodic pyroxene (aegirine to aegirine-augite) is pleochroic from yellowish-green to deep olive-green to emerald green (Figure 51). The thin section also contains a number of cavities infilled by turbid siderite crystals, irregular patches of fine-grained decussate stilpnomelane and fine-grained chalcedonic quartz, as well as more coarsely crystalline quartz, and a slightly later clear carbonate mineral that is probably calcite (Figure 51). Microperthite exsolved from the alkali feldspar is marked by sericite alteration, and some pyroxene had undergone minor replacement by carbonate minerals and actinolite.

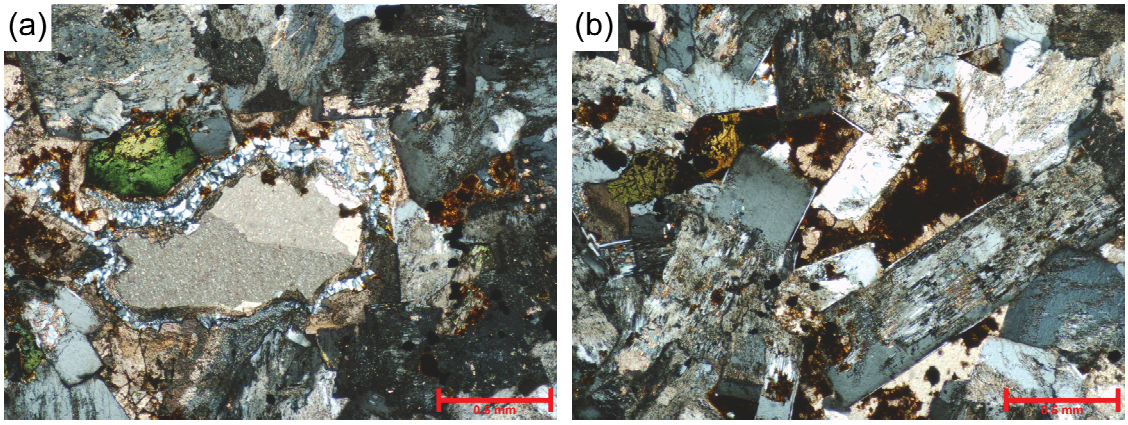

Figure 51: *Representative photomicrographs (in cross-polarised light) of the 'Mount Gibraltar microsyenite' (GSNSW 8928LMC0366, GA 1985437). (a) Small cavity successively filled (from outside rim inwards) by siderite, chalcedonic quartz, a narrow siderite band, and finally coarsely crystalline calcite. The cavity is hosted by microsyenite featuring green aegirine (upper left) and grey, columnar to equant alkali feldspar. (b) Microsyenite comprising columnar to subhedral alkali feldspar crystals, and green aegirine (left). Dark, rhomb-shaped areas (centre) are cavities, filled by pale-brown siderite and very dark brown masses of fine-grained stilpnomelane.*

Zircon Description

Zircons from this sample were extremely sparse, with only about 30 grains recovered in total (Figure 52). The crystals range from euhedral to anhedral, with external morphologies ranging from rounded and anhedral grains to euhedral prisms with pyramidal terminations. Aspect ratios (length/width) are 1–3 (but rarely exceed 2), and long axes are 60–180 µm (Figure 52). In transmitted light, two main zircon types are evident, in approximately equal proportions. The more uniform of the two is euhedral to subhedral, mostly transparent and colourless to pale pink, and often hosts inclusions of dark-coloured minerals. The subordinate population is mostly subhedral to anhedral rounded or irregular shapes, translucent to mottled, and typified by abundant internal cracking.

Cathodoluminescence (CL) images reveal characteristic emission patterns for each of the populations identified in transmitted light. Euhedral zircons are characterised by moderate to high CL emission, and predominantly high-contrast concentric oscillatory zoning parallel to the crystal faces, or less well-defined broad banding parallel to the long axes (Figure 52). The subhedral to anhedral grains show a wide range of CL emission intensities and zoning patterns. Some crystals feature disconformable contacts where cores are overgrown by rim zircon with contrasting CL emission; others display significant distortion of the original zoning patterns, consistent with recrystallisation (Figure 52).

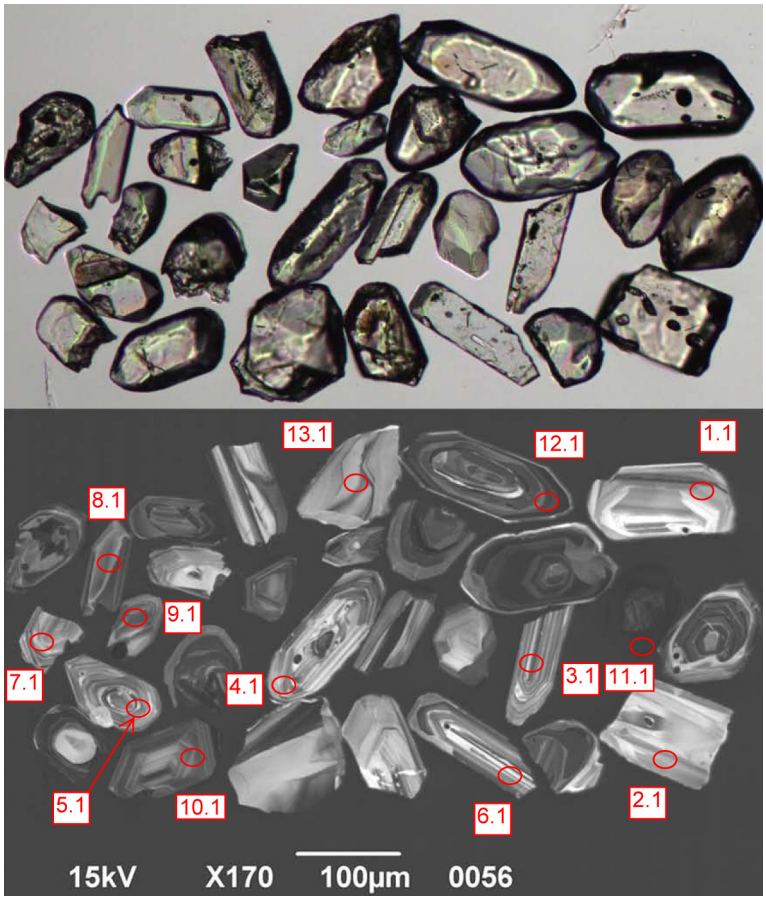

Figure 52: *Representative zircons from the 'Mount Gibraltar microsyenite' (GSNSW 8928LMC0366, GA 1985437). Transmitted-light image is shown in the upper half; cathodoluminescence image in the lower half. SHRIMP analysis sites are indicated, and labelled with grain and spot number.*

U-Pb Isotopic Results

Thirteen analyses were obtained from 13 individual zircons, and the results are presented in Figure 53, and Table 14. Most of the zircons analysed were selected from the euhedral zircons with high CL emission, which are characterised by low to moderate U contents (90–610 ppm, median 147 ppm), whereas Th/U are generally high but vary widely (0.33–1.94, median 1.05). Analyses of the lower-CL, irregularly-shaped zircons yielded higher U contents (314–522 ppm, median 343 ppm) and lower Th/U (0.02–0.58, median 0.43).

Two analyses (6.1.1 and 7.1.1; red fill in Figure 53) yielded high common Pb contents ($^{206}Pb_c$ > 1.3%), and are interpreted to have been affected by loss of radiogenic Pb during one or more events of unknown age. Consequently, their $^{238}U/^{206}Pb$ dates are unreliable, and these analyses are not considered further.

The remaining 11 analyses are mostly characterised by low $^{206}Pb_c$ (maximum 0.98%, median 0.17%), and can be divided into three groups (Table 14):

- seven analyses of seven zircons (Group 1; yellow fill in Figure 53) with individual $^{238}U/^{206}Pb$ dates between c. 333 Ma and c. 320 Ma, which yielded a weighted mean date of 325.4 ± 4.1 Ma (MSWD = 0.90),

- three analyses of three zircons (Group 2; blue fill in Figure 53) with individual $^{238}U/^{206}Pb$ dates between c. 390 Ma and c. 366 Ma, and
- a single analysis (Group 3; pink fill in Figure 53) with a $^{207}Pb/^{206}Pb$ date of 1588 ± 13 Ma (2σ).

Geochronological Interpretation

All of the individual $^{238}U/^{206}Pb$ dates are much older than the hornblende K-Ar date of ~178 Ma obtained by Evernden and Richards (1962), and also significantly predate the Triassic maximum age dictated for the Mount Gibraltar microsyenite by the depositional age for the host Wianamatta Group sedimentary succession. Consequently, all of the analysed zircons are interpreted as inheritance.

The statistical coherence of the weighted mean date obtained from the seven analyses in Group 1 implies the presence of a relatively uniform source of Carboniferous-aged zircons in the source region for the microsyenite. In fact, the weighted mean date of 325.4 ± 4.1 Ma for the zircons in Group 1 is indistinguishable from the magmatic crystallisation ages obtained for the 325.5 ± 2.6 Ma Touga Granite (GSNSW 8928LMC0363, GA 1985433; this volume) and the 324.4 ± 3.2 Ma Bundundah Granite (GSNSW 8928LMC0365, GA 1985435; this volume) in southern MOSS VALE, and raises the possibility that Carboniferous granites are present in significant volumes beneath the Sydney Basin.

Similarly, the Middle to Late Devonian $^{238}U/^{206}Pb$ dates obtained from the three analyses in Group 2 are broadly comparable to the magmatic crystallisation ages obtained for the 384.5 ± 4.4 Ma Grassy Gully Rhyolite (GSNSW 8928LMC0363, GA 1985433; this volume) and the 382.4 ± 3.0 Ma Tullyangela Granite (GSNSW 8928LMC0364, GA 1985434; this volume) in southern MOSS VALE, and potentially indicate the presence of zircon-bearing rocks contemporaneous with the Yalwal Volcanics in the source region of the Mount Gibraltar microsyenite.

Table 14: SHRIMP U-Pb zircon data from the 'Mount Gibraltar microsyenite' (GSNSW 8928LMC0366, GA 1985437). All dates are $^{238}U/^{206}Pb$ unless otherwise indicated.

Sess. no.	Grain.area .replicate	$^{206}Pb_c$ (%)	U (ppm)	Th (ppm)	$^{232}Th/^{238}U$	$^{238}U/^{206}Pb$	±1σ (%)	$^{207}Pb/^{206}Pb$	±1σ (%)	Date (Ma)	±1σ (Ma)	Disc. (%)
Group 3: Mesoproterozoic inherited individual (n = 1; $^{207}Pb/^{206}Pb$ date tabulated)												
90064	11.1.1	0.03	522	10	0.02	3.571	1.30	0.09809	0.34	1588	6	0
Group 2: Devonian inherited individuals (n = 3)												
90064	10.1.1	0.01	314	151	0.50	16.056	1.31	0.05561	1.44	389.5	5.0	12
90064	9.1.1	-0.09	366	205	0.58	16.603	1.30	0.05575	1.57	377.0	4.8	17
90064	8.1.1	0.17	320	113	0.37	17.112	1.54	0.05384	1.88	366.1	5.5	0
Group 1: Carboniferous inherited component (n = 7)												
90064	12.1.1	0.10	610	194	0.33	18.882	1.26	0.05200	1.33	332.7	4.1	-14
90064	13.1.1	0.19	145	102	0.73	19.060	2.54	0.05437	3.21	329.6	8.2	17
90064	1.1.1	0.93	122	132	1.12	19.284	1.60	0.05011	6.57	325.9	5.1	-39
90064	2.1.1	0.18	91	93	1.05	19.402	1.58	0.05706	3.35	324.0	5.0	52
90064	5.1.1	0.11	174	215	1.28	19.431	1.41	0.05522	2.09	323.5	4.4	30
90064	3.1.1	0.98	113	211	1.94	19.478	1.62	0.04719	7.99	322.7	5.1	-82
90064	4.1.1	0.56	147	131	0.92	19.655	1.47	0.05098	5.32	319.9	4.6	-25
Not considered, due to high $^{206}Pb_c$ (> 1.3%; n = 2)												
90064	7.1.1	1.37	103	105	1.05	19.758	1.59	0.04694	7.61	318.3	4.9	-85
90064	6.1.1	1.43	90	150	1.72	20.995	1.64	0.04743	8.80	300.0	4.8	-76

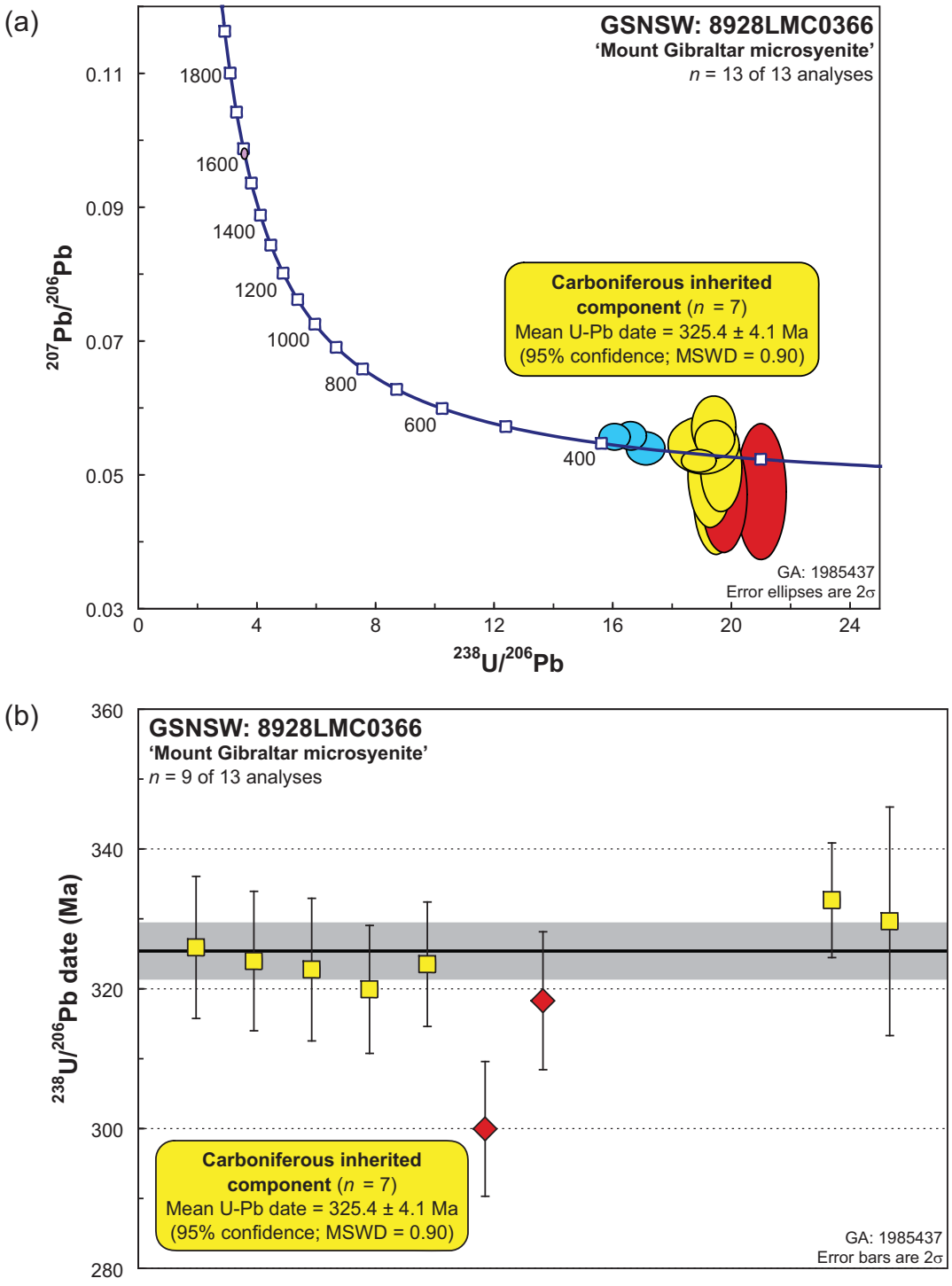

Figure 53: *SHRIMP U-Pb data for zircons from the 'Mount Gibraltar microsyenite' (GSNSW 8928LMC0366, GA 1985437). (a) Tera-Wasserburg concordia diagram; (b) $^{238}U/^{206}Pb$ dates in order of acquisition (four analyses with pre-360 Ma dates are not shown). Yellow fill: Carboniferous inheritance; blue fill: Devonian inheritance; blue fill: Mesoproterozoic inheritance; red fill: not considered due to high $^{206}Pb_c$. Heavy black line and grey band: weighted mean $^{238}U/^{206}Pb$ date and its 95% confidence interval, respectively.*

Boorowa 1:100 000 sheet area

HOVELLS SUITE: RYE PARK GRANITE

GA SAMPLENO:	**1989773**
GSNSW SITEID:	**WRP-046**
PARENT UNIT(S):	Hovells Suite
FORMAL NAME:	Rye Park Granite
INFORMAL NAME:	—
LITHOLOGY:	Medium-grained leucocratic monzogranite
PROVINCE:	Eastern Lachlan Orogen
1:250 000 SHEET:	GOULBURN (SI/55-12)
1:100 000 SHEET:	BOOROWA (8629)
LOCATION (GDA94):	34.498924 °S, 148.904956 °E
LOCATION (MGA94):	Zone 55, 674868 mE, 6180925 mN
ANALYTICAL SESSION NO(S):	90068 (see Table 1 for parameters derived from concurrent measurements of $^{238}U/^{206}Pb$ and $^{207}Pb/^{206}Pb$ reference zircons)
INTERPRETED AGE:	**431.4 ± 4.9 Ma** (95% confidence; 28 analyses of 28 zircons)
GEOLOGICAL ATTRIBUTION:	Magmatic crystallisation
ISOTOPIC RATIO(S) USED:	$^{238}U/^{206}Pb$ (^{204}Pb-corrected)

Sampling Details

This sample was obtained via reverse circulation (RC) drilling by Paradigm Metals Ltd. The drillhole (WRP-046) was collared in granitic rock, and the sampled material was sourced from a depth of 37–41 m. The collar is located near the northern bank of Pudman Creek, about 600 m west of the Rye Park–Rugby Road, and about 1.2 km north-northwest of the locality of Rye Park.

Relationships and Rationale for Dating

The unit sampled is a medium-grained leucocratic monzogranite within the Rye Park Granite, which is part of the Hovells Suite in the eastern Lachlan Orogen (Johnston *et al.*, 2001, in press). The Rye Park Granite intrudes the 433.7 ± 3.0 Ma Hawkins Volcanics (Black, 2005), which is part of the Middle Silurian Douro Group. Farther east and south, on CROOKWELL and GUNNING (Thomas *et al.*, 2001; Johnston *et al.*, 2004), the Hovells Suite includes the 430 ± 6 Ma Bigga Granite (Wilde, 2001), and this age is indistinguishable from those of the S-type Burrawinda Suite (427.8 ± 2.7 Ma Mulgowrie Granodiorite and 427.9 ± 3.0 Ma Winduella Tonalite) and the I-type Gunning Suite (428.6 ± 2.4 Ma Gunning Granite and 429.2 ± 2.3 Ma Cumberoona Tonalite) obtained by Bodorkos and Simpson (2008).

The aim was to obtain a magmatic crystallisation age for the Rye Park Granite, for comparison with the existing data described above.

Petrography

The sample is a medium-grained, equigranular to weakly seriate, bone-coloured leucocratic monzogranite. It comprises 40% greisenised alkali feldspar, 30% quartz, and 30% plagioclase, with accessory biotite, muscovite, apatite and zircon. Alkali feldspars are up to 4.5 mm in length, and display simple twinning. Perthitic exsolution is strongly developed, as is microcline twinning in the

K-feldspar component (Figure 54). Quartz forms anhedral angular to rounded grains up to 3.5 mm in diameter, and is strained and recrystallised. It hosts minerallic inclusions as well as abundant fluid inclusions with variable liquid-vapour ratios. Plagioclase crystals up to 4 mm in length are predominantly albitic in composition, and commonly heavily flecked with sericite and minor carbonate minerals, although some plagioclase rims comprise clear and unaltered albite, especially in contact with (and replacing) alkali feldspar (Figure 54). Where unaltered, biotite is straw-yellow to medium brown in colour, and occurs as rare, fine-grained aggregates.

Replacement of the microcline component of the alkali feldspars by quartz and muscovite (incipient selective greisenisation) occurs mostly on or near through-going fractures as well as internal cracks and structures within the feldspar. Greisenisation postdates perthite development, as euhedral exsolved albite lamellae are enveloped by muscovite during selective removal of the microcline component (Figure 54). Where reactivated, the fractures comprise narrow zones of crushing and diminution, with development of fine-grained secondary sericite and associated replacement of biotite aggregates by very fine-grained aggregates of sericite and titanite. Greisen muscovite adjacent to these fractures is weakly deformed, indicating that at least some alteration postdates deformation.

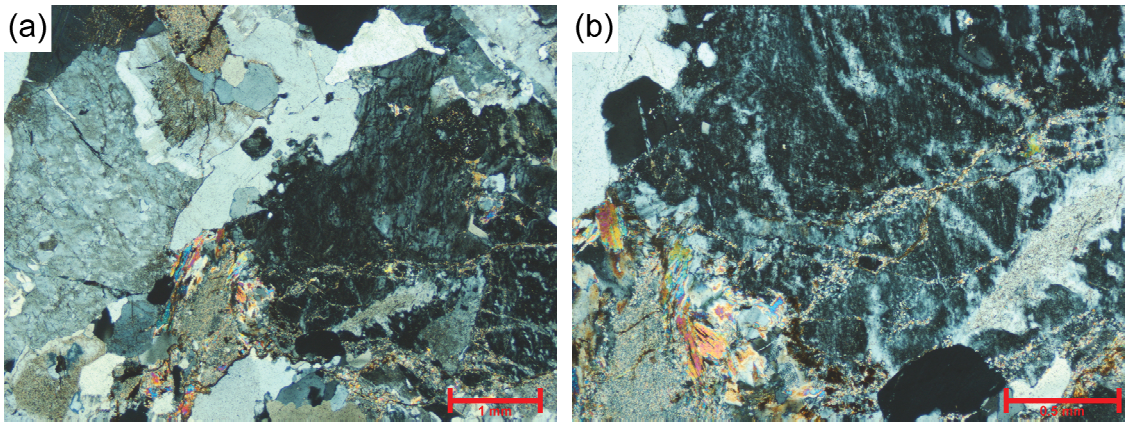

Figure 54: *Representative photomicrographs (in cross-polarised light) of the Rye Park Granite (GSNSW WRP-046, GA 1989773). (a) Large perthitic alkali feldspar (right and left sides), strained and recrystallised quartz (top and base), plagioclase with sericitised cores, and incipient greisenisation along rock fractures, delineated by zones of sericite, coarser-grained white mica and minor fine quartz (lower half). (b) Greisen development within a perthitic alkali feldspar crystal, consisting mainly of fine- and minor coarser-grained white mica and quartz along fractures that crosscut the exsolution texture.*

Zircon Description

Zircons from this sample are euhedral to subhedral, with external morphologies ranging from prismatic crystals with well-developed pyramidal terminations to equant, blocky grains with occasionally irregular shapes. Aspect ratios (length/width) are 1–5 and vary widely, and long axes are 30–240 µm (Figure 55). Most of the crystals are transparent, colourless to pale pink, and notably free of inclusions. A subordinate population of grains is relatively heavily fractured, and is much richer in fine inclusions of pale- and dark-coloured minerals.

Cathodoluminescence (CL) images reveal a range of emission patterns and intensities, but most grains are characterised by an outer region of zircon with moderate CL emission and well-developed concentric oscillatory zoning parallel to the external crystal faces. In many crystals, this outer mantle of oscillatory-zoned zircon disconformably overgrows a core with strongly contrasting (low or high)

CL emission (Figure 55). The zoning is consistent with a diverse suite of inherited cores serving as nucleation sites for oscillatory-zoned zircon rims during magmatic crystallisation, and this pattern is commonly observed in Paleozoic S-type granites of the eastern Lachlan Orogen. Magmatic zircons lacking an inherited core are relatively rare: one example is the crystal above and to the right of grain 11.1 (Figure 55).

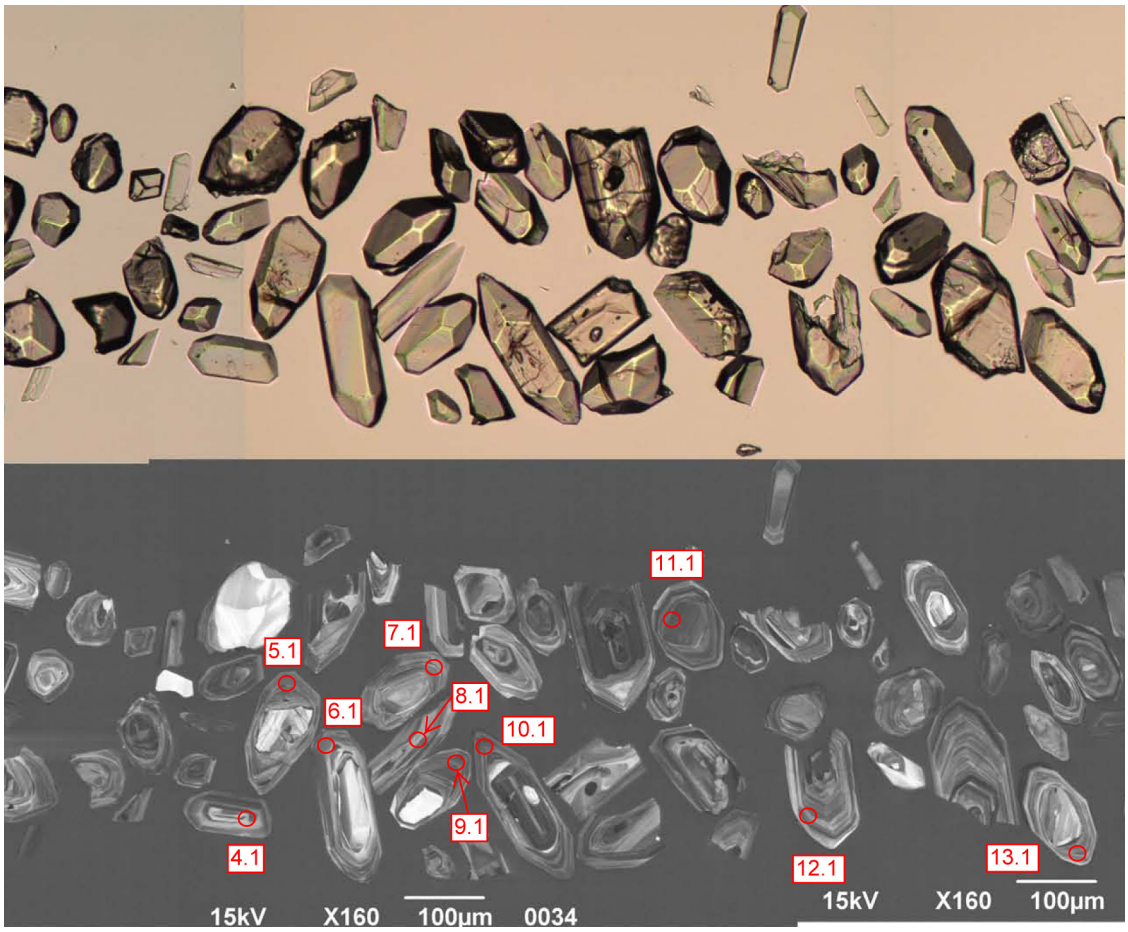

Figure 55: *Representative zircons from the Rye Park Granite (GSNSW WRP-046, GA 1989773). Transmitted-light image is shown in the upper half; cathodoluminescence image in the lower half. SHRIMP analysis sites are indicated, and labelled with grain and spot number.*

U-Pb Isotopic Results

Thirty-two analyses were obtained from 32 individual zircons, and the results are presented in Figure 56, and Table 15. The concentrically-zoned outer mantles of the zircons were preferentially targeted during analysis, in order to derive a magmatic crystallisation age. These areas are characterised by uniformly moderate U contents (152–564 ppm, median 368 ppm) and relatively low Th/U (0.13–0.53, median 0.21).

One analysis (14.1.1; red fill in Figure 56) yielded a high common Pb content ($^{206}Pb_c$ > 2%), and is interpreted to have been affected by loss of radiogenic Pb during one or more events of unknown age. Consequently, its $^{238}U/^{206}Pb$ date is unreliable, and this analysis is not considered further.

The remaining 31 analyses have uniformly low $^{206}Pb_c$ (maximum 0.81%, median 0.15%), and can be divided into three groups (Table 15):

- 28 analyses of 28 zircons (Group 1; yellow fill in Figure 56) with individual $^{238}U/^{206}Pb$ dates between c. 446 Ma and c. 406 Ma, which yielded a weighted mean date of 431.4 ± 4.9 Ma (MSWD = 1.21),
- two analyses of two zircons (Group 2; blue fill in Figure 56) with individual $^{238}U/^{206}Pb$ dates between c. 511 Ma and c. 458 Ma, and
- a single analysis (Group 3; white fill in Figure 56) with a $^{238}U/^{206}Pb$ date of 406 ± 15 Ma (2σ).

Geochronological Interpretation

The weighted mean date of 431.4 ± 4.9 Ma obtained from the 28 analyses in Group 1 is indistinguishable from the median $^{238}U/^{206}Pb$ date for the same 28 analyses (433.5 +6.5/-8.5 Ma), and the absence of significant asymmetry in the uncertainties associated with the latter suggests that Group 1 represents a single population of analyses with an approximately normal distribution. Consequently, the weighted mean $^{238}U/^{206}Pb$ date of 431.4 ± 4.9 Ma is interpreted as the best estimate of the age of magmatic crystallisation of the Rye Park Granite.

The magmatic crystallisation age of 431.4 ± 4.9 Ma for the Rye Park Granite is indistinguishable from that of the 430 ± 6 Ma Bigga Granite (Wilde, 2001) within the Hovells Suite, and it is also indistinguishable from those of the S-type Burrawinda Suite (427.8 ± 2.7 Ma Mulgowrie Granodiorite and 427.9 ± 3.0 Ma Winduella Tonalite) and the I-type Gunning Suite (428.6 ± 2.4 Ma Gunning Granite and 429.2 ± 2.3 Ma Cumberoona Tonalite) obtained by Bodorkos and Simpson (2008). These results establish the temporal equivalence of the Hovells, Burrawinda and Gunning Suites in west-central GOULBURN (Johnston *et al.*, 2001, 2004, in press; Thomas *et al.*, 2001).

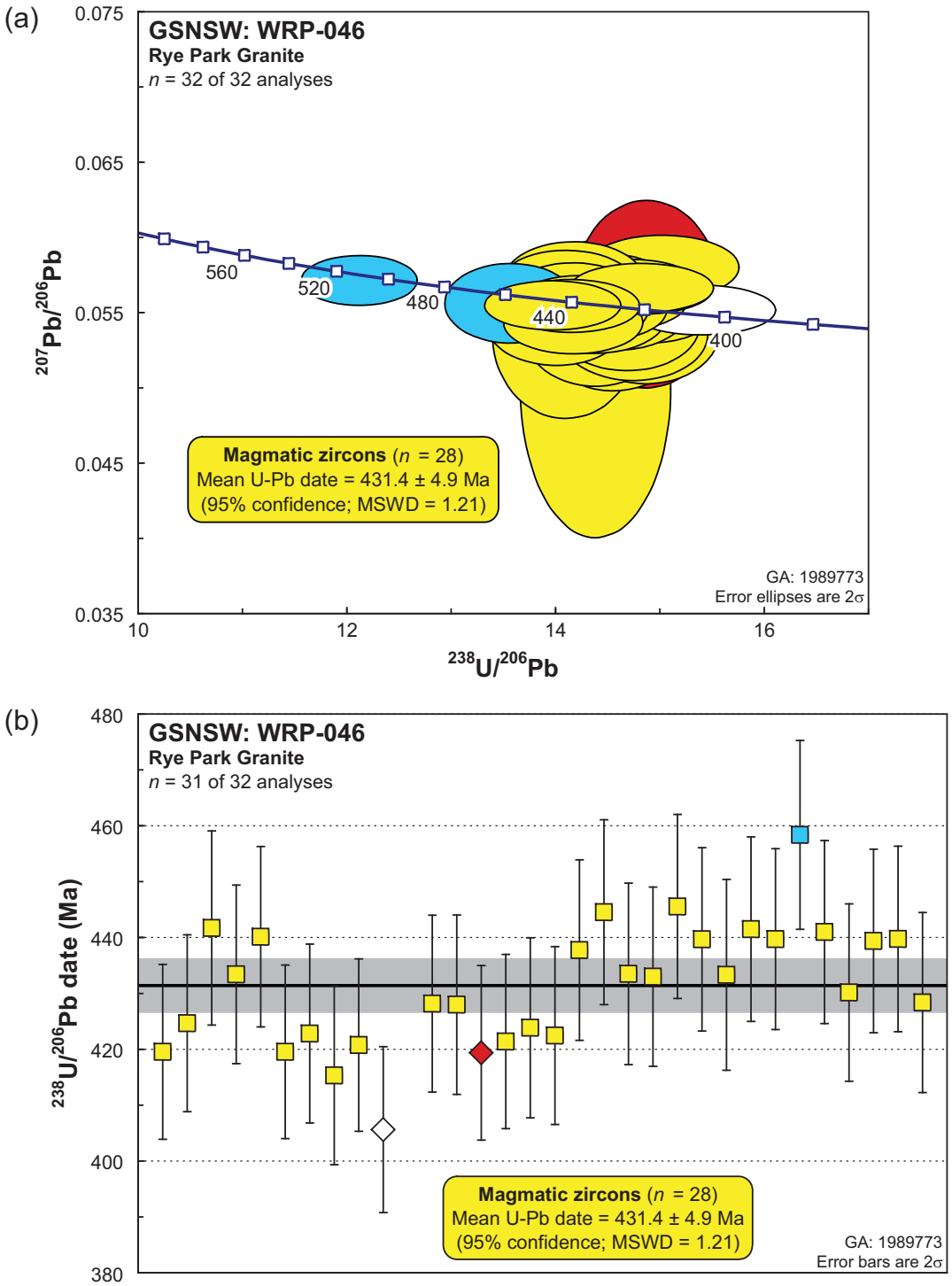

Figure 56: *SHRIMP U-Pb data for zircons from the Rye Park Granite (GSNSW WRP-046, GA 1989773). (a) Tera-Wasserburg concordia diagram; (b) $^{238}U/^{206}Pb$ dates in order of acquisition (one analysis with a pre-480 Ma date is not shown). Yellow fill: magmatic zircons; blue fill: Cambrian–Ordovician inheritance; white fill: affected by loss of radiogenic Pb; red fill: not considered due to high $^{206}Pb_c$. Heavy black line and grey band: weighted mean $^{238}U/^{206}Pb$ date and its 95% confidence interval, respectively.*

Table 15: SHRIMP U-Pb zircon data from the Rye Park Granite (GSNSW WRP-046, GA 1989773). All dates are $^{238}U/^{206}Pb$ unless otherwise indicated.

Sess. no.	Grain.area .replicate	$^{206}Pb_c$ (%)	U (ppm)	Th (ppm)	$^{232}Th/^{238}U$	$^{238}U/^{206}Pb$	±1σ (%)	$^{207}Pb/^{206}Pb$	±1σ (%)	Date (Ma)	±1σ (Ma)	Disc. (%)
Group 2: Cambrian–Ordovician inherited individuals (n = 2)												
90068	11.1.1	0.08	564	274	0.50	12.118	1.88	0.05714	1.19	511.1	9.2	-3
90068	27.1.1	0.29	560	77	0.14	13.570	1.91	0.05564	1.95	458.4	8.5	-4
Group 1: Magmatic zircons (n = 28)												
90068	22.1.1	0.03	365	68	0.19	13.974	1.91	0.05549	1.21	445.6	8.2	-3
90068	19.1.1	0.16	346	75	0.22	14.007	1.93	0.05416	2.02	444.5	8.3	-15
90068	3.1.1	0.66	152	31	0.21	14.100	2.03	0.05352	4.27	441.7	8.7	-21
90068	25.1.1	-0.04	382	55	0.15	14.107	1.93	0.05675	1.74	441.5	8.3	9
90068	28.1.1	0.19	441	114	0.27	14.124	1.92	0.05559	2.64	441.0	8.2	-1
90068	5.1.1	0.07	444	82	0.19	14.152	1.90	0.05545	1.29	440.1	8.1	-2
90068	31.1.1	0.14	302	83	0.28	14.165	1.95	0.05523	2.66	439.7	8.3	-4
90068	26.1.1	0.29	561	94	0.17	14.166	1.91	0.05584	1.83	439.7	8.1	1
90068	23.1.1	0.12	305	136	0.46	14.168	1.93	0.05436	1.58	439.7	8.2	-12
90068	30.1.1	-0.04	372	83	0.23	14.177	1.93	0.05720	1.82	439.4	8.2	14
90068	18.1.1	0.17	428	108	0.26	14.232	1.91	0.05523	1.66	437.8	8.1	-4
90068	20.1.1	0.53	300	38	0.13	14.376	1.94	0.05369	2.74	433.5	8.1	-17
90068	4.1.1	0.19	387	107	0.29	14.379	1.91	0.05467	1.78	433.4	8.0	-8
90068	24.1.1	0.81	249	128	0.53	14.383	2.04	0.04992	8.12	433.3	8.5	-56
90068	21.1.1	0.11	368	65	0.18	14.394	1.91	0.05519	1.54	433.0	8.0	-3
90068	29.1.1	0.18	510	98	0.20	14.492	1.91	0.05622	1.98	430.2	7.9	7
90068	32.1.1	0.32	358	65	0.19	14.554	1.94	0.05382	3.07	428.4	8.1	-15
90068	12.1.1	0.15	386	80	0.21	14.561	1.91	0.05484	1.75	428.2	7.9	-5
90068	13.1.1	0.11	291	49	0.17	14.568	1.94	0.05577	1.47	428.0	8.0	4
90068	2.1.1	0.20	319	45	0.14	14.686	1.93	0.05418	2.29	424.7	7.9	-11
90068	16.1.1	-0.04	245	107	0.45	14.715	1.96	0.05650	1.49	423.8	8.1	11
90068	7.1.1	0.34	249	35	0.15	14.752	1.96	0.05353	2.31	422.8	8.0	-17
90068	17.1.1	0.27	292	137	0.48	14.765	1.95	0.05503	2.44	422.5	8.0	-2
90068	15.1.1	0.02	392	80	0.21	14.803	1.91	0.05650	1.17	421.4	7.8	12
90068	9.1.1	-0.07	463	83	0.19	14.827	1.89	0.05665	1.18	420.7	7.7	14
90068	6.1.1	0.11	377	86	0.24	14.871	1.91	0.05519	1.65	419.5	7.8	0
90068	1.1.1	0.28	321	53	0.17	14.871	1.93	0.05375	2.67	419.5	7.8	-14
90068	8.1.1	-0.08	232	43	0.19	15.027	1.99	0.05802	1.51	415.3	8.0	28
Group 3: Affected by loss of radiogenic Pb (n = 1)												
90068	10.1.1	-0.04	557	190	0.35	15.398	1.89	0.05517	1.24	405.6	7.4	3
Not considered, due to high $^{206}Pb_c$ (> 2%; n = 1)												
90068	14.1.1	2.07	427	83	0.20	14.877	1.92	0.05623	4.54	419.4	7.8	10

References

Black, L. P., 1998. SHRIMP zircon U/Pb isotopic age dating of samples from the Dubbo 1:250 000 Sheet area. Geological Survey of New South Wales Report **GS1998/127**, 2pp.

Black, L. P., 2005. SHRIMP U-Pb zircon ages obtained during 2004/05 for GSNSW. Geological Survey of New South Wales Report **GS2005/745**, 22pp.

Black, L. P., 2006. SHRIMP U-Pb zircon ages obtained during 2005/06 for NSW Geological Survey projects. Geological Survey of New South Wales Report **GS2006/821**, 37pp.

Black, L. P., Kamo, S. L., Allen, C. M., Davis, D. W., Aleinikoff, J. N., Valley, J. W., Mundil, R., Campbell, I. H., Korsch, R. J., Williams, I. S. and Foudoulis, C., 2004. Improved $^{206}Pb/^{238}U$ microprobe geochronology by the monitoring of a trace-element-related matrix effect; SHRIMP, ID-TIMS, ELA-ICP-MS and oxygen isotope documentation for a series of zircon standards. Chemical Geology **205**, 115–140.

Bodorkos, S. and Simpson, C. J., 2008. Summary of results for the joint GSNSW–GA geochronology project: Eastern Lachlan Orogen July 2007–June 2008. Geological Survey of New South Wales Report **GS2008/0505**, 79pp.

Claouè-Long, J. C., Compston, W., Roberts, J. and Fanning, C. M., 1995. Two Carboniferous ages: a comparison of SHRIMP zircon dating with conventional zircon ages and $^{40}Ar/^{39}Ar$ analysis. *In* Berggren, W. A., Kent, D. V., Aubry, M.-P. and Hardenbol, J., editors, Geochronology, Time Scales and Global Stratigraphic Correlation. SEPM Special Publication **54**, pp. 3–21. Society for Sedimentary Geology, Tulsa, Oklahoma, USA.

Compston, W., Williams, I. S. and Meyer, C., 1984. U-Pb geochronology of zircons from lunar breccia 73217 using a sensitive high-mass resolution ion microprobe. Journal of Geophysical Research **89** (Supplement), B525–B534.

Evernden, J. F. and Richards, J. R., 1962. Potassium-argon ages in eastern Australia. Journal of the Geological Society of Australia **9**, 1–49.

Fanning, C. M., 1997. SHRIMP zircon U/Pb age dates from the Dubbo 1:250 000 map sheet — a report by Precise Radiometric Isotope Services. Geological Survey of New South Wales Report **GS1997/590**, 2pp.

Felton, E. A. and Huleatt, M. B., 1976. Geology of the Braidwood 1:100 000 Sheet 8827, first edition. Geological Survey of New South Wales, Sydney.

Fitzherbert, J. A., Thomas, O. D., Deyssing, L. J., Bewert-Vassallo, K. E., Simpson, C. J. and Sherwin, L., in press. Braidwood 1:100 000 Geological Sheet 8827, second edition. Geological Survey of New South Wales, Orange.

Glen, R. A., Dawson, M. W. and Colquhoun, G. P., 2006. Eastern Lachlan Orogen Geoscience Database (DVD-ROM) Version 2. Geological Survey of New South Wales, Maitland.

Hoaglin, D. C., Mosteller, F. and Tukey, J. W., 1983. Understanding Robust and Exploratory Data Analysis. John Wiley and Sons, New York, pp. 345–349.

Johnston, A. J., Pogson, D. J., Thomas, O. D., Watkins, J. J. and Glen, R. A., 2001. Boorowa 1:100 000 Geological Sheet 8629, first edition (Provisional Geology: November 2008). Geological Survey of New South Wales, Orange.

Johnston, A. J., Scott, M. M., Thomas, O. D., Pogson, D. J., Warren, A. Y. E., Sherwin, L., Colquhoun, G. P., Watkins, J. J., Cameron, R. G., MacRae, G. P. and Glen, R. A., in press. Goulburn 1:250 000 Geological Sheet SI/55-12, second edition. Geological Survey of New South Wales, Orange.

Johnston, A. J., Scott, M. M., Watkins, J. J., Sherwin, L., Warren, A. Y. E., Pogson, D. J. and Glen, R. A., 2004. Crookwell 1:100 000 Geological Sheet 8729, first edition (Provisional Geology: November 2008). Geological Survey of New South Wales, Orange.

Ludwig, K. R., 2002. SQUID 1.02: A User's Manual. Berkeley Geochronology Center Special Publication **2**, 19pp.

Ludwig, K. R., 2003. User's Manual for Isoplot 3.6 (April 2008 revision). Berkeley Geochronology Center Special Publication **4**, 77pp.

McQueen, K. G. and Perkins, C., 1995. The nature and origin of a granitoid-hosted gold deposit at Dargues Reef, Majors Creek, New South Wales. Economic Geology **90**, 1646–1662.

McQueen, K. G., 2003. Evidence of a granite-related source for the Braidwood-Araluen-Majors Creek goldfields, NSW, Australia. *In* Blevin, P., Jones, M. and Chappell, B., editors, Magmas to Mineralisation: The Ishihara Symposium. Geoscience Australia Record **2003/14**, 97–100.

Meakin, N. S. and Morgan, E. J., 1999. Dubbo 1:250 000 Geological Sheet SI/55-4, second edition: Explanatory Notes. Geological Survey of New South Wales, Sydney, xvi + 504 pp.

Moffitt, R. S., 1999. Southern Coalfields Regional Geology 1:100 000, first edition. Geological Survey of New South Wales, Sydney.

Nelson, D. R., 1997. Compilation of SHRIMP U-Pb zircon geochronology data, 1996. Geological Survey of Western Australia Record **1997/2**, 189pp.

Pogson, D. J. and Watkins, J. J., 1998. Bathurst 1:250 000 Geological Sheet SI/55-8, second edition: Explanatory Notes. Geological Survey of New South Wales, Sydney, xiv + 430 pp.

Rock, N. M. S., Webb, J. A., McNaughton, N. J. and Bell, G. D., 1987. Nonparametric estimation of averages and error for small data-sets in isotope geoscience: a proposal. Chemical Geology **66**, 163–177.

Rose, G., 1966. Wollongong 1:250 000 Geological Sheet SI/56-9, second edition. Geological Survey of New South Wales, Sydney.

Sircombe, K. N., Cassidy, K. F., Champion, D. C. and Tripp, G., 2007. Compilation of SHRIMP U-Pb geochronological data: Yilgarn Craton, Western Australia, 2004–2006. Geoscience Australia Record **2007/01**, 182pp.

Stacey, J. S. and Kramers, J. D., 1975. Approximation of terrestrial lead isotope evolution using a two-stage model. Earth and Planetary Science Letters **26**, 207–221.

Steiger, R. H. and Jäger, E., 1977. Subcommission on geochronology: convention on the use of decay constants in geo- and cosmochronology. Earth and Planetary Science Letters **36**, 359–362.

Stern, R. A., Bodorkos, S., Kamo, S. L., Hickman, A. H. and Corfu, F., 2009. Measurement of SIMS instrumental mass fractionation of Pb isotopes during zircon dating. Geostandards and Geoanalytical Research **33**, 145–168.

Thomas, O. D., Johnston, A. J., Scott, M. M., Pogson, D. J., Sherwin, L. and MacRae, G. P., 2002. Goulburn 1:100 000 Geological Sheet 8828, first edition (Provisional Geology: November 2008). Geological Survey of New South Wales, Orange.

Thomas, O. D., Scott, M. M., Warren, A. Y. E. and Sherwin, L., 2001. Gunning 1:100 000 Geological Sheet 8728, first edition (Provisional Geology: November 2008). Geological Survey of New South Wales, Orange.

Trigg, S. J. and Campbell, L. M., in prep. Moss Vale 1:100 000 Geological Sheet 8928, first edition. Geological Survey of New South Wales, Orange.

Wilde, S. A., 2001. SHRIMP U-Pb dating of seven samples from the Crookwell area, NSW. Unpublished report to the Geological Survey of New South Wales.

Wilde, S. A., 2002. SHRIMP U-Pb dating of four samples from the Goulburn 1:250 000 map sheet area, NSW. Geological Survey of New South Wales Report **GS2009/0158**, 20pp.

Williams, I. S., 1998. U-Th-Pb geochronology by ion microprobe. *In* McKibben, M. A., Shanks III, W. C. and Ridley, W. I., editors, Applications of Microanalytical Techniques to Understanding Mineralizing Processes. Reviews in Economic Geology **7**, 1–35. Society of Economic Geologists, Littleton, Colorado, USA.

Williams, I. S. and Claesson, S., 1987. Isotopic evidence for the Precambrian provenance and Caledonian metamorphism of high grade paragneisses from the Seve Nappes, Scandinavian Caledonides: II. Ion microprobe zircon U-Th-Pb. Contributions to Mineralogy and Petrology **97**, 205–217.

Wyborn, D. and Owen, M., 1986. 1:100 000 Geological Map Commentary: Araluen 8826, New South Wales. Bureau of Mineral Resources, Geology and Geophysics, Canberra.